2-24-2022 3:30 PM

The role of galectins in differentiation of acute myeloid leukemia cells

Jolaine Smith, *The University of Western Ontario*

Supervisor: Alexander Timoshenko, *The University of Western Ontario*

A thesis submitted in partial fulfillment of the requirements for the Master of Science degree in Biology

Abstract

Galectins are a family of β-galactoside binding proteins with roles in cellular differentiation, apoptosis, and cancer progression. To better understand this important class of proteins, HL-60 acute myeloid leukemia cells were used as a model for comparative study of the effects of recombinant galectins, galectin inhibitors, and all-*trans* retinoic acid (ATRA) on granulocytic differentiation. Targeted inhibition of galectin-1 or -3 induced characteristics of neutrophilic differentiation including segmentation of nuclei, upregulation of neutrophil cytosolic factor 1 gene expression, and a global decrease in protein glycosylation with *O*-linked *N*-acetylglucosamine. Recombinant galectin-8 or -9 also induced granulocytic differentiation that was not observed with recombinant galectin-1 or -3. However, the galectin induced differentiation was moderate relative to the strong stimulatory effects observed with ATRA. *In silico* analysis of acute myeloid leukemia data from the Cancer Genome Atlas revealed changes in galectin gene expression profiles related to the various molecular subtypes of acute myeloid leukemia. A ratio of galectin-12/galectin-9 gene expression was identified as a potential diagnostic marker of leukemia subtypes. Correlation analysis between galectin gene pairs revealed changes to the glycobiological landscape and relation to granulocytic differentiation markers in leukemia cells. Among galectin genes, only the increased galectin-1 gene expression was indicative of patient poor prognosis in all acute myeloid leukemia cohorts. These results indicate that while galectins share similar structures, they elicit different responses and display different gene expression patterns in relation to granulocytic differentiation in acute myeloid leukemia. Furthermore, these findings suggest the possible utility of galectins as targets for differential therapeutics.

Keywords

Galectins, Cell differentiation, All-*trans* retinoic acid, Acute myeloid leukemia, HL-60 cells, OTX008, GB1107, *O*-GlcNAcylation, Neutrophil cytosolic factor 1

Summary for Lay Audience

Galectins are a group of sugar binding proteins involved with the immune system and cancer. Acute myeloid leukemia (AML) is a fast-acting cancer of the blood and bone marrow. Patients with AML have weaker immune systems and lower immune cell counts because of a larger number of cancer cells. To date, the treatments for AML include chemotherapy and many drugs including all-*trans* retinoic acid (ATRA). AML poses issues in treatment and diagnosis due to the wide range of genetic changes that occur within the cancer cells. In this study, different galectins in HL-60 cells (an AML cancer cell line) were used to see how these proteins influence the cell development of the immune system for possible new targets in AML therapies. In HL-60 cells, the inhibition of galectin-1 or galectin-3 as well as the supplementary addition of galectin-8 or galectin-9 resulted in an increase in developed immune cells. However, all galectin responses were weaker when compared to ATRA treated cells. Galectins were also investigated to find new diagnostic and prognostic markers of AML. When comparing galectins between healthy and cancer cells, galectin-9 and galectin-12 showed changes specific to cancer cells, serving as a new diagnostic marker. Additionally, increased expression of galectins-1, -4 and -10 all serve as new prognostic markers in AML. Overall, my findings revealed that galectins are related to the development of the immune system and serve as new diagnostic and prognostic markers. This suggests that galectins might prove useful as potential new targets for AML therapies.

Acknowledgments

I would like to start by thanking my graduate supervisor, Dr. Alexander Timoshenko for accepting me as a graduate student. I appreciate the time, guidance, supervision, and patience you have shown during my time here at Western. You have helped me further develop my skills in more ways than one that have made me a better researcher. I would also like to thank my advisory committee members, Dr. Jim Karagiannis and Dr. Patrick Lajoie, for all your guidance over my years here at Western. Thank you for all the feedback during committee meetings, defense preparation, and questions to prepare me for what comes ahead.

I would like to thank fellow students in the Timoshenko lab; Adam McTague, Philipp Guevorguian, and Rada Tazhitdinova. Thank you all for the help in learning new techniques, trouble shooting, and when learning new methods in our lab. Thank you, Adam, for letting me bounce ideas off you and helping me trouble shoot protocols. I would also like to thank other cell biology graduate students: Mohammed Gatie and Alexandra Kozlov. Thanks to the both of you for the scientific and administrative advice and wisdom you have passed onto me during my time here.

I would also like to thank Dr. Rob Cumming, Dr. Jim Karagiannis, Kim Loney, and Chunhui Li for the use of their labs and equipment, technical assistance, and advice.

I would also like to acknowledge the Cancer Genome Atlas, the Common Fund's Genotype-Tissue Expression program, the CBioPortal, and the *recount2* databases for the public access and normalization of data used in this study.

Lastly, I would like to thank my friends and family that have supported me during my journey of post-secondary education. A special thanks to Alisha Moynahan for helping me and supporting me during all my post-secondary education from undergraduate at Waterloo to our graduate studies at Western.

Table of Contents

List of Abbreviations

ALL	Acute lymphoblastic leukemia
AML	Acute myeloid leukemia
ANOVA	Analysis of variance
APL	Acute promyelocytic leukemia
ATRA	All-*trans* retinoic acid
BAX	Bcl-2 associated X-protein
BFA	Brefeldin A
C/EPB	CCAAT enhancer binding protein
CD	Cluster of differentiation
CHOP	DNA damage inducible transcript 3
CLC	Charcot-Leyden Crystal Galectin or Galectin-10
CLL	Chronic lymphoblastic leukemia
CML	Chronic myeloid leukemia
MYC	MYC proto-oncogene
CRD	Carbohydrate recognition domain
CYB	Cytochrome B
DAPI	4’,6-diamidino-2-phenylindole
DMSO	Dimethyl sulfoxide
ERK	Extracellular signal regulated kinase
FAB	French-American-British
FBS	Fetal bovine serum
FOX	RNA Binding Fox-1
GFAT	Glutamine fructose-6-phosphate aminotransferase
GTEx	Genotype-Tissue Expression
HL-60	Human promyelocytic leukemia cells
HSC	Hematopoietic stem cells
IL	Interleukin
IMDM	Iscove’s modification of Dulbecco’s modified Eagle medium
ITS	Insulin, transferrin, selenous acid
KLF4	Kruppel like factor 4

LGALS	Lectin, Galactoside-Binding, Soluble
MAPK	Mitogen activated protein kinase
MSC	Mesenchymal stem cells
MLL	Mixed lineage leukemia
mTOR	Mechanistic target of rapamycin
NADPH	Nicotinamide adenine dinucleotide phosphate
NANOG	Nanog Homeobox
NCF	Neutrophil cytosolic factor
NuMa	Nuclear mitotic apparatus protein
OCT4	POU Class 5 Homeobox
OGA	O-GlcNAcase
O-GlcNAc	O-linked β-N-acetyl-D-glucosamine
OGT	O-GlcNAc transferase
PML	Promyeloid leukemia gene
PU.1	Spi-1 proto-oncogene
RARα	Retinoic acid receptor alpha
ROS	Reactive oxygen species
RT-qPCR	Quantitative Reverse transcription polymerase chain reaction
RT-PCR	Reverse transcription polymerase chain reaction
RUVg	Removal of unwanted variation
RXR	Retinoic X receptor
SD	Standard deviation
shRNA	Short hairpin RNA
Sp1	Specificity protein 1
STAT3	Signal transducer and activator of transcription 3
TCGA	The Cancer Genome Atlas
TDG	Thiodigalactoside
TIM-3	T-cell immunoglobin domain and mucin domain 3
UDP	Uridine diphosphate
Wnt	Wingless-related integration site

List of Tables

List of Figures

List of Appendices

Chapter 1

1 Introduction

1.1 Acute Myeloid Leukemia (AML)

There are four different leukemias impacting immune cells including acute/chronic myeloid and lymphocytic (AML, CML, ALL, CLL) leukemia. Acute myeloid leukemia (AML) is a fast-progressing blood cancer that affects myeloid origin cells including leukocytes, erythrocytes and megakaryoblasts (Luczak et al., 2012; De Kouchkovsky & Abdul-Hay 2016). The result of AML is an increased amount of terminally undifferentiated and immature cancerous cells in the bone marrow, preventing healthy blood cell production, differentiation, and maturation (De Kouchkovsky & Abdul-Hay, 2016; Lohse et al., 2018). Side effects that can be observed in AML patients include improper immune function, anemia, and hemorrhaging. The incidence of AML has increased over the past decade, especially among older adults who demonstrate poor prognosis (Lohse et al., 2018; Short et al., 2018). Currently, AML subtype identification follows the French-American-British (FAB) classification system, where the eight different subtypes of AML are categorized as M0 through M7. Patient classification is based on cell nuclearmorphology, cytochemical testing, and genetic abnormalities (Dalton et al., 1988; Hassan et al., 1993; De Kouchkovsky & Abdul-Hay, 2016; Walter et al., 2013; Asthana et al., 2018; Lohse et al., 2018; Short et al., 2018). Current treatments for AML include cytotoxic chemotherapy and various other drugs, including all-*trans* retinoic acid (ATRA). However, AML has high genetic heterogeneity due to distinct cytogenetic abnormalities, somatic mutations, and changes in the epigenome, resulting in difficult subtype classification and difficult treatment (Walter et al., 2013; Lohse et al., 2018). Induced differentiation therapies are one of many new treatments being investigated for AML, with galectins representing an intriguing target for these therapies.

1.1.1 AML FAB subtype classification

AML FAB subtype classification indicates which cells during myeloid cell maturation are cancerous, resulting in the accumulation and secretion of these cells from the bone marrow

into the blood (**Figure 1**). Each subtype represents a different stage of maturation when looking at myeloid cell differentiation (Lohse et al., 2018). M6 and M7 are rarer forms of AML and are not associated with leukocyte differentiation (Hassan et al., 1993). There are various genetic mutations that occur resulting in inhibited leukocyte differentiation, including mutations in the *RUNX1, C/EBPα, PU.1*, among other transcription factors (De Kouchkovsky & Abdul-Hay, 2016; Lohse et al., 2018). When looking at leukocyte maturation, subtypes closer to the HSCs are considered more immature and contain more stem-like properties. AML FAB subtypes include M0 (undifferentiated acute myeloblastic leukemia), M1 (acute myeloblastic leukemia, <10% maturation), M2 (acute myeloblastic leukemia, >10% maturation), M3 (acute promyelocytic leukemia, APL), M4 (acute myelomonocytic leukemia), M5 (acute monocytic leukemia), M6 (acute erythroid leukemia), and M7 (acute megakaryoblastic leukemia) (Hassan et al., 1993).

The M3 subtype, also known as acute promyelocytic leukemia (APL), is a form of AML occurring in 5% of all leukemia cases. APL demonstrates a specific chromosomal translocation t(15:17) that results in a gene fusion of the retinoic acid receptor alpha (RARα) with the promyelocytic leukemia gene (PML) denoted as the PML-RARα translocation. This translocation was reported in 98% of APL patients and was not observed in other FAB subtypes. Additionally, this PML-RARα gene fusion allows for APL cells to be susceptible to ATRA as a differential treatment, resulting in a remission rate of over 90% (Lohse et al., 2018) In non-ATRA treated APL, the PML-RARα protein binds to a co-repressor preventing the expression of differentiation genes. When APL is treated with ATRA, the co-repressor is replaced with a co-activator allowing for the activation and transcription of leukocyte differentiation genes. To date, ATRA research into other FAB subtypes demonstrates no effect apart from M2 with vitamin-D3 demonstrating a lesser effect than observed in M3 subtype (Johnson & Redner, 2015).

1.2 The *recount2* database

Galectin gene expression can be examined using the Cancer Genome Atlas (TCGA) database. The TCGA was created in 2006 by the National Cancer Institute and the National Human Genome Research Institute to provide a public catalogue of the full spectrum of genomic changes involved in human cancers. To date, there are over 20,000 primary

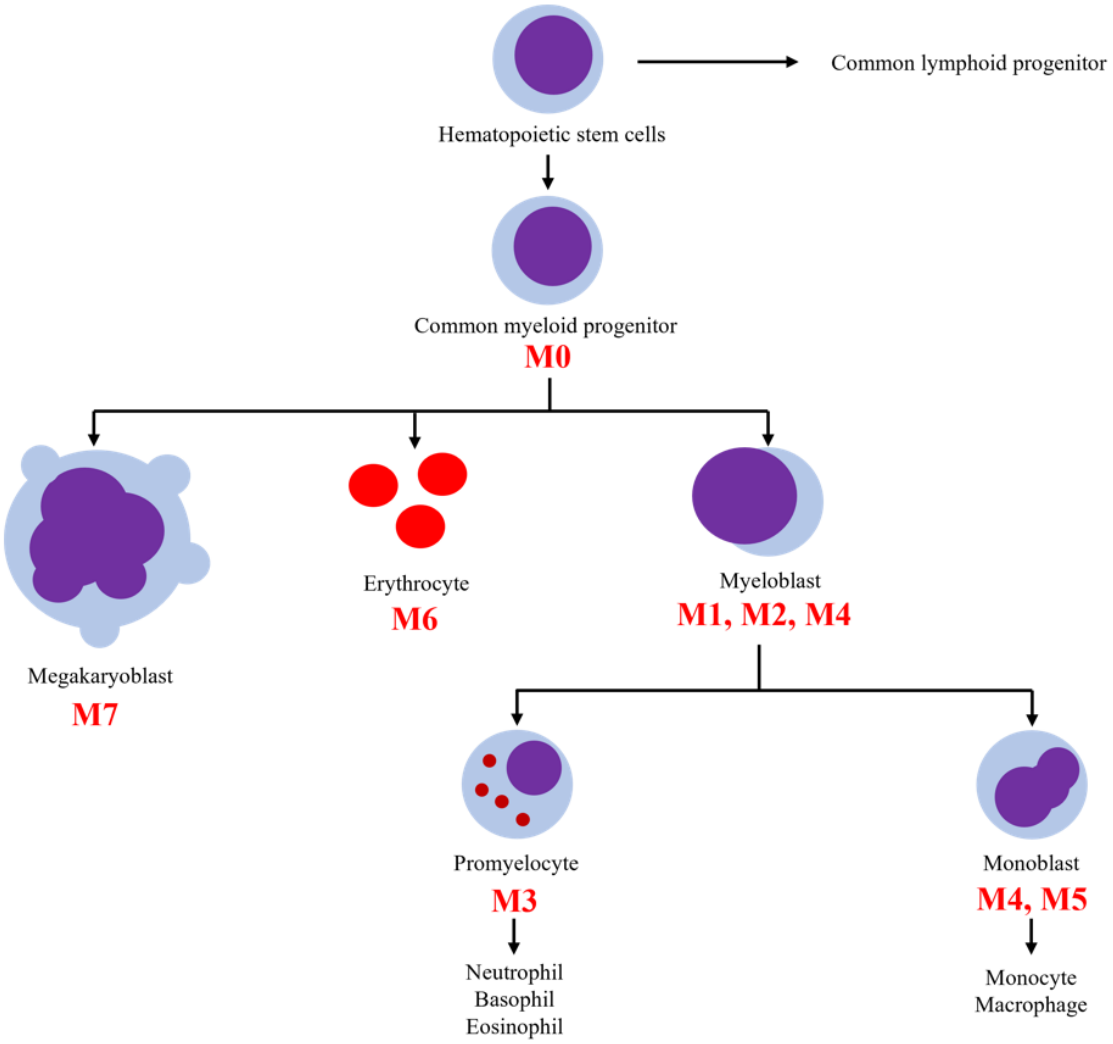

Figure 1: Hematopoiesis of myeloid origin cells related to the French-American-British classification system of acute myeloid leukemia.

AML is classified into eight different molecular subtypes depicted as M0-M7 based on the originating cancerous cell. Leukemias are classified based on the maturation of the cell type within their related lineage. This figure is adapted from Agarwal et al. (2019). Subtype identification is performed through light microscopy of nuclear morphology, as well as genetic abnormalities and biomarkers.

cancers characterized, including AML. However, accessing AML TCGA data does not provide a normal control sample with which to compare. AML TCGA data can be obtained from the recount2 database where healthy bone marrow samples can also be investigated. The recount2 database provides access to 2041 different studied systems. Recount2 obtains raw RNA-seq data of various other databases, including TCGA and the Common Fund's Genotype-Tissue Expression (GTEx) program. Recount2 normalizes the data following the protocol detailed by Nellore et al. (2016) and was verified by Collado-Torres et al. (2017). This normalization technique allows for the comparison of RNA-seq data from different databases, eliminating computational batch effects. Recount2 normalized both AML TCGA data and bone marrow samples from the GTEx database, allowing for the expression profiles of galectins to be examined. FAB subtypes of AML TCGA data can also be determined from recount2, allowing for galectin gene expression profiling to be evaluated. However, there are still lab batch effects between the TCGA and GTEx samples. Risso et al. (2014) demonstrated a differential expression analysis normalization technique that eliminated the lab batch effect. Empirical control genes are identified through differential expression analysis of the two datasets. Once analyzed, 500 empirical control genes are then used to eliminate the variation found between the two datasets, removing the lab batch effect. This normalization allows for the comparison between datasets from different databases without variation (Risso et al., 2014).

1.3 HL-60 cells as a model to study cellular differentiation

HL-60 cells were first classified as a M3 subtype in 1976 when isolated from a 36-year-old female acute myeloid leukemia patient and were immortalized in 1977 by the National Cancer Institute (Collins et al., 1977; Breitman et al., 1980). However, in 1989, HL-60 cells were changed to the M2 FAB classification based on the similarity of morphological characteristics observed in HL-60 cells and cells of the M2 subtype (Dalton et al., 1988). HL-60 cells contain a homozygous deletion of the p53 gene, inhibiting G1 cell growth arrest. This contributes to continuous proliferation while preventing apoptosis and differentiation. However, research has shown that normal cell cycle regulation, apoptosis and differentiation can be restored in HL-60 cells by transfecting cells with p53 (Soddu et al., 1994).

In the 1980s, research showed that HL-60 cells can be cultured in the absence of the growth factors, proteins, and hormones contained in fetal bovine serum (FBS) for *in vitro* culture. For the proliferation and survival of HL-60 cells *in vitro,* a serum-free growth medium containing insulin, transferrin and selenous acid (ITS) is required (Breitman et al., 1980). Undifferentiated HL-60 cells contain surface receptors for insulin (insulin receptor, IR) and transferrin (transferrin receptor, TfR), which allows for binding of these molecules required for HL-60 cell growth. Insulin is involved with glucose uptake and metabolism, while transferrin allows for many cellular processes to occur by iron uptake (Breitman et al., 1980; Chaplinski et al., 1986). Selenous acid provides selenium to cells, which is involved in redox pathways (Guilbert and Iscove, 1976; McKeehan et al., 1976). To understand how galectins are involved in the differentiation of HL-60 cells, it is important to culture in serum-free media due to the galectins present in FBS (Johannes et al., 2018).

HL-60 cells provide a great model to study granulocytic differentiation in relation to AML. An undifferentiated HL-60 cell is classified as a promyelocyte (pre-leukocyte) and has the pluripotency to differentiate into various mature leukocyte-like cells including monocytes, eosinophils, and neutrophils. There are various reagents that induce differentiation of HL-60 cells that are well studied. Terminal differentiation into monocytes is achieved by phorbol 12-myristate 13-acetate, while terminal differentiation into eosinophils is achieved by sodium-butyrate. However, there are several agents that can be used to induce terminal differentiation into the neutrophil or granulocyte lineage.

The two main agents used include DMSO and ATRA (Breitman et al., 1980; Abedin et al., 2003). HL-60 cells have susceptibility to ATRA in the absence of the PML-RARα gene fusion, found in acute promyeloid leukemia (APL), due to the increased progranulocytes. The retinoic acid receptor (RARα) for ATRA is found in progranulocytes and once activated, forms a complex with the retinoid X receptor (RXR) (Breitman et al., 1980; Tassef et al., 2017). This ATRA activation results in downstream activation of transcription factors associated with granulocytic differentiation including C/EBPβ and PU.1 (Bjerregaard et al., 2003; Akagi et al., 2010; Ai & Udalova, 2019). Additionally, the ATRA activation also revealed changes in gene expression and activation of proteins including ERK1/2, p38/MAPK, STAT3, C/EBPα/β, PU.1, integrins, and CD44 (Hickstein

et al., 1989; Liu et al., 2007; Song et al., 2013; Tasseff et al., 2017) (**Figure 2**). Furthermore, previous research with retinoic acid induced differentiation revealed that changes in galectin gene expression were related to Sp1 consensus binding sites (Lu & Lotan, 1999; Lu et al., 2000). Therefore, HL-60 cells provide a good model for studying the effects of galectins during granulocytic differentiation.

1.3.1 Neutrophilic differentiation of HL-60 cells

The innate immune system is made up of many leukocytes including neutrophils. Neutrophils are effective first responders during microbial infection and are often found in high amounts in circulation (Kobayashi et al., 2015; Ai & Udalova, 2019). Neutrophils can have various responses to infections including phagocytosis, release of ROS, degranulation, and release of nuclear extracellular traps (Kolaczkowska & Kubes, 2013). There are many aspects that distinguish neutrophils from other innate immune cells and undifferentiated cells that are reflected in HL-60 cells. Neutrophils have multi-lobular, segmented nuclei with specific envelope protein composition. This is different relative to undifferentiated circular nuclei as well as nuclei portrayed by other innate immune cells. Previous research has reported that HL-60 cells treated with ATRA demonstrate different stages of nuclear transformation into multi-lobular segmented nuclei specifically observed in neutrophils (Olins et al., 2000; Veselská et al., 2003; Olins & Olins, 2004).

Additionally, neutrophils produce ROS when interacting with invading microbes through the NADPH oxidase complex. The NADPH oxidase complex is made up of a group of proteins that serve as markers for neutrophilic differentiation in HL-60 cells due to the upregulation observed in mature neutrophils relative to undifferentiated, immature promyeloid cells (Vinnai et al., 2017; Dakik et al., 2021). The main protein subunits that make up the NADPH oxidase include neutrophil cytosol factors 1 (NCF1/NOXO2) and 2 (NCF2/NOXA2), and cytochrome B subunits α (CYBA/P22-PHOX) and β (CYBB/NOX2) (Sumimoto, 2008; Belambri at al., 2018). Additionally, previous research has shown that activation of transcription factors such as C/EBPα/β and PU.1 allow for the transcription of *NCF1/2* as well as other surface markers like CD11b (Tasseff et al., 2017).

Previous research with DMSO-treated HL-60 cells reported that undifferentiated cells

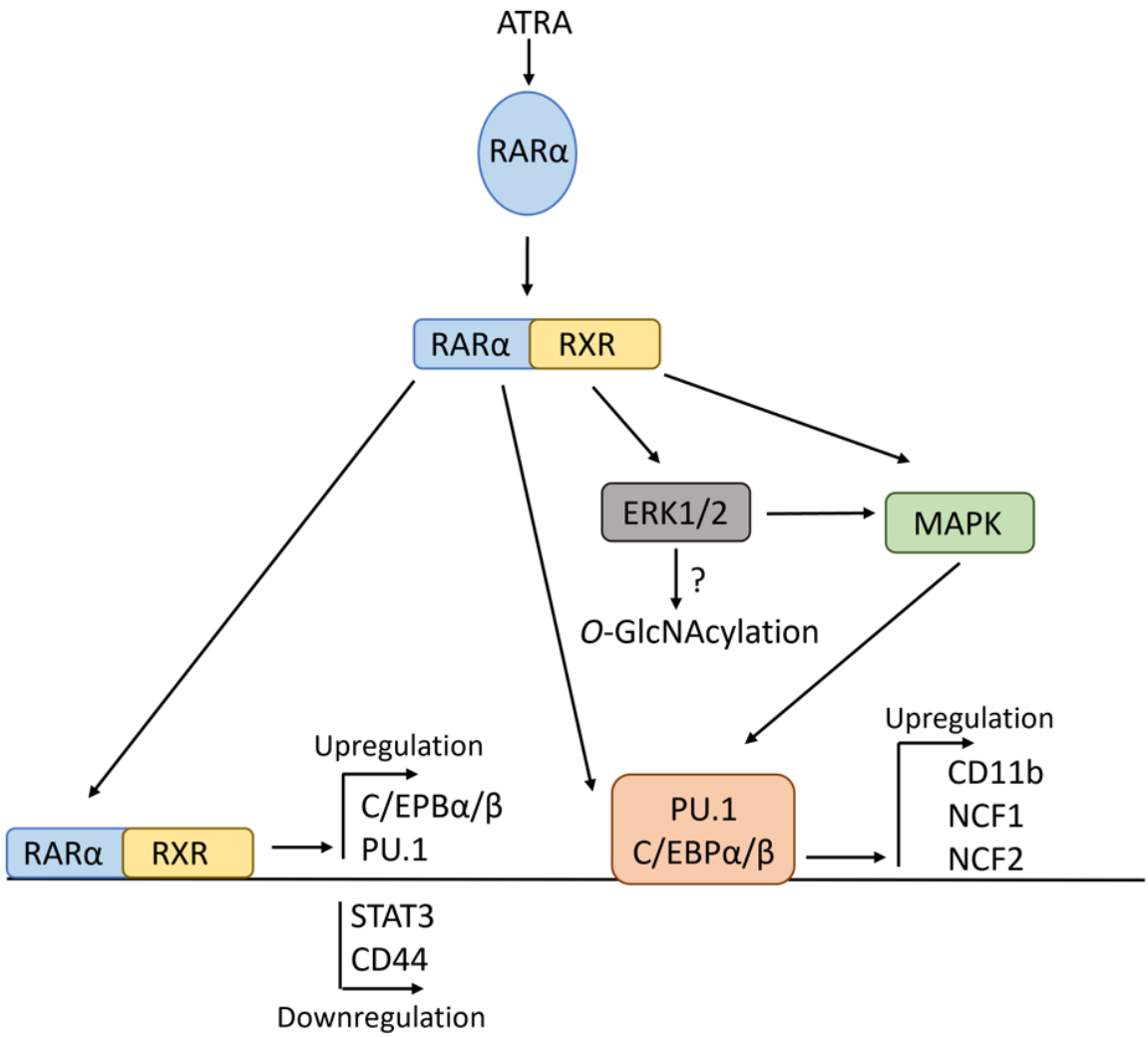

Figure 2: Schematic of ATRA-induced differentiation in HL-60 cells.

Binding of ATRA to RARα results in activation and formation of the RARα-RXR complex. Activation of the RARα-RXR complex leads to downregulation of STAT3 and CD44, and upregulation in PU.1 and C/EBPα/β. Additionally, ATRA activation results in activation of both ERK1/2 and MAPK pathway. ERK1/2 activation also plays a role in the global *O*-GlcNAcylation status of cells. MAPK pathway activation results in PU.1 and C/EBPα/β binding to promoter regions of neutrophil differentiation markers CD11b, NCF1 and NCF2. This figure was adapted from Tasseff et al. (2017).

contain higher levels of *O*-GlcNAcylation relative to differentiation HL-60 cells (Sherazi et al., 2018). Prior investigations with *O*-GlcNAcylation and cancer demonstrated that stem-like cancerous cells also have elevated levels of this cellular protein modification (Sherazi et al., 2018; Akella et al., 2020) *O*-GlcNAcylation is a post-translational modification where an *O*-linked β-N-acetyl-D-glucosamine (*O*-GlcNAc) sugar moiety is added onto the hydroxyl groups of serine and threonine residues of proteins (Yang et al., 2001; Ferrer et al., 2014; Yang & Qian, 2017; Asthana et al., 2018). This protein modification is performed by two enzymes: *O*-GlcNAc transferase (OGT) and *O*-GlcNAcase (OGA). OGT catalyzes the addition of the GlcNAc sugar moiety onto hydroxyl groups through cleavage of the donor substrate uridine diphosphate N-acetylglucosamine (UDP-GlcNAc). OGA catalyzes the removal of the GlcNAc sugar moiety (Yang et al., 2001; Ferrer et al., 2014; Yang & Qian, 2017; Asthana et al., 2018). To obtain the UDP-GlcNAc, cellular respiration needs to occur to obtain fructose-6-phosphate. This sugar is used for the hexosamine biosynthetic pathway converting fructose-6-phosphate into glucosamine-6-phosphate by the enzyme glutamine fructose-6-phosphate aminotransferase (GFAT) (Asthana et al., 2018). The final product of the hexosamine biosynthetic pathway is UDP-GlcNAc (**Figure 3**). In cancerous cells, *O*-GlcNAcylation status is related to a variety of metabolism-sensing signaling pathways including MAPK, mTOR, AMPK, ERK1/2, and STAT3 due to the *O*-GlcNAcylation of these proteins (Moriwaki & Asahi, 2017; Chang et al., 2020; Wu et al., 2020).

1.4 Galectins

Galectins were first characterized in 1975 as soluble S-type lectins found in the electric eel *Electrophorus electricus* (Teichberg et al., 1975). To date, there have been 16 galectin genes discovered, with 12 being found in humans (Timoshenko, 2015). Galectins were first separated from other carbohydrate-binding proteins due to their ability to bind glycans in a calcium-independent manner (Robinson et al., 2019). Galectins have an affinity for β-galactosides through a conserved 130 amino acid sequence called the carbohydrate recognition domain (CRD) (Johannes et al., 2018). When found extracellularly, galectins have been reported to be involved in the activation of signal transduction pathways, cellular

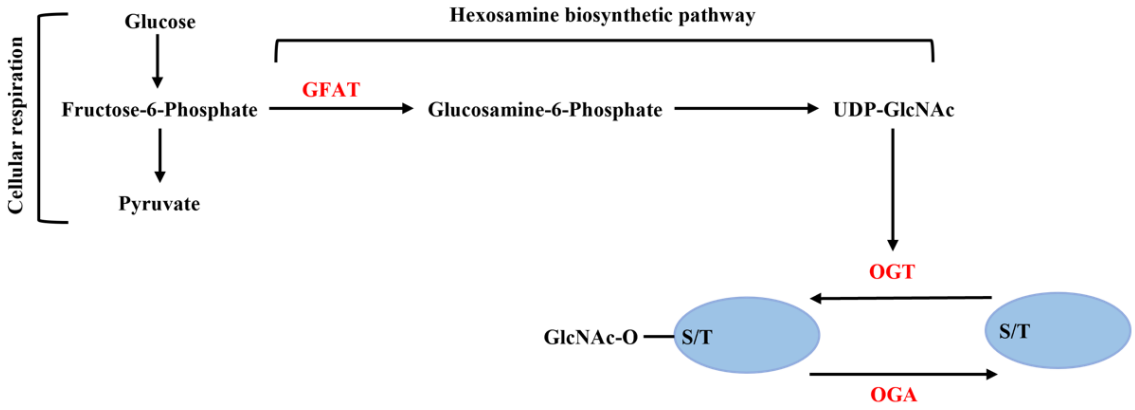

Figure 3: *O*-GlcNAcylation: a post-translational protein modification.

To obtain UDP-GlcNAc, the cell needs to undergo cellular respiration as well as utilize the hexosamine biosynthetic pathway. The activity of the GFAT enzyme is the rate limiting step of this process when converting fructose-6-phosphate to glucosamine-6-phosphate. The resulting product, UDP-GlcNAc, is used to add the GlcNAc sugar moiety to the hydroxyl group of serine and threonine residues of proteins through the enzyme OGT. OGA catalyzes the reverse reaction to remove the GlcNAc sugar moiety. This figure is adapted from Fardini et al. (2013).

adhesion, and migration. When found intracellularly in the cytosol, galectins regulate signal transduction pathways, cellular apoptosis, proliferation, and differentiation. Additionally, nuclear localized galectins are involved with gene splicing and transcriptional activation (Johannes et al., 2018). Importantly, galectins often demonstrate different expression patterns in different cell lines or different tissue types (Liu & Rabinovich, 2010). Furthermore, both CRD-dependent and CRD-independent functions have been reported (Tazhitdinova & Timoshenko, 2020).

The CRD structure of galectins allows for the categorization of each protein into one of three categories: proto-type, tandem-repeat type, and chimeric galectins (**Figure 4**) (Yang et al., 2008). Proto-type galectins are characterized by having a single CRD region and include galectins -1, -2, -5, -7, -10, -11, -13, -14, and -16 (Timoshenko, 2015). This structure allows these galectins to exist as monomers or homodimers (Nishikawa & Suzuki, 2018). Tandem-repeat type galectins are characterized by having two different CRD regions found on either end of the protein connected by a non-CRD linker region (Yang et al., 2008). These galectins are larger than other galectins and include galectins -4, -8, -9, and -12 (Liu & Rabinovich, 2010). These galectins can be found as monomers, homodimers, and heterodimers (Sciacchitano et al., 2018). There is only one chimeric type galectin characterized to date, galectin-3. Galectin-3 was characterized as having one CRD region and a proline-rich N-terminal domain (Yang et al., 2008). The structure of galectin-3 allows for it to be found as a monomer, homodimer, N-type pentamer, or C-type pentamer (Nishikawa & Suzuki, 2018).

1.4.1 Galectins in HL-60 cells and AML

Previous research into galectins has documented their role in cancer progression and in adaptive immunity. However, little is known with respect to their roles in innate immune cell differentiation and in AML. AML is the most common type of leukemia in adults and previous RT-qPCR data has determined that there are 8 galectins expressed, including proto-type galectins -1, -7, and -10, tandem-repeat galectins -4, -8, -9, and -12, and chimeric galectin -3 (El Leithy et al., 2015; De Kouchkoveky & Abdul-Hay, 2016; Su, 2018). Previous RT-qPCR research also indicates that there are 6 galectins expressed in the HL-60 cell line including galectins -1, -3, -8, -9, -10, and -12 (Abedin et al., 2003;

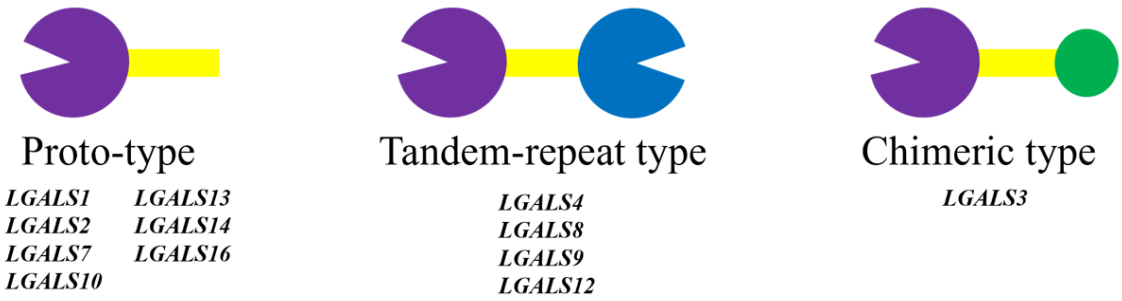

Figure 4: The CRD structure of galectins.

Galectins are classified based on their carbohydrate recognition domains (purple and blue), linker domain (yellow), and N-terminal domain (green). Proto-type galectins contain one CRD. Tandem-repeat type galectins contain two different CRDs (found on the C- and N-termini), connected by a linker peptide region. The chimeric type includes galectin-3 which contains one CRD domain and one N-terminal domain. This figure is adapted from Timoshenko (2015).

Timoshenko et al., 2016; Vinnai et al., 2017). Previous research with HL-60 cells has indicated that galectin gene expression and protein levels change during induced granulocytic differentiation (Abedin et al., 2003; Timoshenko et al., 2016; Vinnai et al., 2017; Vakhrusnev et al., 2018). Additionally, it has also been reported that galectins play a variety of roles in neutrophil function *in vitro* and *in vivo* (Abedin et al., 2003; Liu & Rabinovich, 2009; Robinson et al., 2019). HL-60 cells provide a good model to investigate the effects of galectins during granulocytic differentiation of HL-60 cells with relation to the M2 and M3 molecular subtypes of AML.

1.4.2 Proto-type galectins and cellular differentiation

1.4.2.1 Galectin-1

Galectin-1 was the first galectin to be identified and has been extensively investigated due to its role in cellular differentiation, cancer progression, and immune cell function. Galectin-1 is a proto-type galectin that promotes the differentiation of early hematopoietic stem cells (HSCs), trophoblast stem cells, muscle cells and many others (Vas et al., 2005; Chan et al., 2009; Tang et al., 2018). However, the direct role of galectin-1 in granulocytic differentiation of HL-60 cells has not been examined. The expression of galectin-1 in undifferentiated HL-60 cells is well documented. However, depending on the stimuli used, galectin-1 expression varies in neutrophil-like differentiated cells (Abedin et al., 2003; Timoshenko et al., 2016; Vinnai et al., 2017; Vakhrusnev et al., 2018). There are two stimuli that can be used for induced granulocyte differentiation of HL-60 cells: dimethyl sulfide (DMSO) and all-*trans* retinoic acid (ATRA). DMSO-induced differentiated cells exhibit constant expression of galectin-1 (Abedin et al., 2003; Timoshenko et al., 2016; Vinnia et al., 2017), whereas ATRA- induced differentiated cells exhibit a downregulation in galectin-1 (Vakhrusnev et al., 2018).

Although the expression of galectin-1 has been reported to vary, there are known effects elicited by galectin-1 on neutrophil function in innate immunity. Galectin-1 was reported to be involved with the migration of neutrophils in anti-inflammatory states through the p38/MAPK and PKC pathway. Additionally, galectin-1 has also been reported to activate the nicotinamide adenine dinucleotide phosphate (NADPH) oxidase in primed neutrophils

(Almkvist et al., 2002; Auvynet et al., 2013). Previous studies into galectin-1 have also reported induced lysosome release, degranulation, and neutrophil extravasation (Almkvist et al., 2002; Elola et al., 2005; Ashraf et al., 2018).

Galectin-1 has also been investigated with respect to its role in adaptive immunity. Galectin-1 was reported to be a suppressor of adaptive immunity through the regulation of T cell development. Studies have shown that galectin-1 impacts effector T cell viability through induced apoptotic death, altered cytokine production, and increased survival of naïve T cells (Teichberg et al., 1975; Levi et al., 1983; Perillo et al., 1995; van der Leij et al., 2004). Studies have also reported that galectin-1 in plasma cells enhances antibody production, B cell development and survival, as well as plasma cell differentiation (Rossi et al., 2006; Tsai et al., 2008; Espeli et al., 2009; Anginot et al., 2013).

In AML, galectin-1 has been reported to be a pro-survival molecule by RAS activation intracellularly, activating the MAPK pathway through P13K/AKT signaling for continued cell proliferation (Ruvolo, 2019). Galectin-1 has also been reported to degrade p53 to further enhance cell survival while also preventing the migration of HSCs in a cancerous state (Ruvolo, 2019; Ruvolo et al., 2020).

1.4.2.2 Galectin-7 and -10

Galectin-7 is a proto-type galectin that is not well documented with respect to its role in granulocytic differentiation or neutrophil function. Previous research with HL-60 cells has revealed no expression of galectin-7 in this model (Abedin et al., 2003). However, in breast cancer cells, galectin-7 allows for cancer progression by impairing p53 function (Wang et al., 2018). Additionally, in colorectal cancer and sunburnt keratinocytes, galectin-7 exhibits p53 induced apoptosis, which indicates that galectin-7 is a pro-apoptotic protein (Polyak et al., 1997; Bernerd et al., 1999).

Galectin-10 is the last proto-type galectin found in HL-60 cells and was originally referred to as Charcot-Leyden crystal protein. It was initially defined as part of the lysophopholipase family in 1853 due to lysophospholipase binding (Su, 2018). Once the Charcot-Leyden crystal protein gene was sequenced and a crystalized structure obtained,

it became apparent that it resembled the secondary structures of the CRD of galectins, contained no lysophospholipase activity and was promptly renamed (Mastrianni et al., 1992; Ackerman et al., 1993; Leffler et al., 2002).

Previous research with HL-60 cells has demonstrated that cells induced to differentiate with DMSO have upregulated galectin-10 (Abedin et al., 2003; Timoshenko et al., 2016; Vinnai et al., 2017). Furthermore, Kubach et al. (2007) reported that galectin-10 had an important role in the suppressed function of T regulatory cells. Additionally, accumulated galectin-10 crystals in allergic reactions and in parasitic infections is associated with hypereosinophilia (Ackeman et al., 1993). It was then proposed that galectin-10 had a regulatory role in eosinophil function (Arthur et al., 2014). To date, both galectin-7 and galectin-10 have had no investigations to their relations to AML.

1.4.3 Chimeric type galectin-3 and cellular differentiation

Galectin-3 is the only chimeric galectin known to date and has been studied nearly as much as galectin-1. Galectin-3 has demonstrated roles in immune cell function and cancer progression. It is well documented that HL-60 cells express galectin-3, and that galectin-3 expression is upregulated during DMSO-induced granulocytic differentiation (Abedin et al., 2003; Timoshenko et al., 2016; Vinnai et al., 2017). Neutrophils also have elevated levels of galectin-3 (Robinson et al., 2019). Galectin-3 is found in circulation (20-313 ng/mL) which results in the activation of various immune cell functions (Iurisci et al., 2000). Furthermore, it is often found at elevated levels in cancerous conditions (Iurisci et al., 2000; Eliaz, 2013). Secreted galectin-3 has been reported to interact with immunoglobin E (IgE) and the IgE receptor, which activates the NADPH-oxidase complex in neutrophils during pro-inflammatory responses and when exposed to gram-negative bacteria (Sundqvist et al., 2018; Robinson et al., 2019). Additionally, galectin-3 signaling through carcinoembryonic antigen related cell adhesion molecules (CD66a and CD66b) also results in the production of reactive oxygen species (ROS) (Robinson et al., 2019). Galectin-3 has also been reported to be involved with neutrophil response to infection by *Candida albicans*, *Streptococcus pneumoniae*, and *Aspergillus fumigatus* by extravasation., recruitment, and ROS production (Nieminen et al., 2008; Wu et al., 2017; Snarr et al., 2020). Additionally, inhibition of galectin-3 results in a reduction in various

cytokine and chemokine levels, as well as decreased neutrophil accumulation. This indicates that galectin-3 facilitates neutrophil extravasation (Pan et al., 2018).

Galectin-3 has also been shown to be involved in other immune system functions. Previous studies have reported that galectin-3 elicited increased calcium flux to induce apoptosis and decrease interleukin 5 secretion in T cells. This affected T cell viability, activation, and differentiation (Cortegano et al., 1998; Stowell et al., 2008). Additionally, Acosta-Rodrígues et al. (2004) reported that galectin-3 elicited interleukin 4induced T cell differentiation and survival.

Previous research with galectin-3 has revealed relationships to AML prognosis, subtype identification, and patient age (Cheng et al., 2013). When looking at the AML microenvironment, mesenchymal stromal cells (MSCs) had elevated level of galectin-3 protein positively correlated with the expression of MYC, β-catenin, and AKT2. Suppression of galectin-3 also results in a reduction of MYC expression (Ruvolo et al., 2018). Galectin-3 also exhibits inhibitor effects on immune cell surveillance through MSCs binding of CD45 and T cell receptors, suppressing T cell function (Ruvolo, 2016). When looking at the microenvironment of acute leukemia cells, galectin-3 also enabled drug-resistance through the Wnt/β-catenin pathway (Hu et al., 2015). Galectin-3 also has activity in mitosis through its binding with the nuclear mitotic apparatus protein (NuMa) during daughter cell DNA separation (Magescas et al., 2017).

1.4.4 Tandem-repeat type galectins and cellular differentiation

1.4.4.1 Galectin-4 and -8

Galectin-4 is a tandem-repeat galectin often associated with intestinal inflammation that is not as well documented in the regulation of neutrophils (Timoshenko, 2015). Previous research with HL-60 cells indicates no expression of galectin-4 in undifferentiated or differentiated cells (Abedin et al., 2003). However, galectin-4 is proposed to play a role in the oxidative burst of neutrophils (Huflejt & Leffler, 2004). Additionally, galectin-4 exhibited pro-inflammatory activity by inducing interleukin6 production and CD4+ T cells activation (Hokama et al., 2004). To date, little is known to the role of galectin-4 in AML, with its expression being upregulated in younger AML patients (El Leithy et al., 2015).

Galectin-8 is another tandem-repeat type galectin that demonstrates constant, unchanged gene expression in HL-60 cells during DMSO-induced granulocytic differentiation (Abedin et al., 2003; Timoshenko et al., 2016; Vinnai et al., 2017). Galectin-8 has been reported to stimulate ROS production in neutrophils through binding of its CRD C-terminal domain to integrin-αM (Nishi et al., 2003). Galectin-8 also aids in neutrophil adhesion to endothelial cells through integrin-αM, indicating that galectin-8 has a role in regulating neutrophil extravasation (Yamamoto et al., 2008; Liu & Rabinovish, 2010). Additionally, thrombin mediated cleavage of galectin-8 nullifies neutrophil adhesion during the inflammatory response (Esmon et al., 2005).

The role of galectin-8 in adaptive immunity is better understood. T cell proliferation and apoptosis of activated T cells has been reported to be induced by galectin-8 (Norambuena et al., 2009; Tribulatti et al., 2012). Tsai et al. (2011) also reported that galectin-8 plays a role in B cell differentiation, with knockdown inhibition resulting in inhibited plasma cell differentiation and decreased antibody production.

Galectin-8 has been detected in patients with AML. However, the role of galectin-8 in AML has not been elaborated upon (El Leithy et al., 2015). In colon cancer, galectin-8 has been observed to have lower concentrations when compared to healthy cells, (Nagy et al., 2002). Additionally, elevated levels of galectin-8 serve as an enhancer for cancer progression in prostate and breast cancer (Genetilini et al., 2017; Trebo et al., 2020).

1.4.4.2 Galectin-9 and -12

Galectin-9 is a tandem-repeat type galectin that is expressed in HL-60 cells. Previous research with HL-60 cells indicates that galectin-9 expression is constant during DMSO-induced granulocytic differentiation (Abedin et al., 2003; Timoshenko et al., 2016; Vinnai et al., 2017). Galectin-9 has been reported to be involved with neutrophil degranulation and ROS production by binding to T-cell immunoglobin domain and mucin domain 3 (Tim-3) (Vega-Carrascal et al., 2014; Steichen et al., 2015; Robinson et al., 2019). Furthermore, galectin-9 binding to Tim-3 resulted in IL-8 production, regulating neutrophil recruitment (Vega-Carrascal et al., 2011; Hirao et al., 2015). Additionally, surface galectin-9 was highly expressed in the neutrophils of healthy individuals and was

downregulated once neutrophils were activated (Dunsmore et al., 2021). Furthermore, investigation into adaptive immunity has shown that galectin-9 regulates T cell viability through apoptosis in a Tim-3 dependent manner (Kashio et al., 2003; Zhu et al., 2005).

Interest into the role of galectin-9 in AML stems from to its interaction with Tim-3. Previous research revealed that the activation of Tim-3 by galectin-9 allows for cancer progression through evasion from the immune system. Additionally, activation of protein kinase C and the mTOR pathway allows for increased expression and secretion of Tim-3 and galectin-9 resulting in the apoptosis of natural killer cells, decreased T cell activating cytokine interleukin 2, and a reduction in T cell viability through apoptosis (Gonçalves Silva et al., 2017). Furthermore, the blocking of galectin-9 binding to Tim-3 in AML prevented the reconstitution, self-renewal, and leukemic burden in a mouse transplant model (Kikushige et al., 2015)

Galectin-12 is another tandem-repeat type galectin that is located primarily in adipocytes and leukocytes (Yang et al., 2001). Previous research has reported that galectin-12 is expressed in HL-60 cells and is downregulated upon DMSO-induced granulocyte differentiation (Vinnai et al., 2017). High levels of galectin-12 increased adipocyte differentiation and played a critical role in lipolysis adipocyte signaling (Yang et al., 2004). In ATRA-induced differentiated NB4 cells, knockdowns of galectin-12 resulted in enhanced neutrophilic differentiation and high production of ROS (Xue et al., 2016). In AML, Zheng et al. (2019) demonstrated that galectin-12 gene expression is upregulated in the M3 subtype. Helbawi et al. (2021) also reported that the methylation status of the galectin-12 gene was related to patient outlook.

1.5 Overarching hypothesis and objectives

Galectins have been extensively investigated with respect to their roles in cellular differentiation, immune cell functions, and cancer progression. However, little is known with respect to the role of galectins in the differentiation of myeloid cells and AML. Previous research has shown that there are changes in galectin gene expression during DMSO and ATRA induced granulocytic differentiation of HL-60 cells. When looking at the galectins expressed in HL-60 cells, DMSO and ATRA induced differentiation resulted

in an upregulation of galectin-3 and -10, and a downregulation of galectin-1 and -12 depending on the stimuli used. Galectin-8 and galectin-9 have shown constant expression during differentiation of HL-60 cells (Abedin et al., 2003; Timoshenko et al., 2016; Vinnai et al., 2017). Furthermore, little is understood with respect to galectin gene changes in AML cells relative to healthy bone marrow cells, and the relationships galectins have with the differentiation of innate immune cells.

For these reasons, I tested the hypothesis that galectins are essential regulators of neutrophilic differentiation of promyelocytic HL-60 cells and define phenotypic differences between subtypes of acute myeloid leukemia. The rationale behind this study is that galectins demonstrate variable expression patterns during DMSO and ATRA induced granulocytic differentiation of HL-60 cells. By using recombinant galectins and galectin inhibitors (OTX008, GB1107, thiodigalactoside), I assessed the role of galectins in neutrophilic differentiation in the absence and presence of ATRA. Additionally, an *in silico* analysis of AML TCGA cohorts allowed for the assessment of galectin gene expression profiles in AML FAB subtypes for diagnostic and prognostic purposes.

Objective 1: To evaluate the effects of proto-type, chimeric-type, and tandem-repeat type recombinant galectins on markers of neutrophilic differentiation of the HL-60 cell line in comparison to ATRA-induced responses.

Objective 2: To examine the effects of CRD and non-CRD specific inhibition of galectin-1 and galectin-3 on markers of neutrophilic differentiation of the HL-60 cell line in comparison to ATRA-induced responses.

Objective 3: To perform an *in silico* analysis on galectin gene expression from the Cancer Genome Atlas AML patient samples for new FAB subtype diagnostics, prognosis, and to evaluate changes in the glycobiological landscape.

Chapter 2

2 Materials and Methods

2.1 Chemicals and solutions

Dulbecco's Phosphate Buffer Saline (DPBS) without calcium and magnesium (311-424-CL), Iscove's Modification of Dulbecco's Modifed Eagle Medium (IMDM) (319-105-CL), and 100x ITS Universal Culture Supplements (315-081-QL) were purchased from Wisent Bio Products (Saint-Jean-Baptiste, QC). Fetal Bovine Serum (FBS) (12484-028), and SYBR™ Safe DNA Gel Stain (s33102) were purchased from ThemoFisher (Mississauga, ON). All-*trans*-retinoic acid (ATRA) (R2625), dimethyl sulfide (DMSO) (D26500), and Immobilon Classico Western HRP substrate (WBLUC500) were purchased from Sigma-Aldrich Canada (Oakville, ON). Recombinant human galectin-1 animal-free protein (NBP2-76255-50ug), recombinant human galectin-3 protein (NBP2-34881-50ug), and recombinant human galectin-8 protein (NBP1-48335-0.05mg) were purchased from Bio-Techne (Kanata, ON). Recombinant human galectin-9 protein (2045-GA) was purchased from R&D Systems (Oakville, ON). GB1107 (HY-114409), and OTX008 (HY-19756) were kindly provided from MedChemExpress (Burlington, ON). Thiodigalactoside (TDG) (OG05033) was purchased from Carbosynth Ltd (San Diego, CA). Brefeldin A (11861) was purchased from Cayman Chemicals (Ann Arbor, MI). Bovine serum albumin (BSA) (AD0023), mammalian Protease Inhibitor Cocktail (BS386), sodium azide (NaN_3) (S2002), (AD0023), sodium orthovanadate (Na_3VO_4) (SB0869), and 2x RIPA Buffer IIII with EDTA and EGTA (pH 7.4) (RB4477) were purchased from BioBasic (Markham, ON). Non-fat dry milk blotting-grade blocker (1706404), and SsoAdvanced Universal SYBR® Green Supermix (1725274) were purchased from Bio-Rad (Mississauga, ON). TRIzol® (15596018) was purchased from Life Technologies (Toronto, ON). VECTASHIELD Vibrance Mounting Medium with DAPI (H-1800) was purchased from Vector Laboratories (Burlingame, CA). Froggarose LE Molecular Biology Grade Agarose (A87) was purchased from FroggaBio (Concord, ON).

2.2 Cell culture and treatments

Cell culture – Human acute promyelocytic leukemia HL-60 (ATCC® CCL-240™) cells were cultured in suspension with IMDM without antibiotics and sub-cultured to maintain a cell concentration under 1 x 10^6 cells/mL in either Ø60 mm (82.1194.500) or Ø100 mm suspension culture dishes (83.3902.500) from SARSTEDT and grown in a humidified incubator at 37°C with 5% CO_2. IMDM media was supplemented with 1% ITS (5 µg/mL human insulin, 5 µg/mL human transferrin, 5 ng/L selenous acid) (IMDM-ITS) or 10% FBS (IMDM-FBS). Cell viability was determined using the trypan blue (0.4%) exclusion test and was not less than 90%.

Treatment of HL-60 cells with all-trans retinoic acid – Cells concentrated at 4 x 10^5 – 5 x 10^5 cells/mL in IMDM-ITS were grown in either Ø60 mm or Ø35 mm (80.1135.500) suspension culture dishes, 6 well (83.3920.500) plates, 42 well (83.3922.500) plates or 48 well plates (83.3923.500) from SARSTEDT and treated with 1 µM ATRA for 72 h as described by Gupta et al. (2014) to induce neutrophil-like differentiation.

Treatment of HL-60 cells with recombinant galectins – Cells in IMDM-ITS were treated with 10 ng/mL, 100 ng/mL and 1000 ng/mL of human recombinant galectin-1, -3, -8 or -9 to determine a dose-dependent effects in the presence or absence of ATRA. Cells treated with recombinant galectins were plated at a cell concentration of 1 x 10^5 cells/mL, and cells treated with recombinant galectins + ATRA were treated at a cell concentration of 4 x10^5 cells/mL. Cells were also treated with 1000 ng/mL of human recombinant galectin-1, -3, -8 or -9 daily every 24 h in the presence or absence of ATRA. Cells were also treated with combinations of 500 ng/mL of human recombinant galectin-1, -3 and/or -8. Cells that were daily supplemented with recombinant galectins were plated at a concentration of 3 x 10^5 cells/mL, and ATRA treated cells daily supplemented with recombinant galectins were plated at a concentration of 6 x 10^5 cells/mL. Cells were grown in Ø35 mm suspension culture dishes, 6 well plates, 42 well plates or 48 well plates from SARSTEDT. All recombinant galectin treatments were over 72 h, and cells grown in a humidified incubator at 37°C with 5% CO_2.

Treatment of HL-60 cells with CRD and non-CRD inhibitors – Cells in IMDM-ITS were treated with 5 µM OTX08 (K_d = 30 µM) galectin-1 inhibitor, 2 µM GB1107 (K_d = 37 nM) (Vuong et al., 2019) galectin-3 inhibitor, or 100 µM TDG broad galectin-1 (K_d = 24 µM) and -3 (K_d = 48 µM) (van Hattum et al., 2013) inhibitor daily for 72 h. Inhibitor treatment cells were plated at a concentration of 2.5 x 10^5 cells/mL, and inhibitor + ATRA treated cells were plated at a concentration of 5 x 10^5 cells/mL. Cells were grown in Ø60 mm suspension culture dishes from SARSTEDT and in humidified conditions at 37°C with 5% CO_2.

Treatment of HL-60 cells with brefeldin A – Cells in IDMD-ITS were plated at a concentration of 4 x 10^5 cells/mL in Ø35 mm suspension culture dishes from SARSTEDT. Cells were treated with 1 µM brefeldin A for 24 h in a humidified incubator at 37°C with 5% CO_2.

2.3 Nuclear staining and fluorescence microscopy

To prepare HL-60 cells for nuclear staining, cell concentrations and viability were determined using hemocytometer and trypan blue (0.4%) exclusion test. Cells were diluted to 3 x 10^5 – 5 x 10^5 cells/mL with DPBS and 200 µL of cells were centrifuged onto glass slides for 5 min at 500 rpm using the Shandon Cytospin 2 centrifuge. Cells were stained with 4',6-diamidino-2-phenylindole (DAPI)-contained VECTASHIELD Vibrance Mounting Medium. An AxioImager A1 fluorescent microscope (Carl Zeiss) with DAPI filter cube was used to view slides. Images of cells were captured using a high-resolution monochrome XCD-X700 CCD camera (Sony Corporation) while using the Northern Eclipse 8.0 software from Empix Imaging (Mississauga, ON). Images of cells were used to calculate differentiation and apoptotic indices based on nuclear morphology.

2.4 RNA isolation, cDNA synthesis, RT end-point PCR, and RT-qPCR gene expression

Total mRNA isolation and cDNA synthesis – HL-60 cells were centrifuged for 5 min at 300 x g and washed once with ice-cold DPBS. Total mRNA was isolated from cell pellets using the TRIzol ® method according to manufacturer's protocol. The mRNA samples were resuspended in sterile nuclease-free water and the Thermo Scientific™ Nanodrop

2000c UV-Vis spectrophotometer was used to determine the $A_{260/280}$ ratio with a threshold of >1.8. cDNA was synthesized from mRNA (200 ng – 1 µg) using the High-Capacity cDNA reverse transcription Kit from Applied Biosystems (4368813) following the manufacturer's protocol.

Reverse transcription real-time and end-point polymerase chain reaction – All primers for reverse transcription real-time polymerase chain reaction (RT-qPCR) assays were synthesized by BioCorp UWO OligoFactory (Western University, ON) and verified by BLAST (Table S1). End-point PCR amplification was performed using the T100 Thermo Cycler (Bio-Rad) in 20 µL (1 µM forward primer, 1 µM reverse primer, 1 µL cDNA) reactions using the 2X Taq FroggaMix (FroggaBio) (FBTAQM). PCR amplicons were separated on a 2% agarose gel containing SYBR® Safe in TAE buffer (20 mM Tris, 40 mM Acetic Acid, 1.2 mM EDTA) and visualized using a Molecular Imager GelDoc XR+ (Bio-Rad) with Image Lab software V6.0 (Bio-Rad). The SsoAdvanced Universal SYBR® Green supermix was used for RT-qPCR amplification of samples with 20 µL (1 µM forward primer, 1 µM reverse primer, and1 µL cDNA) volumes. The CFX Connect™ Real-Time PCR Detection System from Bio-Rad was used to quantify mRNA transcripts by a 2 min at 95°C polymerase activation, followed by a 2-step cycling regime of 40 cycles of denaturation (5 s, 95°C) and annealing (25 s, 60 - 62°C) (**Table S1**). Relative transcript levels were calculated using the Livak method ($2^{-\Delta\Delta CT}$) with β-actin (*ACTB*) as a reference gene.

2.5 Protein isolation and immunodot blot

Protein isolation – HL-60 cells were centrifuged for 5 min at 300 x g and washed twice with ice-cold DPBS. Cell pellets were lysed in 50-200 µL of 1X RIPA buffer (50 mM Tris-HCl, pH 7.5, 0.1% sodium dodecyl sulfate, 0.5% w/v sodium deoxycholate. 5 mM EGTA and 150 mM NaCl) containing 100 µM Na_3VO_4, 1 µM 4-(2-aminoethyl)benzenesulfonyl fluoride hydrochloride, 100 µM phenylmethylsulfonyl fluoride, 1.4 µM E-64, 1 mM bestatin, 1 µM leupeptin, 1.5 µM pepstatin A, and 0.08 µM aprotinin then incubated on ice for 10 min. Cell lysates were centrifuged at 12,000 x g for 12 min at 4°C. Total protein concentrations were determined using the DC™ Protein

Assay Kit II (5000112) from Bio-Rad with BSA standards. Absorbances were measured at 655 nm using a model 3550 Miscroplate Reader from Bio-Rad.

Immunodot blot – Nitrocellulose membranes (0.22 mm pore size) from GE Healthcare (16060006) were prewetted in Tris-buffer saline (TBS) (20 mM Tris-HCl, pH 7.5, 150 mM NaCl) and then placed on a Bio-Dot® Microfiltration apparatus from Bio-Rad as described by Sherazi et al. (2018). Each well was loaded with 200 mL of total protein extract (5-12.5 µg/mL in DPBS) and immobilized by gravity filtration for 2 h. Membranes were blocked with a 3% non-fat dry milk solution in TBST buffer (TBS and 0.05% Tween 20) for 60 min at room temperature. Membranes were washed three times with TBST and incubated overnight at 4°C with 1:1,000 *O*-GlcNAc (RL2) mouse monoclonal antibody from ThermoFisher (MA1-072) in TBST containing 5% BSA and 0.05% sodium azide. Membranes were washed three times with TBST and then incubated with 1:10,000 goat anti-mouse polyclonal IgG-HRP conjugated from ThermoFisher (A16066) in TBST containing 5% non-fat dry milk solution for 1.5 h at room temperature. Membranes were visualized using 2 mL of Immobilon Classico chemiluminescent reagent from Sigma-Aldrich (WBLUC0500) as well as the ChemiDoc XRS system with Quantity One Software V4.6.6.

2.6 Retrieval and RUVg normalization of AML and BM samples

Genes of interest – Various galectin genes (galectin-1 (*LGASL1),* galectin-3 (*LGALS3*), galectin-4 (*LGALS4*), galectin-8 (*LAGLS8*), galectin-9 (*LGALS9*), galectin-10 (*CLC*), and galectin-12 (*LGALS12*)) were investigated and compared to different marker genes (neutrophil cytosolic factor 1 and 2 (*NCF1/2*), and cytochrome B α and β (CYBA/B), *O*-GlcNAc cycle enzymes (*O*-GlcNAcase (*OGA*), *O*-GlcNAc transferase (*OGT*), and glutamine fructose-6-phosphate aminotransferase (*GFAT1*)), and cell stemness marker genes (octamer-binding protein 4 (*OCT4*), nanog homeobox (*NANOG*), RNA binding Fox-1 homolog 2 (*FOX2*), proto-oncogene (*C-MYC*), Kruppel like factor 4 (*KLF4*), and CD34 molecule (*CD34*)).

Retrieval of acute myeloid leukemia patient RNA-Seq data – AML patient RNA-Seq by Expectation Maximization (RSEM) (n=160) data for from The Cancer Genome Atlas (TCGA) for survival curve analysis was extracted from cBioPortal for cancer genomic (https://cbioportal.org/) platform and converted to a $\log_2$ scale in Microsoft Office Excel prior to survival curve statistical analysis in GraphPad Prism (V8.01-9.01). Additional patient data were determined using TCGA biolinks R-package (https://bioconductor.org/) in R studios. TCGA AML raw RNA-Seq counts (n=126) and Genotype-Tissue Expression (GTEx) bone marrow raw RNA-Seq counts (n=70) were extracted from recount2 (https://jhubiostatistics.shinyapps.io/recount/) for differential expression analysis. Data were opened in R studios and TCGA Biolinks R package and Ensembl ID annotation package were used to determine AML subtype and gene names. Raw RNA-seq counts were filtered where genes with less than 5 reads between 2 samples were removed from the data sets. The filter raw RNA-seq data were then upper quartile normalized prior to RUVg normalization (Nellore et al., 2016; Collado-Torrse et al., 2017).

Removal of unwanted variation (RUVg) – Differential expression analysis between AML and GTEx was performed to identify 500 least differential expression empirical control genes for normalization. The RUVg normalization algorithm linear model of Log E [Y| W, X, O] = Wα + Xβ + O was used where, Y represents the observed matrix of gene-level counts, W represents the contribution of each factor of unwanted variation to each sample, α represents the contribution of each factor of unwanted variation to each gene, X represents the observed matrix stating treatment/condition status, β represents the observed matrix of treatment/condition effect each gene and O represents the offsets that occur due to upper quartile normalization. With the assumption that for some genes β = 0, the final algorithm used was Log E [Y| W, X, O] = Wα + O (Risso et al., 2014). RUVg normalized data were transferred into Microsoft Office Excel and $\log_2$ transformed prior to statistical analysis in GraphPad Prism (V8.01-9.01).

2.7 *In silico* analysis

Determination of the distribution of data – D'Agostino & Pearson normality tests and Shapiro-Wilk normality tests were conducted prior to statistical analysis to determine the

distribution of the data. Based on the results of the normality tests, non-parametric analysis was conducted for all statistical tests.

Differential expression analysis – For comparison between normal bone marrow samples and all cohorts of AML data, non-parametric Mann-Whitney U test was performed to determine corresponding P-values. For comparison between normal bone marrow samples and FAB subtype classification of M0-M5 AML, non-parametric Kruskal-Wallis test with Dunn's multiple comparisons tests were performed to determine corresponding P-values. The data were presented as means ± SD and as violin plots. Log_2 fold changes (log_2FC) were calculated using mean log_2 normalized RNA-Seq data where a log_2FC of zero represents no change in gene expression with bone marrow serving as a normal control.

Correlation analysis – Pairwise, non-parametric Spearman's correlation analysis was performed in GraphPad Prism (V8.4.3) to determine corresponding correlation coefficient (ρ) and P-values in both bone marrow and AML cohorts. To determine significant differences in gene expression correlation patterns between bone marrow and AML cohorts, the comparing correlations (cocor) R package was used in R studios implementing Fisher's z-transformation of correlation coefficients for comparison between independent groups (Diedenhofen & Much, 2015). The data were presented in heat maps and comparison table.

Survival curve analysis – Survival curve analysis was conducted for all RSEM AML cohorts from cBioPortal as well as the FAB subtype classification M0-M5 for galectin gene and *O*-GlcNAc cycle related enzymes using the log-rank (Mantel-Cox) test.

2.8 Statistical Analysis

Unpaired Student's t-test, One-way ANOVA with Tukey's multiple comparison test, and Two-way ANOVA with Tukey's multiple comparison test were performed using GraphPad Prism V8.01 and V9.01 for Windows (GraphPad Software, La Jolla CA, www.graphpad.com). All experiments were performed using a minimum of three biological replicates. Data were presented as means ± SD and differences between means were considered significant at $p<0.05$.

Chapter 3

3 Results

3.1 The impact of galectins on differentiation of HL-60 cells

3.1.1 Hallmarks of all-*trans* retinoic acid-induced neutrophilic differentiation of HL-60 cells

Acute promyeloid leukemia HL-60 cells served as a model system to understand granulocyte differentiation in the context of AML. All-*trans* retinoic acid (ATRA) has been used in various studies and cell models for promyeloid cell induced differentiation into granulocytes. Previous research with HL-60 cells demonstrated that 1 µM ATRA induced high levels of granulocytic differentiation over 72 hours (Gupta et al., 2014). In this study, the degree of differentiation induced by ATRA in an HL-60 cell model was assessed. Nuclear morphology, neutrophil cytosolic factor 1 (*NCF1*) gene expression, and global *O*-GlcNAcylation are several characteristics that change due to stimuli induced differentiation of HL-60 cells (Olins & Olins, 2004; Vinnai et al., 2017; Sherazi et al., 2018).

Upon ATRA-induced differentiation, the nuclear morphology of HL-60 cells was examined using DAPI staining. Over 72 hours, untreated HL-60 cells exhibited circular morphology and ATRA-induced differentiated HL-60 cells exhibited multi-lobular, segmented nuclei (**Figure 5A**). Upon quantification, ATRA-induced HL-60 cells exhibited 87.4% (± 0.2%) segmented nuclei relative to untreated cells (2.4 ± 0.6%, $p<0.0001$) (**Figure 5B**). Vinnai et al. (2017) reported that DMSO-induced differentiated HL-60 cells had an upregulation in *NCF1* expression by RT-qPCR. In this study, ATRA-induced differentiated HL-60 cells also caused an upregulation in *NCF1* expression of 178.6-fold relative to untreated cells ($p<0.0001$) (**Figure 5C**). Sherazi et al. (2018) reported that DMSO-induced differentiation of HL-60 cells also caused a decrease in global *O*-GlcNAcylation by immunodot blot assay. In this study, ATRA-induced differentiated HL-60 cells also caused a decrease in global *O*-GlcNAcylation of 57% relative to untreated cells ($p<0.01$) (**Figure 5D**).

Figure 5: ATRA-induced granulocytic differentiation of HL-60 cells.

HL-60 cells were treated with 1 µM ATRA to induce granulocytic differentiation for 72 h. (A) HL-60 cell nuclear morphology visualized by DAPI stain demonstrated undifferentiation promyeloid cells (white arrow) and abnormal, multi-lobular granulocyte-like differentiated cells (red arrow), with example nuclei found in the top left corners. Scale bar represents 20 µm. (B) The differentiation index was determined as the percent of nuclei demonstrating segmented, multi-lobular granulocyte-like shape of 100 – 400 cells counted. (C) Granulocyte specific genes *NCF1* was quantified by RT-qPCR with the Livak Method ($2^{-\Delta\Delta Ct}$) using *ACTB* as an internal control. (D) *O*-GlcNAcylation was assessed by immunodot blot using the RL2 antibody. Data are presented as the mean ± SD, n=3. Significant differences were determined using unpaired Student's t-test. ***p<0.01*, *****p<0.0001*.

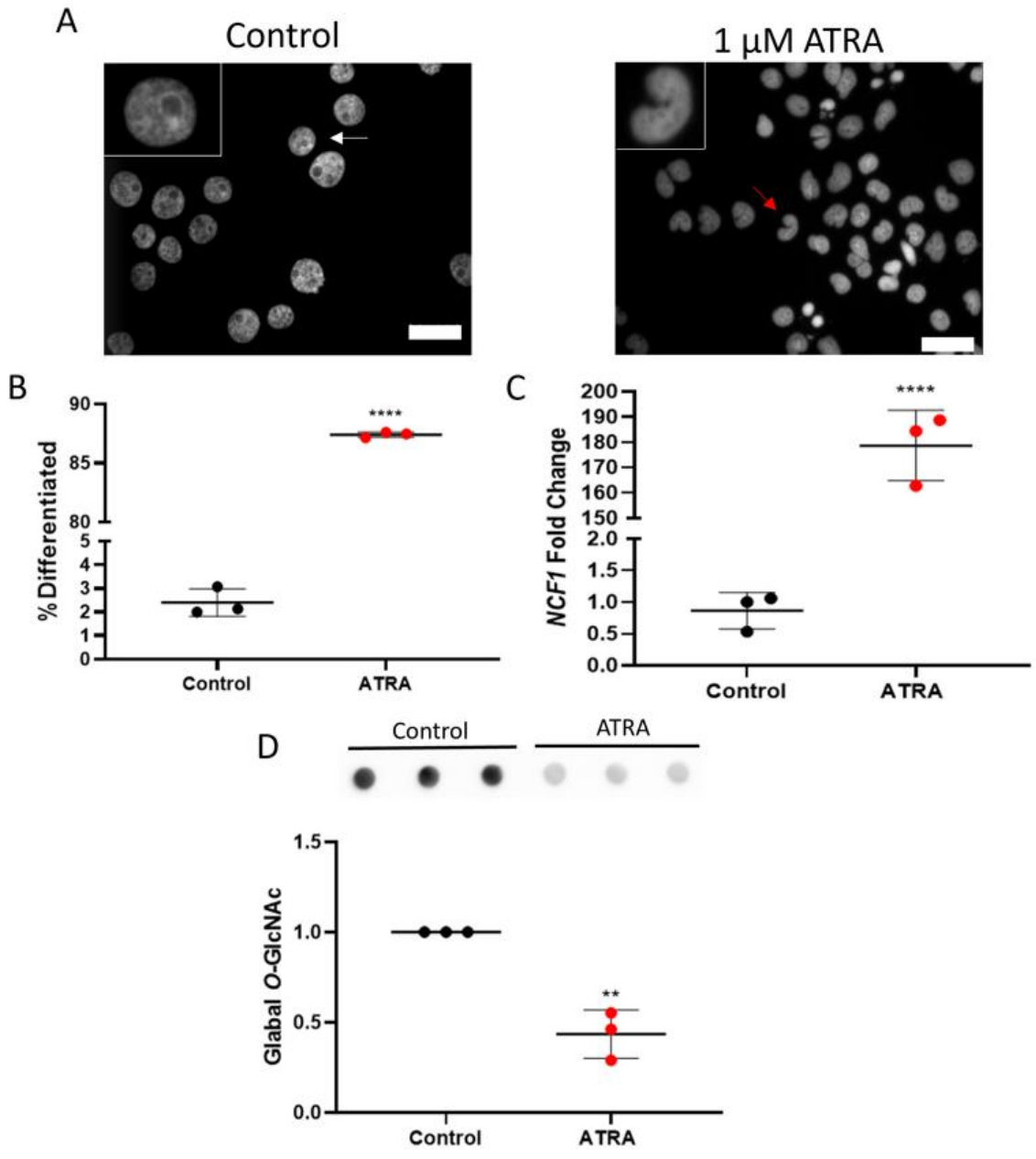
A
Control
1 μM ATRA
B
% Differentiated
90
85
80
5
4
3
2
1
0
****
Control
ATRA
C
NCF1 Fold Change
200
190
180
170
160
150
2.0
1.5
1.0
0.5
0.0
****
Control
ATRA
D
Control
ATRA
Glabal O-GlcNAc
1.5
1.0
0.5
0.0
**
Control
ATRA

3.1.2 The effects of proto-type recombinant galectin-1 and galectin-1 inhibitors on differentiation of HL-60 cells

Galectin-1 is one of the 6 galectins expressed in HL-60 cells that were previously investigated by Vinnai et al. (2017). However, the impact galectin-1 has on granulocytic differentiation of HL-60 cells is unknown. The dose-dependent effects of 10, 100 or 1000 ng/mL of human recombinant galectin-1 on HL-60 cells differentiation over 72 hours was assessed. Galectin-1 treated cells exhibited no significant changes in the percentage of segmented nuclei at all concentrations (3.5 ± 0.4, 3.0 ± 0.9, and 3.8 ± 1.3% respectively) relative to untreated cells (3.5±1.0 %) (**Figure 6A-B**). Galectin-1 dose-dependent treated cells also had no significant change in the regulation of *NCF1* at all concentrations (0.8-fold, 0.9-fold, and 1.3-fold, respectively) relative to untreated cells (**Figure 6D**). Additionally, HL-60 cells treated with 1000 ng/mL of recombinant galectin-1 had no significant decrease in global *O*-GlcNAcylation (16.6%) relative to untreated cells (**Figure 6F**).

To further evaluate the effects of recombinant galectin-1, daily supplementation with 1000 ng/mL for 72 hours was conducted. Daily supplementation with galectin-1 exhibited no significant change in the percentage of segmented nuclei (1.3 ± 0.6%) compared to untreated cells (1.1 ± 0.5%) (**Figure 7A-B**). Furthermore, there was no significant changes in the regulation of *NCF1* (2.7-fold) relative to untreated cells (**Figure 7D**). Global *O*-GlcNAcylation demonstrated no significant change (105.7%) when treated with 1000 ng/mL galectin-1 relative to untreated cells (**Figure 7E**).

Combination treatments with 1 µM ATRA were also conducted with dose-dependent (10, 100 and 1000 ng/mL) and daily supplementation (1000 ng/mL) of recombinant galectin-1. Dose-dependent treatments with galectin-1 + ATRA demonstrated no significant change in the percentage of segmented nuclei with 10 ng/mL (85.4 ± 2.5%). However, a significant increase was observed with 100 ng/mL (88.5 ± 1.9%, $p<0.01$) and 1000 ng/mL (86.4 ± 1.3%, $p<0.05$) in the percentage of segmented nuclei relative to ATRA treated cells (80.9 ± 1.9 %) (**Figure 6A, C**). Furthermore, there were no significant changes in the expression of *NCF1* with galectin-1 + ATRA treated cells at all concentrations (68.9-fold, 72.2-fold, and 94.1-fold, respectively) relative to ATRA treated cells (44.9-fold) (**Figure**

Figure 6: Dose-dependent effects of human recombinant galectin-1 on granulocytic differentiation of HL-60 cells.

HL-60 cells were treated with 10, 100, or 1000 ng/mL of galectin-1, with half the cells also being treated with 1 µM ATRA to induce granulocytic differentiation for 72 h. (A) Nuclear morphology of control and galectin-1 treated cells were visualized by DAPI staining with the scale bar representing 20 µM. The differentiation index was determined as the percentage of nuclei demonstrating multi-lobular granulocyte-like shape based on galectin-1 (130 – 205 cells counted) (B) and galectin-1+ATRA (150 – 360 cells counted) treatments (C). Granulocyte specific gene *NCF1* was quantified by RT-qPCR with the Livak Method ($2^{-\Delta\Delta Ct}$) using *ACTB* as an internal control for galectin-1 (D) and galectin-1+ATRA treatments (E). (F) *O*-GlcNAcylation was assessed by immunodot blot using the RL2 antibody when HL-60 cells were treated with 1000 ng/mL galectin-1 ± ATRA. Data are presented as mean ± SD, n=3-4. Significant differences were determined using One-way ANOVA and Two-way ANOVA followed by Tukey's HSD test and are represented as different letters with a $p<0.05$.

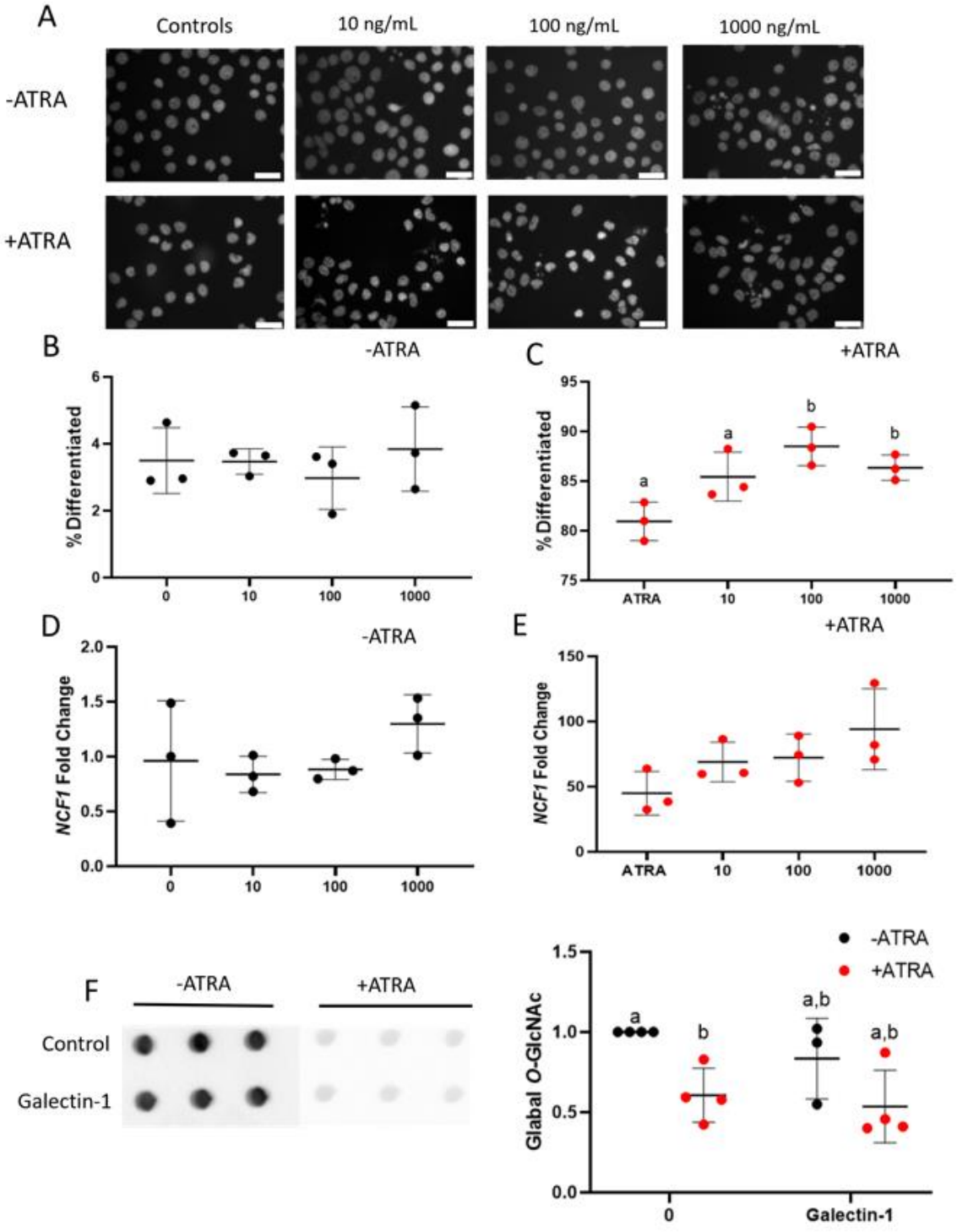
A
Controls
10 ng/mL
100 ng/mL
1000 ng/mL
-ATRA
+ATRA
B
-ATRA
% Differentiated
0
2
4
6
0
10
100
1000
C
+ATRA
% Differentiated
75
80
85
90
95
a
a
b
b
ATRA
10
100
1000
D
-ATRA
NCF1 Fold Change
0.0
0.5
1.0
1.5
2.0
0
10
100
1000
E
+ATRA
NCF1 Fold Change
0
50
100
150
ATRA
10
100
1000
F
-ATRA
+ATRA
Control
Galectin-1
-ATRA
+ATRA
Glabal O-GlcNAc
0.0
0.5
1.0
1.5
a
b
a,b
a,b
0
Galectin-1

Figure 7: Daily supplementation effects of human recombinant galectin-1 on granulocytic differentiation of HL-60 cells.

HL-60 cells were supplemented daily with 1000 ng/mL of galectin-1, with half the cells being treated with 1 µM ATRA for 72 h. (A) Nuclear morphology of control and galectin-1 treated cells were visualized by DAPI staining with the scale bar representing 20 µM. The differentiation index was determined as the percentage of nuclei demonstrating multi-lobular granulocyte-like shape based on galectin-1 (150 – 300 cells counted) (B) and galectin-1 + ATRA (190 – 280 cells counted) treatment (C). (D) Granulocyte specific gene *NCF1* was quantified by RT-qPCR with the Livak Method ($2^{-\Delta\Delta Ct}$) using *ACTB* as an internal control for galectin-1 and galectin-1 + ATRA treatments. (D) *O*-GlcNAcylation was assessed by immunodot blot using the RL2 antibody of galectin-1 ± ATRA treatments. Data are presented as mean ± SD, n=3-4. Significant differences were determined using unpaired Student's t test and Two-way ANOVA followed by Tukey's HSD test and are represented as different letters with a $p<0.05$.

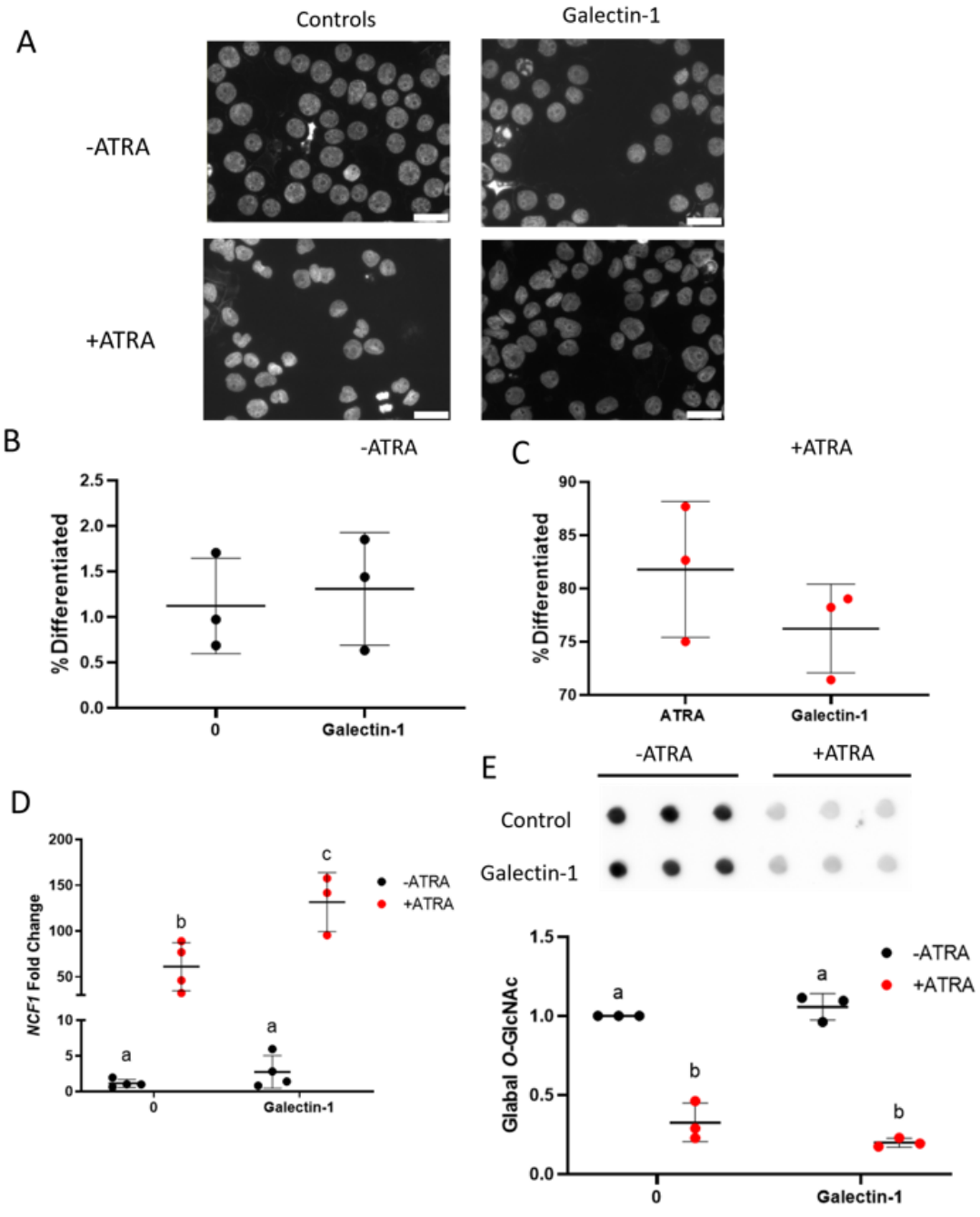
A
Controls
Galectin-1
-ATRA
+ATRA
B
-ATRA
% Differentiated
2.5
2.0
1.5
1.0
0.5
0.0
0
Galectin-1
C
+ATRA
% Differentiated
90
85
80
75
70
ATRA
Galectin-1
D
NCF1 Fold Change
200
150
100
50
10
5
0
a
b
a
c
0
Galectin-1
-ATRA
+ATRA
E
-ATRA
+ATRA
Control
Galectin-1
Global O-GlcNAc
1.5
1.0
0.5
0.0
a
b
a
b
0
Galectin-1
-ATRA
+ATRA

6E). Additionally, global *O*-GlcNAcylation demonstrated no significant changes (46.5%) when treated with 1000 ng/mL of galectin-1 + ATRA compared to ATRA treated cells (39.4%) (**Figure 6F**). The ATRA treatment for the dose dependent concentrations with galectin-1 + ATRA demonstrated an increase in the percentage of segmented nuclei ($p<0.0001$), upregulation in *NCF1* expression ($p<0.05$) and decrease in global *O*-GlcNAcylation ($p<0.05$) relative to untreated HL-60 cells (**Figure 6A-F**).

Daily supplementation of 1000ng/mL of galectin-1 + ATRA exhibited no significant change in the percentage of segmented nuclei (76.2 ± 4.2%) relative to ATRA treated cells (81.8 ± 6.4%) (**Figure 7A, C**). However, an upregulation in the expression of *NCF1* was detected with galectin-1 + ATRA treated cells (131.6-fold) relative to ATRA treated cells (61.0-fold, $p<0.01$) (**Figure 7D**). Furthermore, global *O*-GlcNAcylation demonstrated no significant change with 1000 ng/mL of galectin-1 + ATRA treatment (80.1%) compared to ATRA treated cells (67.4%) (**Figure 7E**). The ATRA treatments for the daily supplementation with galectin-1 + ATRA demonstrated an increase in the percentage of segmented nuclei ($p<0.0001$), upregulation in *NCF1* expression ($p<0.01$), and a decrease in global *O*-GlcNAcylation ($p<0.0001$) relative to untreated cells (**Figure 7A-E**).

During ATRA-induced differentiation, galectin-1 expression in HL-60 cells is downregulated (Vakhrushev ert al., 2018). Therefore, the galectin-1 specific allosteric inhibitor OTX008 and the galectin broad inhibitor TDG were investigated. HL-60 cells were treated with 5 µM OTX008 or 100 µM TDG daily over 72 hours. OTX008 demonstrated a significant increase in segmented nuclei (12.3 ± 1.9%) relative to DMSO vehicle control (8.8 ± 1.7%, $p<0.05$) and untreated cells (2.3 ± 0.7%, $p<0.0001$) (**Figure 8A-B**). Furthermore, a significant upregulation in *NCF1* expression was also observed with OTX008 treatment (26.7-fold) relative to DMSO vehicle control (12.8-fold, $p<0.05$) and untreated cells ($p<0.001$) (**Figure 8D**). Additionally, a significant global decrease in *O*-GlcNAcylation was observed with OTX008 treatment (91.7%) relative to DMSO vehicle control (49.3%, $p<0.01$) and untreated cells ($p<0.0001$) (**Figure 8F-G**). However, daily treatments with galectin broad inhibitor TDG demonstrated no significant effect on granulocytic differentiation of HL-60 cells. Nuclear morphology demonstrated no significant change in the percentage of segmented nuclei (4.1 ± 0.4%) compared to

Figure 8: Allosteric inhibition of galectin-1 with OTX008 induces granulocytic differentiation of HL-60 cells not observed with TDG.

HL-60 cells were supplemented daily with either 5 µM OTX008, 100 µM thiodigalactoside (TDG), or 0.467% (v/v) DMSO as vehicle control, with half the cells treated with 1 µM ATRA for 72 h. (A) Nuclear morphology of untreated and treated cells were visualized by DAPI staining with the scale bar representing 20 µM. The differentiation index was determined as the percentage of nuclei demonstrating multi-lobular granulocyte-like shape based on OTX008 and TDG treatments (120 – 210 cells counted) (B), and OTX008 + ATRA (130 – 250 cells counted) and TDG + ATRA (120 - 240 cells counted) treatments (C). Granulocyte specific gene *NCF1* was quantified by RT-qPCR with the Livak method ($2^{-\Delta\Delta Ct}$) using *ACTB* as an internal control for OTX008 and TDG treatments (D), and OTX008 + ATRA and TDG + ATRA treatments (E). (F) *O*-GlcNAcylation was assessed by immunodot blot using the RL2 antibody for OTX008 and TDG treatments (G), and OTX008 + ATRA and TDG + ATRA treatments (H). Data are presented as mean ± SD, n=3-5. Significant differences were determined using One-way ANOVA followed by Tukey's HSD test and are represented as different letters with a $p<0.05$.

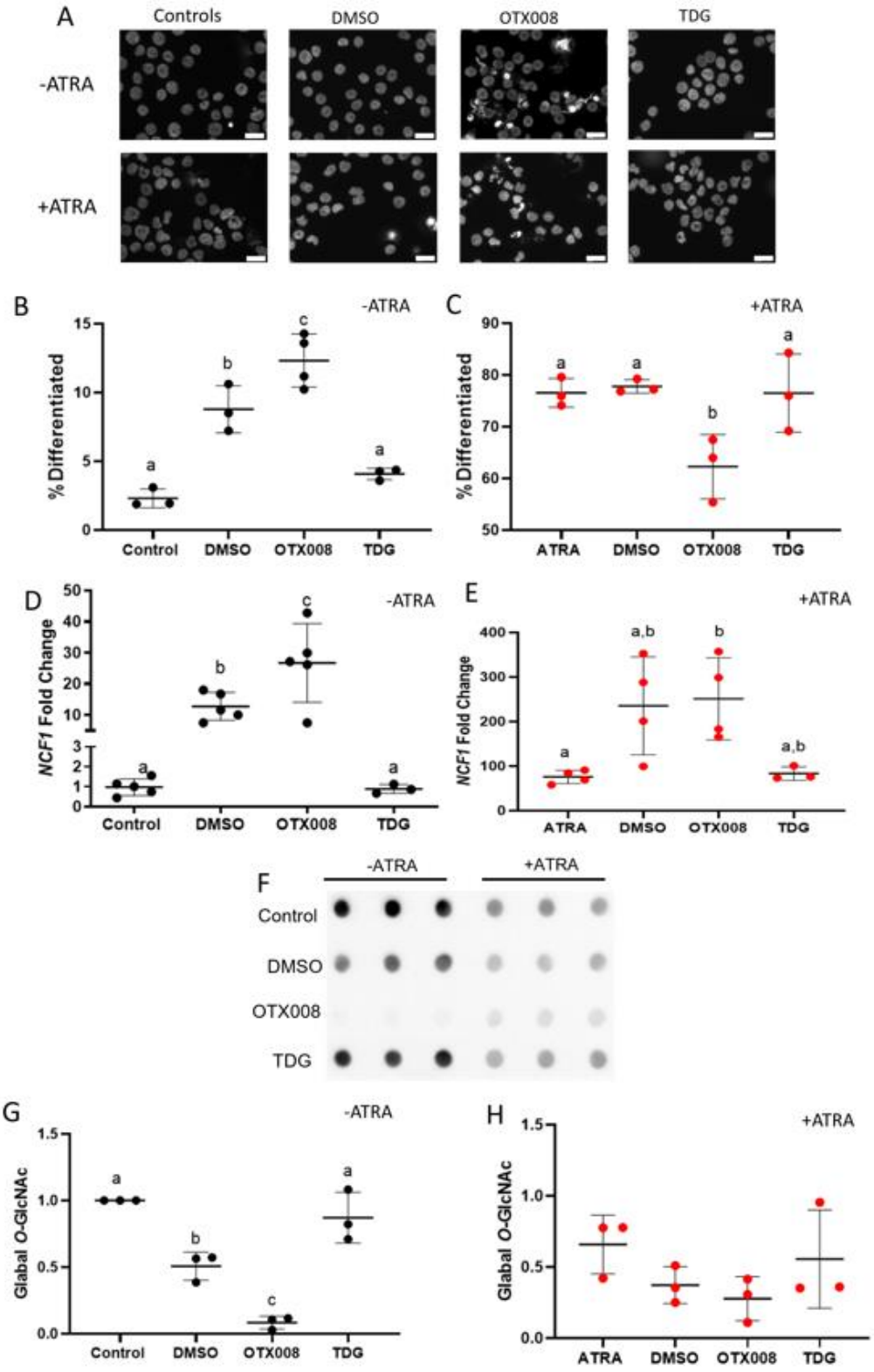
A
Controls
DMSO
OTX008
TDG
-ATRA
+ATRA
B
-ATRA
% Differentiated
Control
DMSO
OTX008
TDG
C
+ATRA
% Differentiated
ATRA
DMSO
OTX008
TDG
D
-ATRA
NCF1 Fold Change
Control
DMSO
OTX008
TDG
E
+ATRA
NCF1 Fold Change
ATRA
DMSO
OTX008
TDG
F
-ATRA
+ATRA
Control
DMSO
OTX008
TDG
G
-ATRA
Glabal O-GlcNAc
Control
DMSO
OTX008
TDG
H
+ATRA
Glabal O-GlcNAc
ATRA
DMSO
OTX008
TDG

untreated cells (2.3 ± 0.7%) (**Figure 8A-B**). Furthermore, there was no significant change in the expression of *NCF1* (0.9-fold) or in global *O*-GlcNAcylation (12.9%) when compared to untreated cells (**Figure 8D, F-G**).

To further understand the effects of OTX008 and TDG on granulocytic differentiation of HL-60 cells, combination treatments with 1 µM ATRA were conducted with daily treatments of 5 µM OTX008 or 100 µM TDG for 72 hours. Daily treatments of OTX008 + ATRA demonstrated a significant decrease in segmented nuclei (62.3 ± 6.2%) relative to DMSO vehicle control (77.8 ± 1.3%, $p<0.05$) and ATRA treated cells (76.5 ± 2.8%, $p<0.05$) (**Figure 8A, C**). When examining *NCF1* expression, there was no significant change in OTX008 + ATRA treated cells (251.1-fold) relative to DMSO vehicle control (235.4-fold). However, the OTX008 treatment demonstrated an upregulation of *NCF1* relative to ATRA treated cells (75.7-fold, $p<0.05$). The DMSO vehicle control demonstrated no significant change in *NCF1* expression relative to ATRA treated cells (**Figure 8E**). Additionally, global *O*-GlcNAcylation had no significant change with OTX008 + ATRA treatment (69.4%) relative to DMSO vehicle control (59.4%), and ATRA treated cells (34.2 %) (**Figure 8F, H**). The ATRA treatment with OTX008 + ATRA demonstrated an increase in the percentage of segmented nuclei ($p<0.0001$), upregulation of *NCF1* expression ($p<0.0001$), and decrease in global *O*-GlcNAcylation ($p<0.05$) relative to untreated cells (**Figure 8A-H**).

Combination treatments of TDG + ATRA demonstrated no significant effect on granulocytic differentiation of HL-60 cells. TDG + ATRA demonstrated no significant change in the percentage of segmented nuclei (76.5 ± 7.6%) relative to ATRA treated cells (76.5 ± 2.8%,) (**Figure 8A, C**). Additionally, TDG + ATRA demonstrated no significant change in *NCF1* expression (83.4-fold) and global *O*-GlcNAcylation (15.46%) relative to ATRA treated cells (75.7-fold and 34.2 %, respectively) (**Figure 8E-F, H**).

3.1.3 The effects of chimeric type recombinant galectin-3 and a galectin-3 inhibitor on differentiation of HL-60 cells

Galectin-3 is another galectin expressed in HL-60 cells reported by Vinnai et al. (2017), that demonstrated upregulation during differentiation. The dose-dependent effects of 10,

100 or 1000 ng/mL human recombinant galectin-3 on HL-60 cell differentiation for 72 hours was thus assessed. Nuclear morphology exhibited no significant changes in the percentage of segmentation for 10 ng/mL (1.8 ± 0.6%) and 100 ng/mL (1.6 ± 0.4%) treated cells, whereas 1000 ng/mL treated cells exhibited an increase in the percentage of segmented nuclei (3.6 ± 0.5%, $p<0.01$) relative to untreated cells (1.8 ± 0.3%) (**Figure 9A-B**). Furthermore, there were no significant changes observed in the regulation of *NCF1* at all concentrations (0.9-fold, 0.9-fold, and 1.1-fold, respectively) relative to untreated cells (**Figure 9D**). Additionally, there were no significant changes observed in the global *O*-GlcNAcylation of the cells treated with 1000 ng/mL of galectin-3 (19% increase) relative to untreated cells (**Figure 9F**).

To provide a further understanding of the effects of galectin-3 on granulocytic differentiation of HL-60 cells, cells were supplemented daily with 1000 ng/mL of galectin-3 for 72 hours. Nuclear morphology exhibited no significant changes in the percentage of segmented nuclei when supplemented daily with galectin-3 (1.8 ± 0.09%) relative to untreated cells (1.0 ± 0.7%) (**Figure 10A-B**). Furthermore, there were no significant changes observed in the expression of *NCF1* (0.9-fold) and global *O*-GlcNAcylation (19.6%) of galectin-3 daily supplemented cells relative to untreated cells (**Figure 10D-E**).

To evaluate the effects of galectin-3 on ATRA-induced differentiated HL-60 cells, combination treatments of 1 µM ATRA and dose-dependent effects (10, 100 and 1000 ng/mL) and daily supplementation (1000 ng/mL) of galectin-3 were conducted for 72 hours. Dose-dependent effects of galectin-3 + ATRA demonstrated no significant effects in the percentage of segmented nuclei (86.8 ± 0.5, 88.3 ± 0.4, and 85.6 ± 3.4%, respectively) relative to ATRA treated cells (85.5 ± 2.2%) (**Figure 9A, C**). Furthermore, there were no significant changes observed in the expression of *NCF1* of galectin-3 + ATRA treated cells (122.6-fold, 118.3-fold, and 114.9-fold, respectively) relative to ATRA treated cells (118.1-fold) (**Figure 9E**). Additionally, there were no significant changes in global levels of *O*-GlcNAcylation observed with 1000 ng/mL of galectin-3 + ATRA treated cells (40.5%) relative to ATRA treated cells (39.4 %) (**Figure 9F**). The ATRA treatment for the dose dependent effects with galectin-3 + ATRA demonstrated an increase in the

Figure 9: Dose-dependent effects of human recombinant galectin-3 on granulocytic differentiation of HL-60 cells.

HL-60 cells were treated with 10, 100, or 1000 ng/mL of galectin-3, with half the cells also being treated with 1 µM ATRA to induce differentiation for 72 h. (A) Nuclear morphology of control and galectin-3 treated cells were visualized by DAPI staining with the scale bar representing 20 µm. The differentiation index was determined as the percentage of nuclei demonstrating multi-lobular granulocyte-like shape based on galectin-3 (170 – 360 cells counted) (B) and galectin-3 + ATRA (230 – 430 cells counted) treatments (C). Granulocyte specific gene *NCF1* was quantified by RT-qPCR with the Livak method ($2^{-\Delta\Delta Ct}$) using *ACTB* as an internal control for galectin-3 (D) and galectin-3 + ATRA treatments (E). (F) *O*-GlcNAcylation was assessed by immunodot blot using the RL2 antibody when HL-60 cells were treated with 1000 ng/mL galectin-3 ± ATRA. Data are presented as mean ± SD, n=3-4. Significant differences were determined using One-way ANOVA and Two-way ANOVA followed by Tukey's HSD test and are represented as different letters with a $p<0.05$.

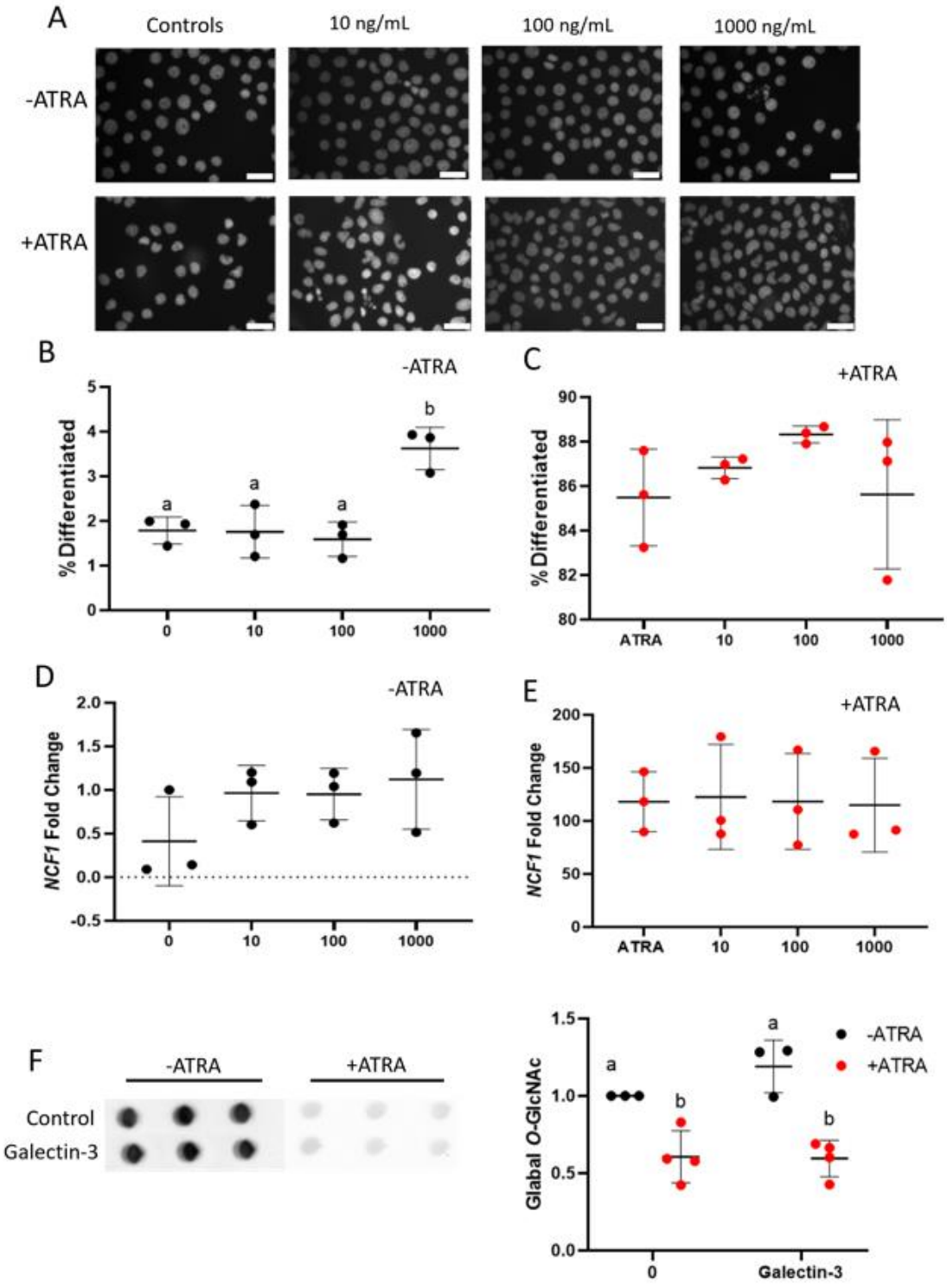
A
Controls
10 ng/mL
100 ng/mL
1000 ng/mL
-ATRA
+ATRA
B
-ATRA
% Differentiated
a
a
a
b
0
10
100
1000
C
+ATRA
% Differentiated
ATRA
10
100
1000
D
-ATRA
NCF1 Fold Change
0
10
100
1000
E
+ATRA
NCF1 Fold Change
ATRA
10
100
1000
F
-ATRA
+ATRA
Control
Galectin-3
Glabal O-GlcNAc
a
b
a
b
-ATRA
+ATRA
0
Galectin-3

Figure 10: Daily supplementation of human recombinant galectin-3 exhibits no effect on granulocytic differentiation of HL-60 cells.

HL-60 cells were supplemented daily with 1000 ng/mL of galectin-3, with half the cells being treated with 1 µM ATRA for 72 h. (A) Nuclear morphology of control and galectin-3 treated cells were visualized by DAPI staining with the scale bar representing 20 µm. The differentiation index was determined as the percentage of nuclei demonstrating multi-lobular granulocyte-like shape based on galectin-3 (340 – 400 cells counted) (B) and galectin-3 + ATRA (230 – 340 cells counted) treatments (C). (D) Granulocyte specific gene *NCF1* was quantified by RT-qPCR with the Livak method ($2^{-\Delta\Delta Ct}$) using *ACTB* as an internal control for galectin-3 and galectin-3+ATRA treatments. (E) *O*-GlcNAcylation was assessed by immunodot blot using the RL2 antibody of galectin-3 ± ATRA treatments. Data are presented as mean ± SD, n=3-4. Significant differences were determined using unpaired Student's t test and Two-way ANOVA followed by Tukey's HSD test and are represented as different letters with a $p<0.05$.

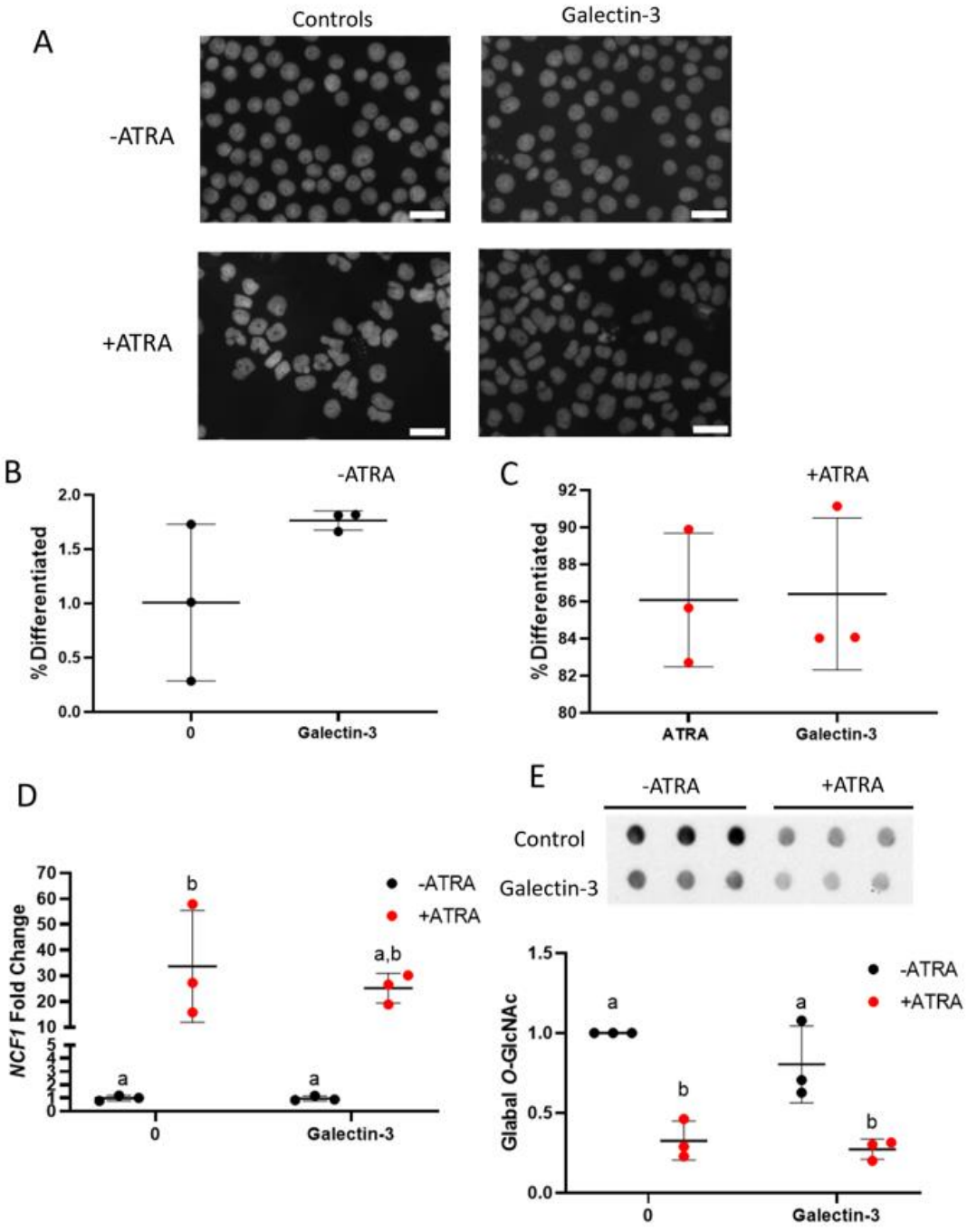
A
Controls
Galectin-3
-ATRA
+ATRA
B
-ATRA
% Differentiated
2.0
1.5
1.0
0.5
0.0
0
Galectin-3
C
+ATRA
% Differentiated
92
90
88
86
84
82
80
ATRA
Galectin-3
D
NCF1 Fold Change
70
60
50
40
30
20
10
5
4
3
2
1
0
b
a,b
a
a
-ATRA
+ATRA
0
Galectin-3
E
-ATRA
+ATRA
Control
Galectin-3
Glabal O-GlcNAc
1.5
1.0
0.5
0.0
a
b
a
b
-ATRA
+ATRA
0
Galectin-3

percentage of segmented nuclei (*p<0.0001*), upregulation in *NCF1* expression (*p<0.01*), and a decrease in global *O*-GlcNAcylation (*p<0.05*) relative to untreated cells (**Figure 9A-F**).

Cells daily supplemented with 1000 ng/mL of galectin-3 + ATRA exhibited no significant change in the percentage of segmented nuclei (86.4 ± 4.1%) relative to ATRA treated cells (86.1 ± 3.6%) (**Figure 10A, C**). Furthermore, there was no significant change in the expression of *NCF1* observed with galectin-3 + ATRA treatment (25.2-fold) relative to ATRA treated cells (33.7-fold) (**Figure 10D**). Additionally, there was no significant change in global *O*-GlcNAcylation levels observed with galectin-3 + ATRA treated cells (72.8%) relative to ATRA treated cells (67.4%) (**Figure 10E**). The ATRA treatment for the daily supplementation with galectin-3 + ATRA demonstrated an increase in the percentage of segmented nuclei (*p<0.0001*), upregulation in *NCF1* expression (*p<0.05*), and a decrease in global *O*-GlcNAcylation (*p<0.01*) relative to untreated cells (**Figure 10A-E**).

GB1107 is a specific allosteric inhibitor of galectin-3 that was used to investigate the effects of galectin-3 inhibition on granulocytic differentiation. HL-60 cells were treated with 2 µM GB1107 daily over 72 hours. GB1107 treated cells exhibited a significant increase in the percentage of segmented nuclei (5.0 ± 0.6%) relative to untreated cells (2.3 ± 0.7%, *p<0.01*) (**Figure 11A-B**). Furthermore, GB1107 treated cells demonstrated a significant upregulation in *NCF1* (2.0-fold) relative to untreated cells (*p<0.05*) (**Figure 11D**). Global *O*-GlcNAcylation levels also significantly decreased in GB1107 treated cells (38.4%) relative to untreated cells (*p<0.01*) (**Figure 11F-G**).

The galectin-3 inhibitor GB1107 was also used in a combination treatment with ATRA to further assess the effect galectin-3 has on granulocytic differentiation of HL-60 cells. HL-60 cells were treated with 1 µM ATRA and daily supplemented with 2 µM GB1107 for 72 hours. Nuclear morphology exhibited no significant change in the percentage of segmented nuclei of GB1107 + ATRA treated cells (69.8 ± 4.3%) relative to ATRA treated cells (76.5 ± 2.8%) (**Figure 11A, C**). Furthermore, there was no significant change in *NCF1* expression of GB1107 + ATRA treated cells (114.7-fold) relative to ATRA treated cells

Figure 11: Allosteric inhibition of galectin-3 with GB1107 induces granulocytic differentiation of HL-60 cells.

HL-60 cells were supplemented daily with 2 µM GB1107, with half the cells being treated with 1 µM ATRA for 72 h. (A) Nuclear morphology of control and GB1107 treated cells were visualized by DAPI staining with the scale bar representing 20 µm. The differentiation index was determined as the percentage of nuclei demonstrating multi-lobular granulocyte-like shape based on GB1107 (150 – 200 cells counted) (B) and GB1107 + ATRA (130 – 230 cells counted) treatments (C). (D) Granulocyte specific genes *NCF1* was quantified by RT-qPCR with the Livak method ($2^{-\Delta\Delta Ct}$) using *ACTB* as an internal control for GB1107 and GB1107 + ATRA treatments. (E) *O*-GlcNAcylation was assessed by immunodot blot using the RL2 antibody GB1107 treatments (G), and GB1107 + ATRA treatments (H). Data are presented as mean ± SD, n=3-4. Significant differences were determined using unpaired Student's t test and Two-way ANOVA followed by Tukey's HSD test and are represented as different letters with a $p<0.05$.

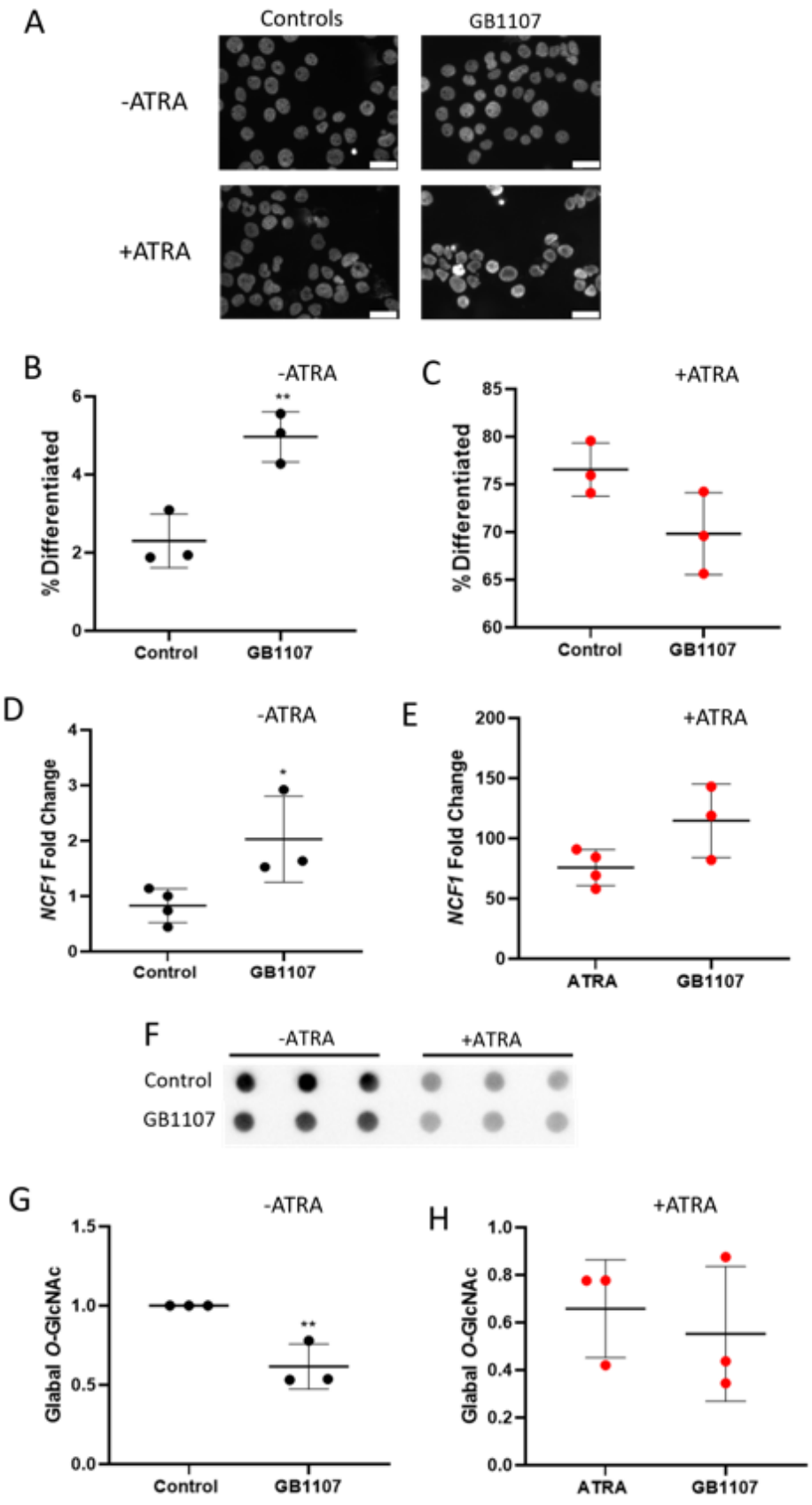
A
Controls
GB1107
-ATRA
+ATRA
B
-ATRA
% Differentiated
Control
GB1107
C
+ATRA
% Differentiated
Control
GB1107
D
-ATRA
NCF1 Fold Change
Control
GB1107
E
+ATRA
NCF1 Fold Change
ATRA
GB1107
F
-ATRA
+ATRA
Control
GB1107
G
-ATRA
Glabal O-GlcNAc
Control
GB1107
H
+ATRA
Glabal O-GlcNAc
ATRA
GB1107

(75.7-fold) (**Figure 11E**). Additionally, there was no significant change observed in global *O*-GlcNAcylation levels of GB1107 + ATRA treated cells (44.8%) relative to ATRA treated cells (34.2%) (**Figure 11F, H**). The ATRA treatment with GB1107 + ATRA demonstrated an increase in the percentage of segmented nuclei ($p<0.0001$), upregulation of *NCF1* expression ($p<0.0001$), and a decrease in global *O*-GlcNAcylation ($p<0.05$) relative to untreated cells (**Figure 11A-H**).

3.1.4 The effects of tandem-repeat type recombinant galectin-8 and galectin-9 on differentiation of HL-60 cells

Galectin-8 is another galectin that exhibits constant expression patterns during differentiation in HL-60 cells (Abedin et al., 2003; Timoshenko et al., 2016; Vinnai et al., 2017). To examine the effects of galectin-8 on HL-60 cell granulocytic differentiation, dose-dependent treatments of human recombinant galectin-8 at 10, 100 or 1000 ng/mL were conducted over 72 hours. Nuclear morphology showed that cell treatments at 1000 ng/mL had a significant increase in the percentage of segmented nuclei (9.1 ± 0.3%, $p<0.05$) relative to untreated cells (3.8 ± 2.8%), whereas cells treated with 10 ng/mL (4.7 ± 0.7%) or 100 ng/mL (6.5 ± 1.5%) exhibited no significant changes in the segmentation of nuclei (**Figure 12A-B**). Furthermore, 1000 ng/mL of galectin-8 demonstrated a significant upregulation in *NCF1* expression (4.3-fold, $p<0.001$) relative to untreated cells, while 10 ng/mL (1.3-fold) and 100 ng/mL (1.0-fold) demonstrated no significant changes in *NCF1* expression (**Figure 12D**). However, there was no significant change observed at 1000 ng/mL of galectin-8 treated cells on global *O*-GlcNAcylation levels (19.5%) relative to untreated cells (**Figure 12F**).

To further understand the effects of 1000 ng/mL of recombinant galectin-8 on HL-60 cell differentiation, daily supplementation of 1000 ng/mL of galectin-8 was conducted over 72 hours. Daily supplemented galectin-8 cells exhibited a significant increase in the percentage of segmented nuclei (6.9 ± 1.5%) relative to untreated cells (2.3 ± 0.6%, $p<0.01$) (**Figure 13A-B**). However, there were no significant changes observed in the expression of *NCF1* (5.3-fold) and global *O*-GlcNAcylation (14.7% increase) relative to untreated cells (**Figure 13D-E**).

Figure 12: Human recombinant galectin-8 induces granulocytic differentiation of HL-60 cells.

HL-60 cells were treated with 10, 100, or 1000 ng/mL of galectin-8, with half the cells also being treated with 1 µM ATRA to induce differentiation for 72 h. (A) Nuclear morphology of control and galectin-8 treated cells were visualized by DAPI staining with the scale bar representing 20 µM. The differentiation index was determined as the percentage of nuclei demonstrating multi-lobular granulocyte-like shape based on galectin-8 (220 – 540 cells counted) (B) and galectin-8+ATRA (230 – 440 cells counted) treatments (C). Granulocyte specific gene *NCF1* was quantified by RT-qPCR with the Livak method ($2^{-\Delta\Delta Ct}$) using *ACTB* as an internal control for galectin-8 (D) and galectin-8 + ATRA treatments (E). (F) *O*-GlcNAcylation was assessed by immunodot blot using the RL2 antibody when HL-60 cells were treated with 1000 ng/mL of galectin-8 ± ATRA. Data are presented as mean ± SD, n=3-4. Significant differences were determined using One-way ANOVA and Two-way ANOVA followed by Tukey's HSD test and are represented as different letters with a $p<0.05$.

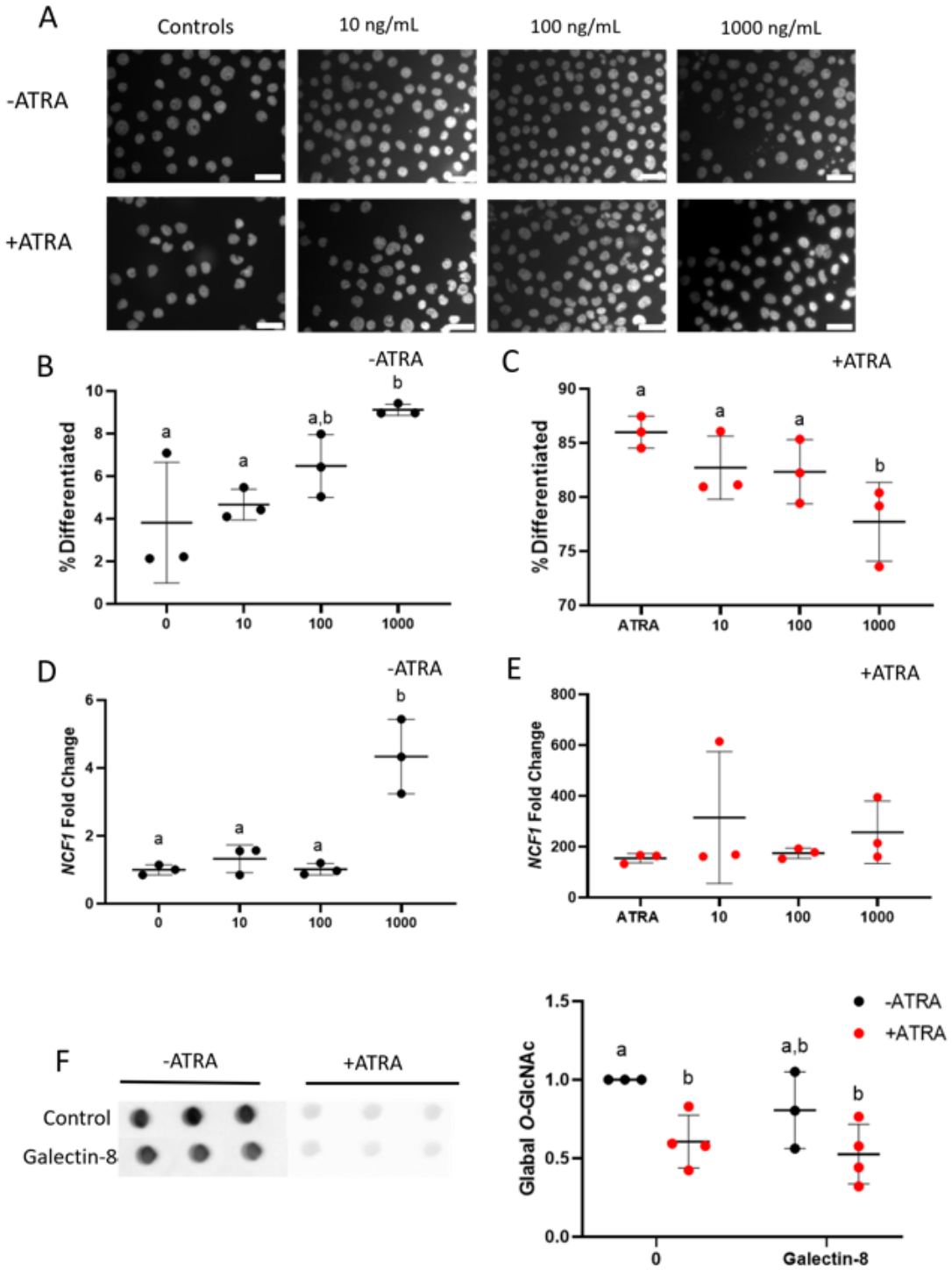
A
Controls
10 ng/mL
100 ng/mL
1000 ng/mL
-ATRA
+ATRA
B
-ATRA
% Differentiated
a
a
a,b
b
0
10
100
1000
C
+ATRA
% Differentiated
a
a
a
b
ATRA
10
100
1000
D
-ATRA
NCF1 Fold Change
a
a
a
b
0
10
100
1000
E
+ATRA
NCF1 Fold Change
ATRA
10
100
1000
F
-ATRA
+ATRA
Control
Galectin-8
-ATRA
+ATRA
Global O-GlcNAc
a
b
a,b
b
0
Galectin-8

Figure 13: Daily supplementation effects of human recombinant galectin-8 on granulocytic differentiation of HL-60 cells.

HL-60 cells were supplemented daily with 1000 ng/mL of galectin-8, with half the cells being treated with 1 µM ATRA for 72 h. (A) Nuclear morphology of control and galectin-8 treated cells were visualized by DAPI staining with the scale bar representing 20 µm. The differentiation index was determined as the percentage of nuclei demonstrating multi-lobular granulocyte-like shape based on galectin-8 (170 – 280 cells counted) (B) and galectin-8 + ATRA (210-290 cells counted) treatments (C). (D) Granulocyte specific gene *NCF1* was quantified by RT-qPCR with the Livak method ($2^{-\Delta\Delta Ct}$) using *ACTB* as an internal control for galectin-8 and galectin-8 + ATRA treatments. (E) *O*-GlcNAcylation was assessed by immunodot blot using the RL2 antibody of galectin-8 ± ATRA treatments. Data are presented as mean ± SD, n=3-4. Significant differences were determined using unpaired Student's t test and Two-way ANOVA followed by Tukey's HSD test and are represented as different letters with a $p<0.05$.

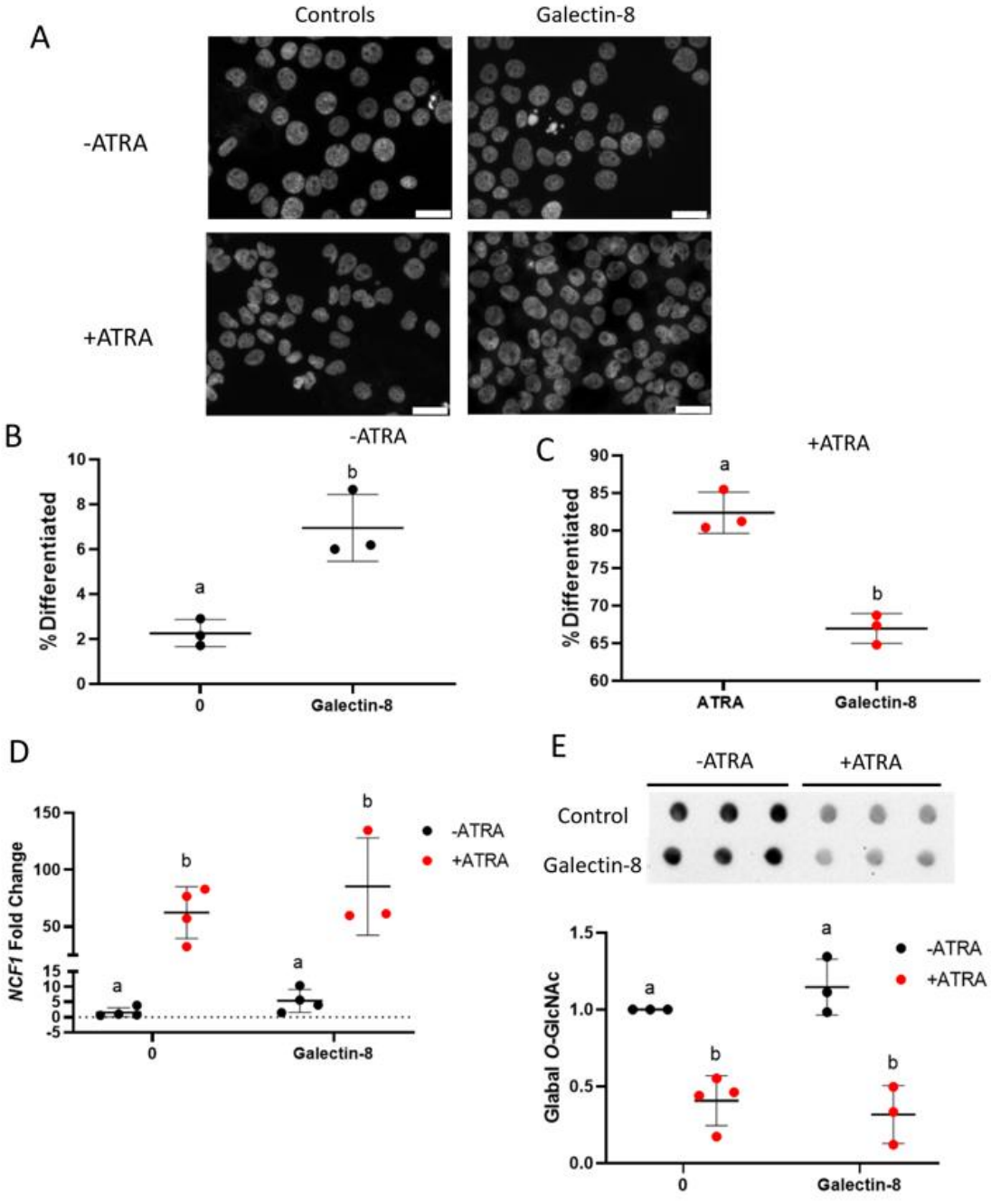
A
Controls
Galectin-8
-ATRA
+ATRA
B
-ATRA
% Differentiated
0
Galectin-8
C
+ATRA
% Differentiated
ATRA
Galectin-8
D
NCF1 Fold Change
-ATRA
+ATRA
0
Galectin-8
E
-ATRA
+ATRA
Control
Galectin-8
Global O-GlcNAc
0
Galectin-8

To get a more in-depth look at the effect of galectin-8 on the granulitic differentiation of HL-60 cells, combination treatments with ATRA were conducted. HL-60 cells were treated with 1 µM ATRA and treated with dose-dependent concentrations (10, 100 or 1000 ng/mL) or supplemented daily with recombinant galectin-8 (1000 ng/mL) for 72 hours. Nuclear morphology of dose-dependent cell treatments of galectin-8 + ATRA exhibited a significant decrease in the percentage of segmented nuclei at 1000 ng/mL (77.7 ± 3.6%, $p<0.05$) relative to ATRA treated cells (86.0 ± 1.5%), whereas 10 ng/mL (82.7 ± 2.9%) and 100 ng/mL (82.3 ± 2.9%) cell treatments demonstrated no significant changes in the percentage of segmented nuclei (**Figure 12A, C**). Furthermore, there were no significant changes in *NCF1* expression at all galectin-8 + ATRA concentrations (314.6-fold, 174.2-fold, and 256.5-fold, respectively) relative to ATRA treated cells (154.2-fold) (**Figure 12E**). Additionally, there was no significant change observed in the global *O*-GlcNAcylation levels when treated with 1000 ng/ml of galectin-8 + ATRA (47.4%) relative to ATRA treated cells (39.4%) (**Figure 12F**). The ATRA treatment for the dose dependent effects with galectin-8 + ATRA demonstrated an increase in the percentage of segmented nuclei ($p<0.0001$), upregulation in *NCF1* expression ($p<0.001$), and decrease in global *O*-GlcNAcylation ($p<0.05$) relative to untreated cells (**Figure 12A-F**).

Daily supplementation of 1000 ng/mL of galectin-8 + ATRA exhibited a significant decrease in the percentage of segmented nuclei (67.0 ± 1.5%, $p<0.01$) relative to ATRA treated cells (82.4 ± 0.6%) (**Figure 13A, C**). Furthermore, there was no significant change in the expression of *NCF1* of galectin-8 + ATRA treated cells (85.2-fold) relative to ATRA treated cells (62.3-fold) (**Figure 13D**). Global O-GlcNAcylation levels demonstrated no significant change with galectin-8+ATRA treated cells (68.3%) relative to ATRA treated cells (59.3%) (**Figure 13E**). The ATRA treatment for the daily supplementation with galectin-8 + ATRA demonstrated an increase in the percentage of segmented nuclei ($p<0.0001$), upregulation of *NCF1* expression ($p<0.05$), and decrease in global *O*-GlcNAcylation ($p<0.01$) (**Figure 13A-E**).

Previous reports have indicated that galectin-9 exhibits constant gene expression during DMSO-induced differentiation of HL-60 cells (Vinnai et al., 2017; Abedin et al., 2003). To see how galectin-9 is involved with the granulocytic differentiation of HL-60 cells, the

dose dependent effects of human recombinant galectin-9 at 10, 100, or 1000 ng/mL were investigated over the 72 hours. Nuclear morphology showed no significant changes in the percentage of segmented nuclei (5.3 ± 0.4, 5.2 ± 1.7, and 11.5 ± 5.2%, respectively) relative to untreated cells (5.1 ± 2.0%) (**Figure 14A-B**). Furthermore, treatment with 1000 ng/mL galectin-9 resulted in a significant upregulation in *NCF1* expression (11.0-fold, $p<0.05$) relative to untreated cells, while 10 ng/mL (0.9-fold) and 100 ng/mL (0.8-fold) demonstrated no significant changes in *NCF1* expression (**Figure 14D**). Additionally, there was no significant change observed in global *O*-GlcNAcylation of cells treated with 1000 ng/mL of galectin-9 (6.6% increase) relative to untreated cells (**Figure 14F**).

Daily supplementation of recombinant galectin-9 at 1000 ng/mL was also conducted over 72 hours. Nuclear morphology exhibited no significant change in the percentage of segmented nuclei of galectin-9 treated cells (2.8 ± 1.2%) relative to untreated cells (1.1 ± 0.5%) (**Figure 15A-B**). Furthermore, there were no significant changes in *NCF1* expression of galectin-9 treated cells (4.4-fold) or in global *O*-GlcNAcylation (3.9%) relative to untreated cells (**Figure 15D-E**).

To understand how galectin-9 is involved in ATRA-induced differentiation of HL-60 cells, combination treatments were also conducted. Cells were treated with 1 µM ATRA and dose-dependent effect concentrations (10, 100, or 1000 ng/mL) or daily supplementation with recombinant galectin-9 (1000 ng/mL) for 72 hours. The dose-dependent treatments of galectin-9 + ATRA exhibited no significant change in the percentage of segmented nuclei (86.9 ± 7.5, 82.5 ± 3.9, and 80.1 ± 6.3%, respectively) relative to ATRA treated cells (91.1 ± 3.5%) (**Figure 14A, C**). Furthermore, there was no significant change observed in the expression of *NCF1* galectin-9 + ATRA treated cells (163.7-fold, 234.9-fold, and 214.0-fold, respectively) relative to ATRA treated cells (142.2-fold) (**Figure 14E**). Additionally, global *O*-GlcNAcylation levels demonstrated no significant change upon treatment with galectin-9 + ATRA (40.1%) relative to ATRA treated cells (39.4%) (**Figure 14F**). The ATRA treatment for the dose dependent effects with galectin-9 + ATRA demonstrated an increase in the percentage of segmented nuclei ($p<0.0001$), upregulation

Figure 14: Dose-dependent effects of human recombinant galectin-9 on granulocytic differentiation of HL-60 cells.

HL-60 cells were treated with 10, 100, or 1000 ng/mL of galectin-9, with half the cells also being treated with 1 µM ATRA to induce differentiation for 72 h. (A) Nuclear morphology of control and galectin-9 treated cells were visualized by DAPI staining with the scale bar representing 20 µm. The differentiation index was determined as the percentage of nuclei demonstrating multi-lobular granulocyte-like shape based on galectin-9 (100 – 380 cells counted) (B) and galectin-9 + ATRA (200 – 370 cells counted) treatments (C). Granulocyte specific gene *NCF1* was quantified by RT-qPCR with the Livak method ($2^{-\Delta\Delta Ct}$) using *ACTB* as an internal control for galectin-9 (D) and galectin-9 + ATRA treatments (E). (F) *O*-GlcNAcylation was assessed by immunodot blot using the RL2 antibody when HL-60 cells were treated with 1000 ng/mL galectin-9 ± ATRA. Data are presented as mean ± SD, n=3-4. Significant differences were determined using One-way ANOVA and Two-way ANOVA followed by Tukey's HSD test and are represented as different letters with a $p<0.05$.

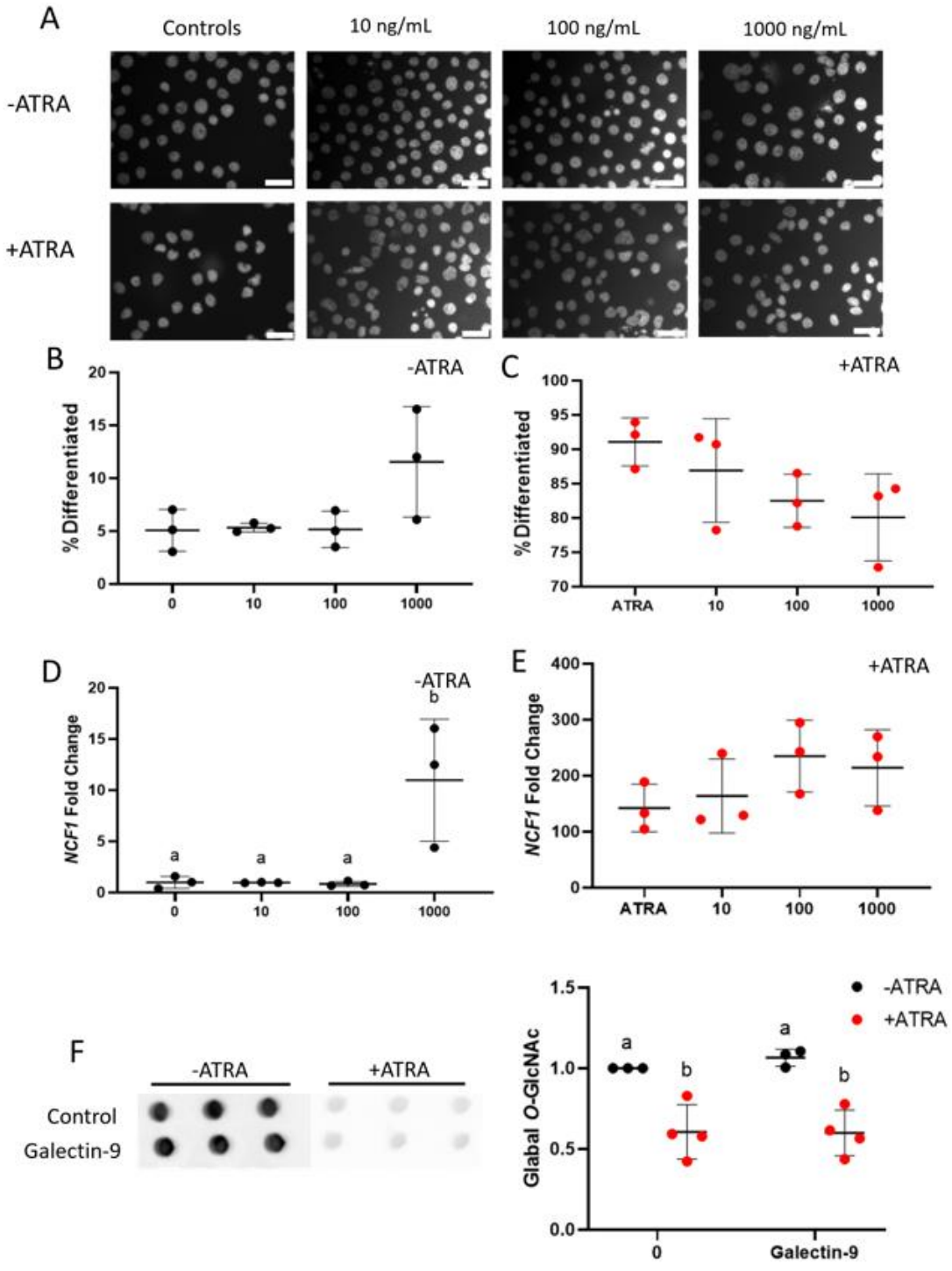
A
Controls
10 ng/mL
100 ng/mL
1000 ng/mL
-ATRA
+ATRA
B
-ATRA
% Differentiated
0
5
10
15
20
0
10
100
1000
C
+ATRA
% Differentiated
70
75
80
85
90
95
100
ATRA
10
100
1000
D
-ATRA
NCF1 Fold Change
a
a
a
b
0
5
10
15
20
0
10
100
1000
E
+ATRA
NCF1 Fold Change
0
100
200
300
400
ATRA
10
100
1000
F
-ATRA
+ATRA
Control
Galectin-9
Glabal O-GlcNAc
-ATRA
+ATRA
a
b
a
b
0.0
0.5
1.0
1.5
0
Galectin-9

Figure 15: Daily supplementation effects of human recombinant galectin-9 on granulocytic differentiation of HL-60 cells.

HL-60 cells were supplemented daily with 1000 ng/mL of galectin-9, with half the cells being treated with 1 µM ATRA for 72 h. (A) Nuclear morphology of control and galectin-9 treated cells were visualized by DAPI staining with the scale bar representing 20 µm. The differentiation index was determined as the percentage of nuclei demonstrating multi-lobular granulocyte-like shape based on galectin-9 (140 – 290 cells counted) (B) and galectin-9 + ATRA (190 – 350 cells counted) treatments (C). (D) Granulocyte specific genes *NCF1* was quantified by RT-qPCR with the Livak method ($2^{-\Delta\Delta Ct}$) using *ACTB* as an internal control for galectin-9 and galectin-9+ATRA treatments. (E) *O*-GlcNAcylation was assessed by immunodot blot using the RL2 antibody of galectin-9 ± ATRA treatments. Data are presented as mean ± SD, n=3-4. Significant differences were determined using unpaired Student's t test and Two-way ANOVA followed by Tukey's HSD test and are represented as different letters with a $p<0.05$.

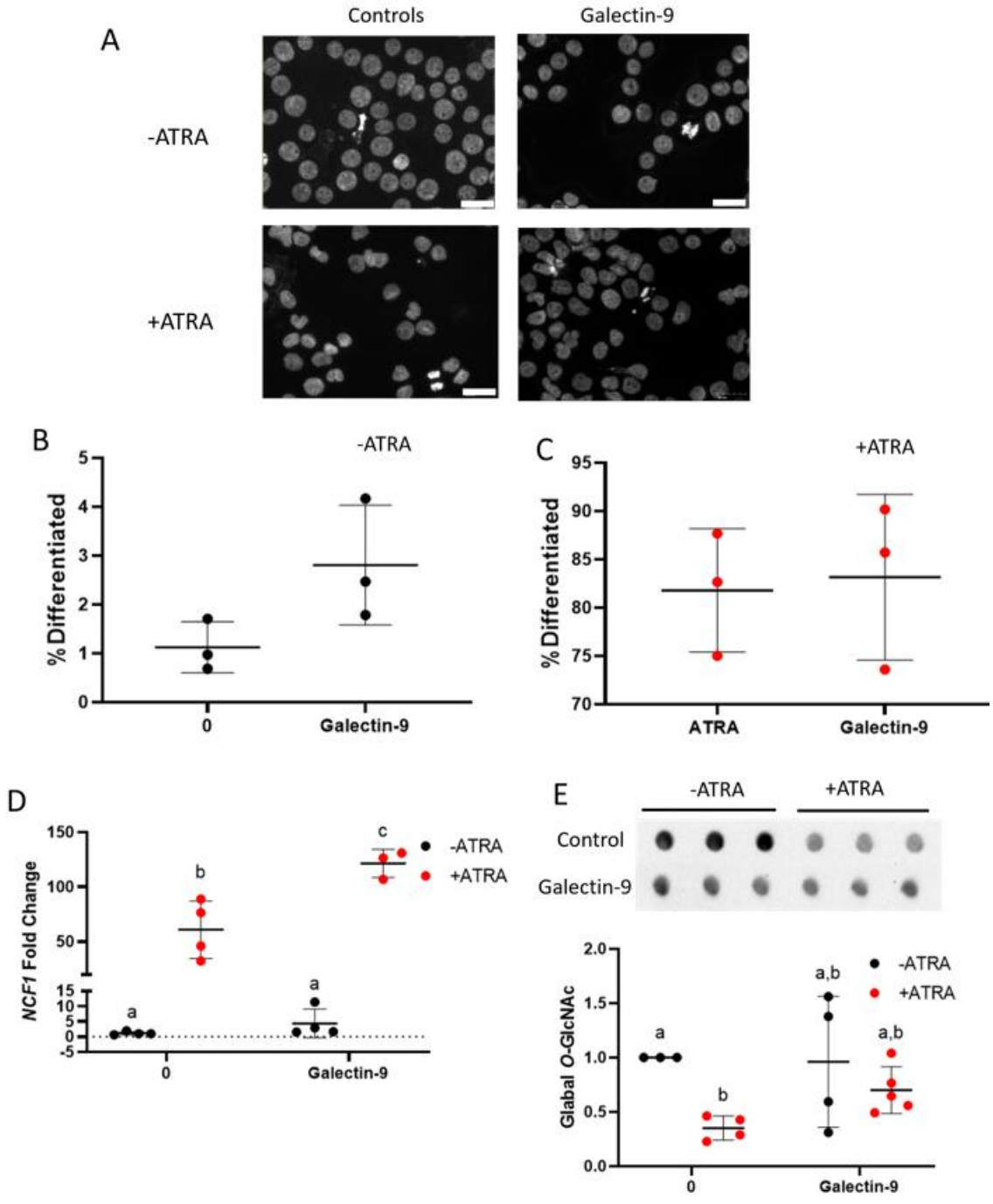
A
Controls
Galectin-9
-ATRA
+ATRA
B
-ATRA
% Differentiated
0
Galectin-9
C
+ATRA
% Differentiated
ATRA
Galectin-9
D
NCF1 Fold Change
-ATRA
+ATRA
a
b
a
c
0
Galectin-9
E
-ATRA
+ATRA
Control
Galectin-9
Glabal O-GlcNAc
a
b
a,b
a,b
0
Galectin-9

of *NCF1* expression (*p<0.01*) and decrease in global *O*-GlcNAcylation (*p<0.05*) relative to untreated cells (**Figure 14A-F**).

When examining the effects of daily supplementation with 1000 ng/mL galectin-9 + ATRA, there was no significant change in the percentage of segmented nuclei (83.2 ± 8.6%) relative to ATRA treated cells (81.8 ± 6.4%) (**Figure 15A, C**). Furthermore, daily supplementation of galectin-9 + ATRA displayed a significant upregulation in the expression of *NCF1* (121.5-fold, *p<0.01*) relative to ATRA treated cells (60.9-fold) (**Figure 15D**). However, there was no significant change observed in the levels of *O*-GlcNAcylation of galectin-9 + ATRA treated cells (29.9%) relative to ATRA treated cells (64.9%) (**Figure 15E**). The ATRA treatment for the daily supplementation with galectin-9 + ATRA demonstrated an increase in the percentage of segmented nuclei (*p<0.0001*), upregulation of *NCF1* expression (*p<0.001*), and decrease in global *O*-GlcNAcylation (*p<0.01*) relative to untreated cells (**Figure 15A-E**).

3.2 HL-60 cells exhibit resistance to galectin-induced apoptosis

3.2.1 Brefeldin-A treatment of HL-60 cells results in hallmarks of apoptosis not observed with all-*trans* retinoic acid

HL-60 cells can undergo apoptosis when treated with various agents. Brefeldin A (BFA) is a lactone produced by fungi that inhibits protein transport between the endoplasmic reticulum and Golgi Apparatus by preventing association of COP-I coat vesicles (Shao et al., 1996). Previous research with HL-60 cells has shown that 0.5-10 µM BFA induced high levels of apoptosis (Andersen et al., 2016). There are several factors that change during cellular apoptosis including the condensation of DNA and changes in gene expression. In this study, the degree of apoptosis induced by BFA in HL-60 cells was assessed. HL-60 cells were treated with 0.01,0.1, 1, or 10 µM BFA for 24 hours prior to nuclear imaging and gene expression analysis.

Untreated HL-60 cells exhibited circular morphology whereas BFA treated HL-60 cells exhibited condensed morphology for apoptotic cells. HL-60 cells treated with 0.01 µM BFA exhibited no significant changes in the percentage of apoptotic cells (2.2 ± 0.1%)

relative to untreated cells (0.6 ± 0.5%). However, 0.1 µM (42.7 ± 14.7%, *p<0.001*), 1 µM (49.3 ± 7.0%, *p<0.0001*), and 10 µM (56.9 ± 7.7%, *p<0.0001*) exhibited an increase in the percentage of apoptotic cells (**Figure 16A-B**). *CHOP* and *BAX* are two proteins that demonstrate increased expression during apoptosis (Choi et al. 2010; Namba et al., 2013). RT-qPCR was performed to assess the changes in expression of *CHOP* and *BAX* of cells treated with 1 µM BFA. BFA treated cells demonstrated 141.3-fold (*p<0.0001*) upregulation in *CHOP* and 8.2-fold (*p<0.01*) upregulation in *BAX* (**Figure 16C-D**).

Previous research with ATRA has shown induced apoptosis at 1 µM ATRA (Veselská et al., 2003). HL-60 cells were treated with 1 µM ATRA for 72 hours and nuclear condensation and associated gene expression changes were assessed. ATRA treated HL-60 cells demonstrated no significant changes in apoptotic cells (2.9 ± 1.3%) relative to untreated cells (0.5 ± 0.9%) (**Figure 17A**). Additionally, there were no changes observed in the expression of both *CHOP* (1.5-fold) and *BAX* (0.9-fold) (**Figure 17B-C**).

3.2.2 Effect of recombinant galectins on HL-60 cell apoptosis

Previous research with galectins has shown induced apoptosis in immune cells. However, little is known with respect to galectin induced apoptosis in HL-60 cells. In this study, HL-60 cells were treated with dose dependent concentrations (10, 100, or 1000 ng/mL) or supplemented daily with human recombinant galectin -1 (1000 ng/mL) for 72 hours. HL-60 cells treated with recombinant galectin-1 demonstrated no change in the percentage of apoptotic cells at 10 ng/mL (0.2 ± 0.4%), with significant increases observed with 100 ng/mL (1.4 ± 0.3%, *p<0.05*) and 1000 ng/mL (1.0 ± 0.4%, *p<0.05*) relative to untreated cells (0.4 ± 0.3%) (**Figure 18A**). Furthermore, HL-60 cells treated with 1000 ng/mL of galectin-1 demonstrated no significant changes in *CHOP* (1.1-fold) or *BAX* (3.0-fold) expression relative to untreated cells (**Figure 18B-C**). Additionally, daily supplemented HL-60 cells with 1000 ng/mL of galectin-1 exhibited no significant change in the percentage of apoptotic cells (1.3 ± 0.6%) relative to untreated cells (1.2 ± 0.4%) (**Figure 18D**). Daily supplemented HL-60 cells also demonstrated no significant changes in *CHOP* (1.2-fold) or *BAX* (1.9-fold) expression relative to untreated cells (**Figure 18E-F**).

To provide further insights into galectins and apoptosis in HL-60 cells, treatments with

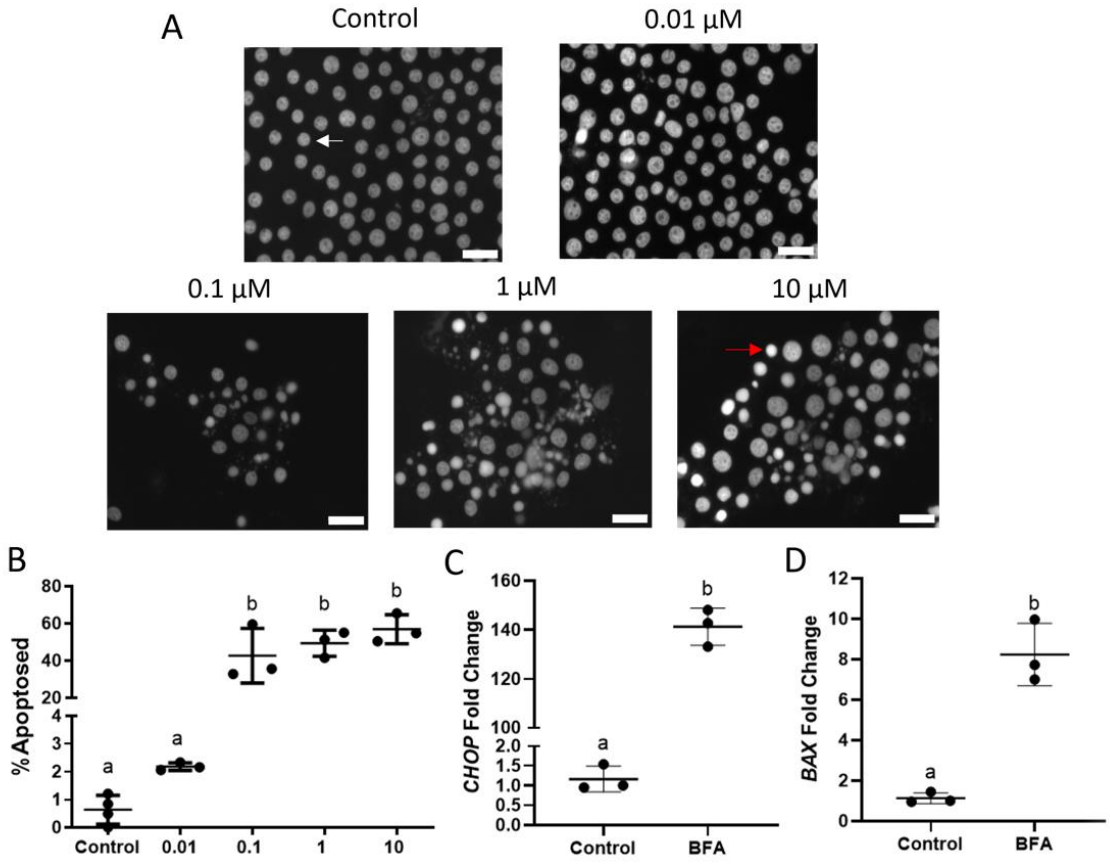

Figure 16: Brefeldin-A induced apoptosis of HL-60 cells.

HL-60 cells were treated with either 0.01, 0.1, 1, or 10 µM BFA for 24 hr. (A) Nuclear morphology of untreated and BFA treated cells were visualized by DAPI staining with the scale bar representing 20 µm. Non-apoptotic cells demonstrated circular nuclei (white arrow) and apoptotic cells demonstrated condensed nuclei (red arrow). (B) The apoptotic index was determined as the percentage of nuclei demonstrating DNA condensation based on BFA treatment (220 – 480 cells counted). Changes in the expression of genetic markers of apoptosis *CHOP* (C) and *BAX* (D) were quantified by RT-qPCR with the Livak method ($2^{-\Delta\Delta Ct}$) using *ACTB* as an internal control. Data are presented as means ± SD, n=3. Statistical differences were determined using the unpair Student's t test and One-way ANOVA followed by Tukey's HSD test and are represented as different letters with a $p<0.05$.

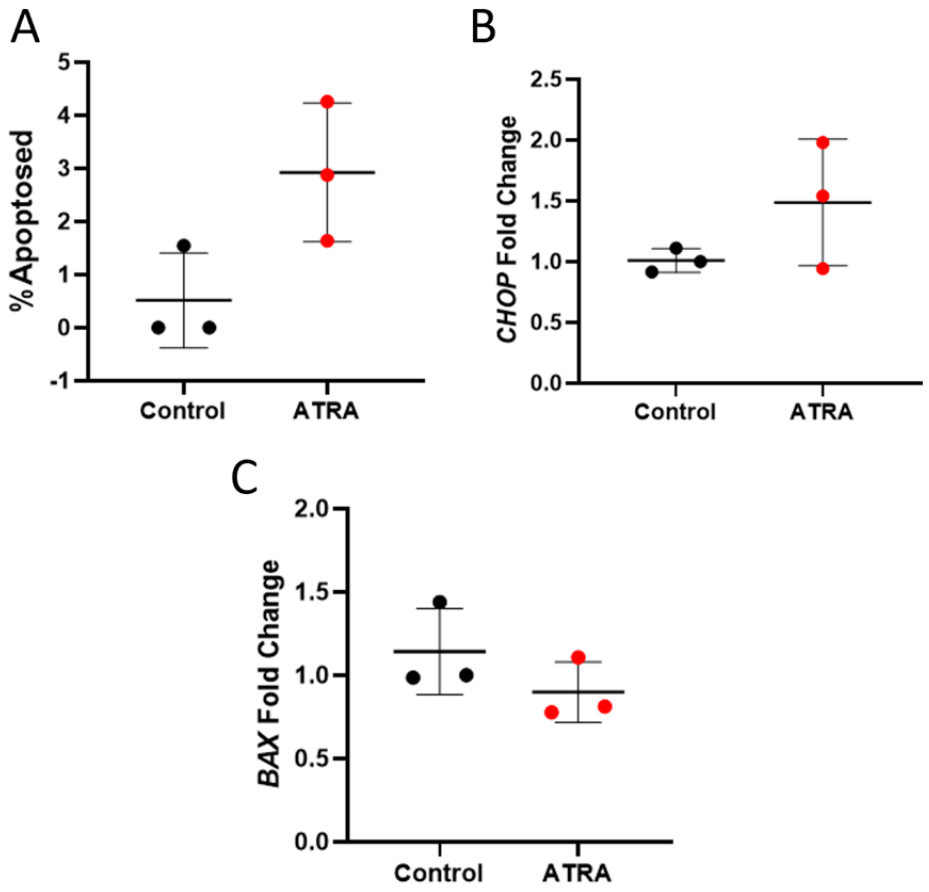

Figure 17: ATRA did not induce apoptosis in HL-60 cells.

HL-60 cells were treated with 1 µM ATRA to induce granulocytic differentiation for 72 h. (A) The apoptotic index was determined as the percentage of nuclei demonstrating DNA condensation (100 – 400 cells counted). Apoptotic gene markers *CHOP* (B) and *BAX* (C) were quantified by RT-qPCR with the Livak method ($2^{-\Delta\Delta Ct}$) using *ACTB* as an internal control. Data are presented as the mean ± SD, n=3. Significant differences were determined using unpaired Student's t-test.

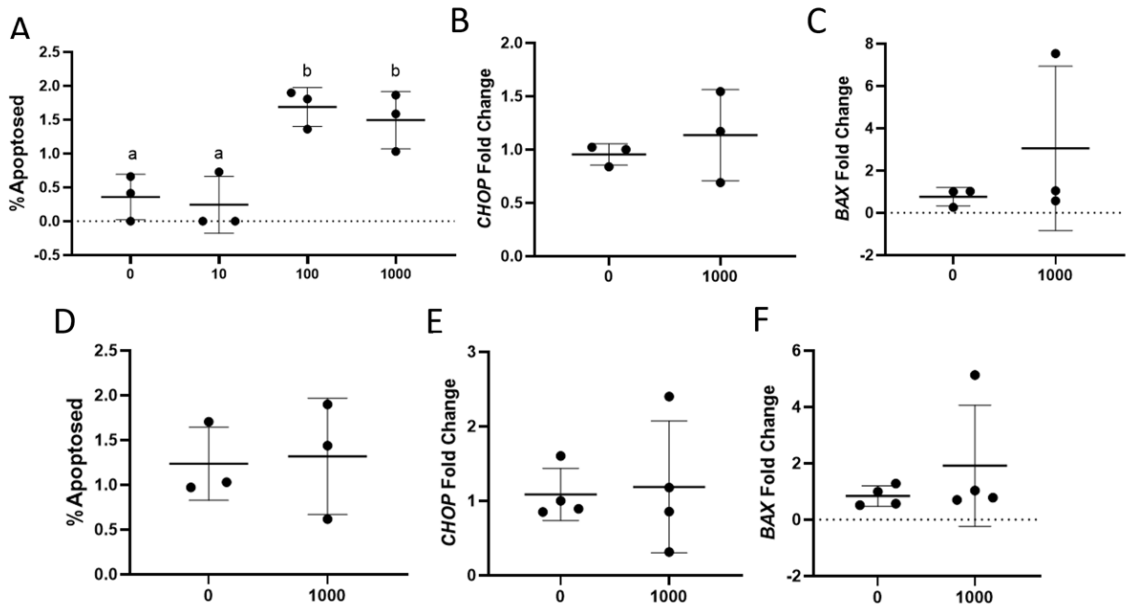

Figure 18: HL-60 cells exhibit resistance to galectin-1 induced apoptosis.

HL-60 cells were treated with dose dependent concentrations of 10, 100, or 1000 ng/mL or daily supplemented with 1000 ng/mL recombinant galectin-1 72 hr. The apoptotic index was determined as the percentage of nuclei demonstrating DNA condensation of dose-dependent (130 – 205 cells counted) (A) and daily supplementation (150 – 300 cells counted) (D). Apoptotic gene markers *CHOP* for dose dependent (B) and daily supplementation (E); and *BAX* for dose dependent (C) and daily supplementation (F) were quantified by RT-qPCR with the Livak method ($2^{-\Delta\Delta Ct}$) using *ACTB* as an internal control. Data are presented as mean ± SD, n=3-4. Significant differences were determined using unpaired Student's t test and One-way ANOVA followed by Tukey's HSD test and are represented as different letters with a $p<0.05$.

galectin-3 were also assessed. Dose dependent concentrations (10, 100, or 1000 ng/mL) of galectin-3 over 72 hours exhibited no significant changes in the percentage of apoptotic cells (0.5 ± 0.3, 0.8 ± 0.3, 1.1 ± 0.4%, respectively) relative to untreated cells (0.6 ± 0.6%) (**Figure 19A**). Furthermore, HL-60 cells treated with 1000 ng/mL of galectin-3 demonstrated no significant changes in *CHOP* (1.0-fold) or *BAX* (0.6-fold) gene expressions relative to untreated cells (**Figure 19B-C**). HL-60 cells were also supplemented daily with 1000 ng/mL of galectin-3 over 72 hours. Daily supplemented cells exhibited no significant change in the percentage of apoptotic cells (0.6 ± 0.1%) relative to untreated cells (0.3 ± 0.4%) (**Figure 19D**). Furthermore, daily supplemented cells demonstrated no significant changes in *CHOP* (0.6-fold) or *BAX* (0.8-fold) gene expressions relative to untreated cells (**Figure 19E-F**).

HL-60 cells were also treated with dose dependent concentrations (10, 100, or 1000 ng/mL) or daily supplemented with human recombinant galectin-8 (1000 ng/mL) over 72 hours. HL-60 cells treated with 1000 ng/mL of galectin-8 exhibited a significant increase in the percentage of apoptotic cells (3.1 ± 0.7%, $p<0.01$) that was not observed with 10 ng/mL (1.0 ± 0.6%) or 100 ng/mL (2.0 ± 0.6%) relative to untreated cells (0.7 ± 0.3%) (**Figure 20A**). However, HL-60 cells treated with 1000 ng/mL of galectin-8 demonstrated no significant changes in *CHOP* (1.4-fold) or *BAX* (1.1-fold) gene expressions relative to untreated cells (**Figure 20B-C**). Additionally, HL-60 cells daily supplemented with 1000 ng/mL of galectin-8 exhibited a significant increase in the percentage of apoptotic cells (6.1 ± 1.3%, $p<0.01$) relative to untreated cells (1.3 ± 0.8%) (**Figure 20D**). Furthermore, HL-60 cells daily supplemented with galectin-8 demonstrated no significant changes in *CHOP* (1.2-fold) or *BAX* (1.2-fold) gene expressions relative to untreated cells (**Figure 20E-F**).

Finally, the effects of galectin-9 on HL-60 cells apoptosis were also assessed. HL-60 cells were treated with the dose dependent concentrations (10, 100 or 1000 ng/mL) or daily supplemented with human recombinant galectin-9 (1000 ng/mL) for 72 hours. Dose dependent concentrations exhibited no significant changes in the percentage of apoptotic cells (0.5 ± 0.4, 0.6 ± 1.1, 1.4 ± 2.3%, respectively) relative to untreated cells (0.5 ± 0.2%)

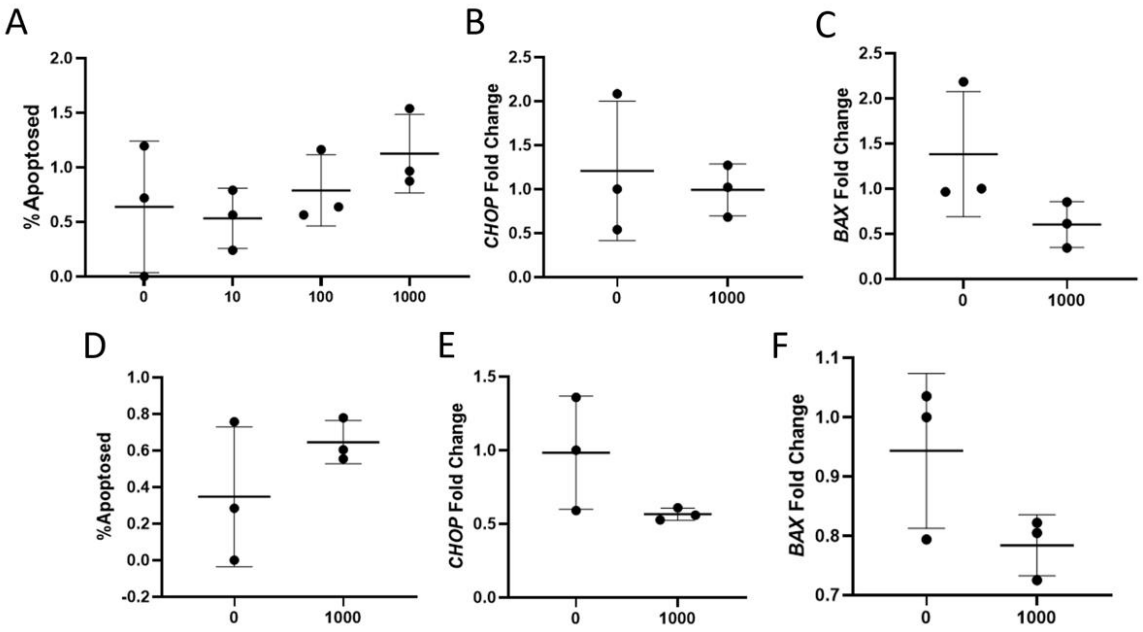

Figure 19: HL-60 cells exhibit resistance to galectin-3 induced apoptosis.

HL-60 cells were treated with dose dependent concentrations of 10, 100, or 1000 ng/mL or daily supplemented with 1000 ng/mL recombinant galectin-3 72 hr. The apoptotic index was determined as the percentage of nuclei demonstrating DNA condensation of dose-dependent (170 – 360 cells counted) (A) and daily supplementation (340 – 400 cells counted) (D). Apoptotic gene markers *CHOP* for dose dependent (B) and daily supplementation (E); and *BAX* for dose dependent (C) and daily supplementation (F) were quantified by RT-qPCR with the Livak method ($2^{-\Delta\Delta Ct}$) using *ACTB* as an internal control. Data are presented as mean ± SD, n=3-4. Significant differences were determined using unpaired Student's t test and One-way ANOVA followed by Tukey's HSD test.

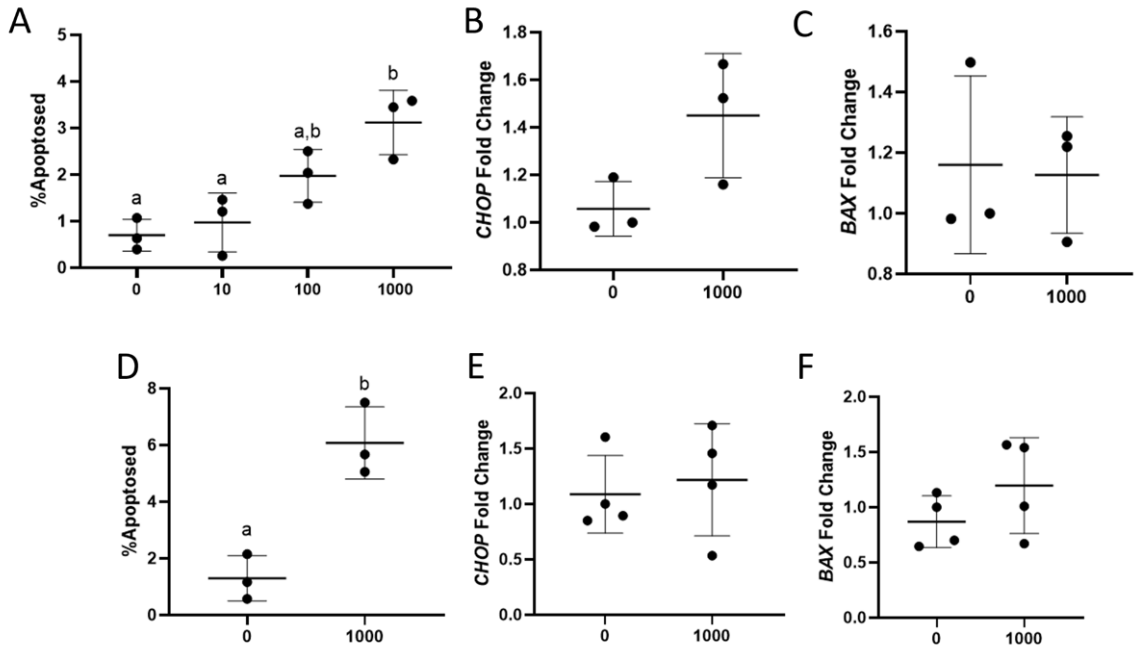

Figure 20: HL-60 cells exhibit resistance to galectin-8 induced apoptosis.

HL-60 cells were treated with dose dependent concentrations of 10, 100, or 1000 ng/mL or daily supplemented with 1000 ng/mL recombinant galectin-8 72 hr. The apoptotic index was determined as the percentage of nuclei demonstrating DNA condensation of dose-dependent (220 – 540 cells counted) (A) and daily supplementation (170 – 280 cells counted) (D). Apoptotic gene markers *CHOP* for dose dependent (B) and daily supplementation (E); and *BAX* for dose dependent (C) and daily supplementation (F) were quantified by RT-qPCR with the Livak method ($2^{-\Delta\Delta Ct}$) using *ACTB* as an internal control. Data are presented as mean ± SD, n=3-4. Significant differences were determined using unpaired Student's t test and One-way ANOVA followed by Tukey's HSD test and are represented as different letters with a $p<0.05$.

(**Figure 21A**). Furthermore, HL-60 cells treated with 1000 ng/mL of galectin-9 demonstrated no significant changes in *CHOP* (1.3-fold) or *BAX* (1.3-fold) gene expressions relative to untreated cells (**Figure 21B-C**). Additionally, HL-60 cells daily supplemented with 1000 ng/mL of galectin-9 exhibited no significant changes in the percentage of apoptotic cells (2.8 ± 1.2%) relative to untreated cells (1.1 ± 0.5%) (**Figure 21D**). HL-60 cells daily supplemented with galectin-9 also demonstrated no significant changes in *CHOP* (0.5-fold) or *BAX* (0.9-fold) gene expressions relative to untreated cells (**Figure 21E-F**).

3.3 *In silico* analysis of the relationship between galectins and cell differentiation biomarkers in acute myeloid leukemia and FAB subtypes

There are various galectins expressed in bone marrow and AML cells. Analysis of TCGA data indicated gene expression of galectin 1, 3, 4, 7, 8, 9, 10, and 12 in both bone marrow and AML cohorts. Differential expression analysis revealed no significant changes in *LGALS* expression, except for *LGALS9* demonstrating a significant upregulation (1.1-fold, $p<0.05$) relative to bone marrow cohorts (**Table 1**) (**Figure 22A**). Additionally, *O*-GlcNAc cycle enzymes, granulocytic differentiation markers, and most stemness markers demonstrated no significant changes in gene expression in AML relative to bone marrow cohorts. Nanog homeobox (*NANOG*) was the only stemness marker revealed to be significantly downregulated in AML cohorts (0.9-fold, $p<0.0001$) relative to bone marrow control (**Table 1**) (**Figure 22B-C**).

To provide a further understanding of galectin gene expression in AML, patient data were separated into individual FAB subtype classification including M0-M5. Differential expression analysis of the FAB subtypes revealed that there were no significant changes in galectin gene expression specifically in the M0-M2 subtype, while the M3-M5 subtypes demonstrated significant changes in galectin gene expression relative to bone marrow cohorts. The M3 subtype exhibited the largest total of significant changes in galectin gene expression. *LGALS1* in the M4 (2.1-fold, $p<0.001$) and M5 (4.2-fold, $p<0.0001$) subtypes, and *LGALS3* in the M4 (2.5-fold, $p<0.001$) and M5 (4.5-fold, $p<0.01$) subtypes demonstrated a significant upregulation in gene expression relative to bone marrow

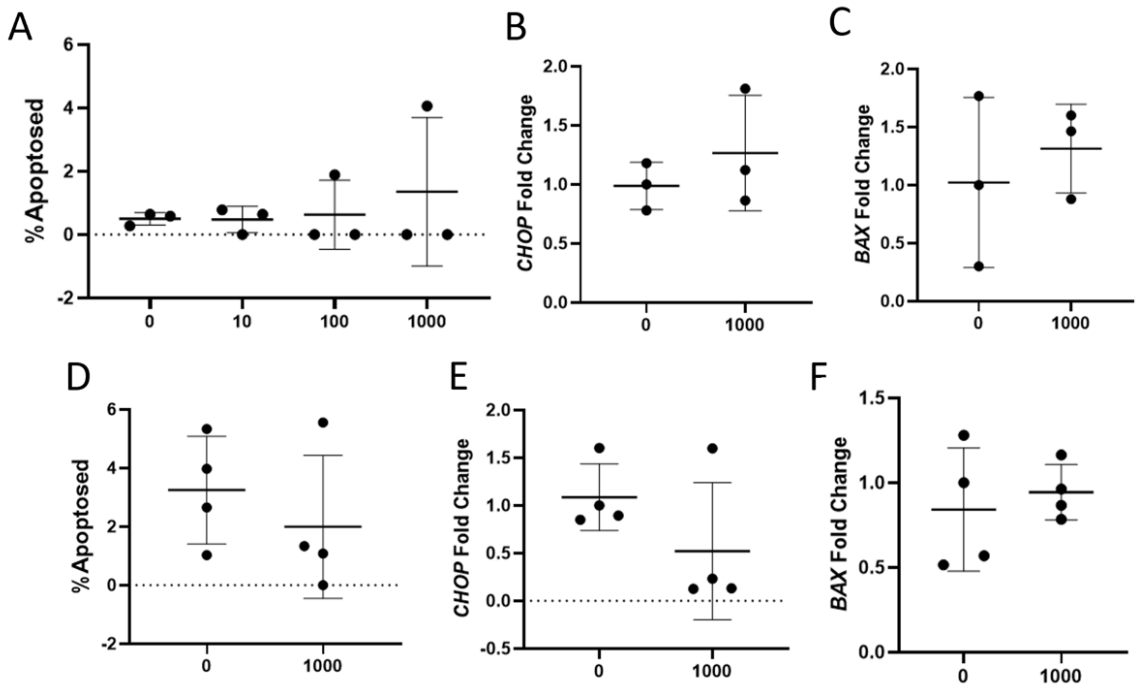

Figure 21: HL-60 cells exhibit resistance to galectin-9 induced apoptosis.

HL-60 cells were treated with dose dependent concentrations of 10, 100, or 1000 ng/mL or daily supplemented with 1000 ng/mL recombinant galectin-9 72 hr. The apoptotic index was determined as the percentage of nuclei demonstrating DNA condensation of dose-dependent (100 – 380 cells counted) (A) and daily supplementation (140 – 290 cells counted) (D). Apoptotic gene markers *CHOP* for dose dependent (B) and daily supplementation (E); and *BAX* for dose dependent (C) and daily supplementation (F) were quantified by RT-qPCR with the Livak method ($2^{-\Delta\Delta Ct}$) using *ACTB* as an internal control. Data are presented as mean ± SD, n=3-4. Significant differences were determined using unpaired Student's t test and One-way ANOVA followed by Tukey's HSD test.

Figure 22: Differential gene expression analysis of TCGA AML cohorts .

GTEx bone marrow (BM) and TCGA AML RNA-Seq data were retrieved from recount2 and RUVg normalized in R studio prior to statistical analysis. Various galectin genes (*LGALS*) (A), *O*-GlcNAc related enzymes *(OGA, OGT, GFAT1*) and granulocyte differentiation marker genes (*NCF1/2, CYBA/N, MPO*) (B), as well as stemness marker genes (*OCT4, NANOG, FOX2, C-MYC, KLF4, CD34*) (C) were $\log_2$ transformed to assess expression. Data is presented as violin plots, n=70-126. Statistical significance was determined using the nonparametric Mann Whitney test. *$p \leq 0.05$, ****$p \leq 0.0001$.

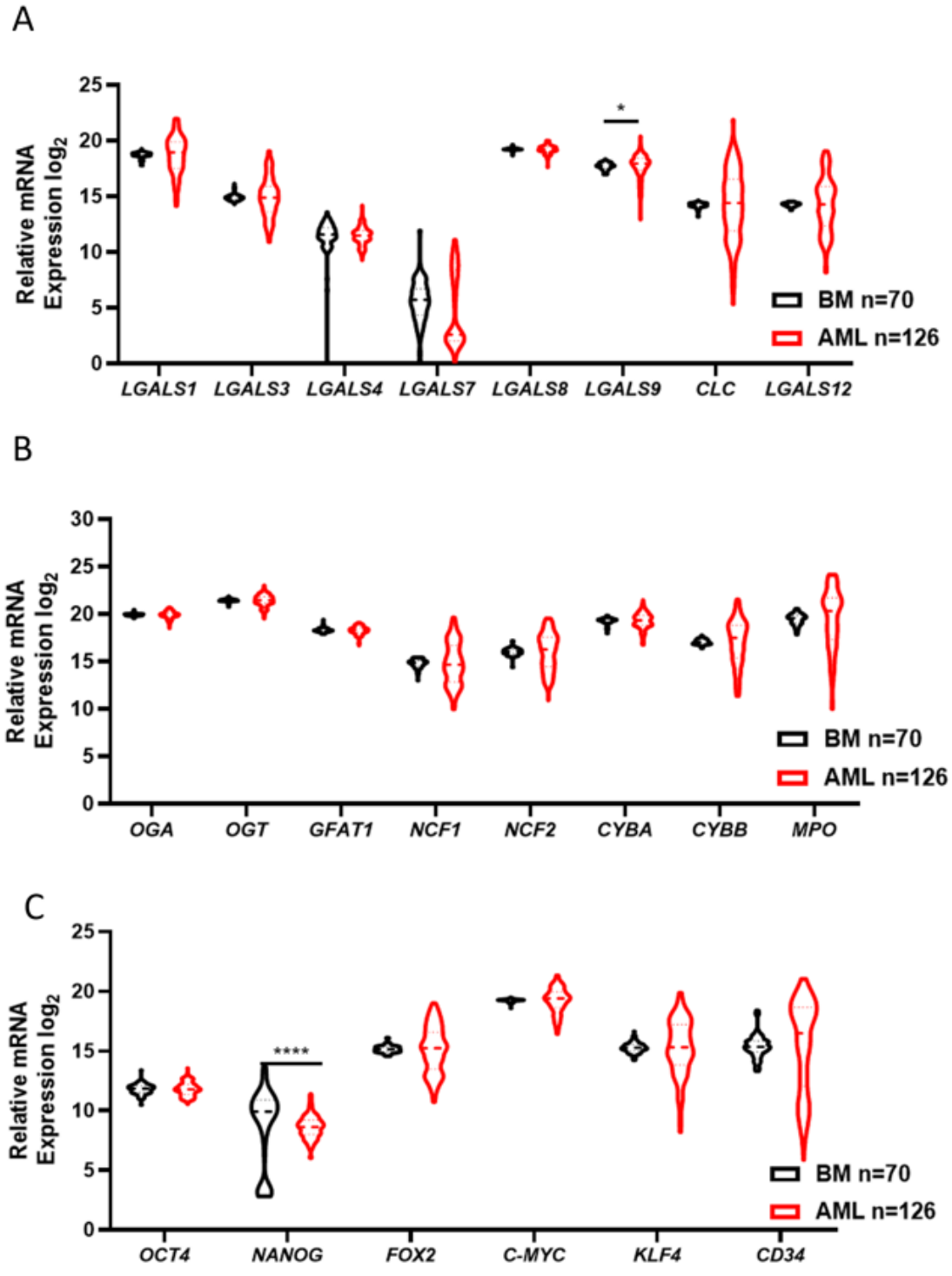
A
Relative mRNA Expression log2
25
20
15
10
5
0
*
BM n=70
AML n=126
LGALS1
LGALS3
LGALS4
LGALS7
LGALS8
LGALS9
CLC
LGALS12
B
Relative mRNA Expression log2
30
25
20
15
10
5
0
BM n=70
AML n=126
OGA
OGT
GFAT1
NCF1
NCF2
CYBA
CYBB
MPO
C
Relative mRNA Expression log2
25
20
15
10
5
0
****
BM n=70
AML n=126
OCT4
NANOG
FOX2
C-MYC
KLF4
CD34

Table 1: Subtype-specific gene expression patterns in TCGA cohort of AML.

Gene	Cell Type						
	AML	**M0**	**M1**	**M2**	**M3**	**M4**	**M5**
Galectins							
LGALS1	0.0414	-0.668	-0.215	-0.829	-0.583	**1.0458*** **	**2.0713**** **
LGALS3	0.0102	-0.845	-0.903	-0.698	0.447	**1.303*** **	**2.170****
LGALS4	0.107	0.184	-0.0215	-0.0323	**1.0852***	-0.314	0.4814
LGALS7	-0.972	-0.578	-0.767	-1.292	-1.568	-1.407	0.0228
LGALS8	-0.0137	-0.0548	-0.0507	0.0513	**-0.298****	0.0769	0.0833
LGALS9	**0.0692***	-0.157	0.343	0.232	**-1.938*** **	0.215	**0.713****
CLC	0.0119	-0.713	-0.123	0.634	0.777	0.649	-1.966
LGALS12	-0.0292	-1.345	-0.907	-0.786	**3.991**** **	-0.0059	1.448
***O*-GlcNAc related cycle enzymes**							
OGA	-0.0195	0.241	0.0146	0.0177	-0.033	0.00096	**-0.428***
OGT	-0.0132	0.169	0.0741	-0.0047	0.393	-0.121	**-0.599***
GFAT1	-0.055	-0.0472	-0.170	-0.0643	**0.312***	0.0555	-0.236
Granulocyte differentiation markers							
NCF1	0.0353	**-1.497***	-0.442	-0.591	**-1.816***	**1.998*** **	**2.374****
NCF2	0.00597	-0.834	-0.606	-0.477	-1.619	**1.744**** **	**1.961*** **
CYBA	0.0538	**-0.878***	0.0362	-0.200	0.178	0.274	**0.972*** **
CYBB	0.02075	-0.971	-1.0602	-0.637	0.426	**2.0047**** **	1.548
MPO	0.171	**-3.890****	0.737	1.041	**4.294**** **	-0.414	-2.217
Stemness markers							
OCT4	0.00818	-0.303	0.105	-0.0749	-0.219	0.0208	0.374
NANOG	**-0.0791**** **	-0.188	**-0.338****	**-0.153***	-0.284	0.185	0.593
FOX2	-0.0355	0.976	0.112	-0.346	-0.542	-0.489	0.509
C-MYC	0.0142	-0.478	0.345	0.536	-0.0301	-0.341	-0.898
KLF4	0.0396	-1.054	-0.648	-0.937	-0.982	**1.889**** **	**2.739**** **
CD34	0.0876	**3.391*** **	-0.302	**2.612**** **	-3.407	0.139	**-4.056***
Housekeeping gene							
HMBS	0.0197	-0.104	0.127	0.133	0.186	-0.286	-0.0475

Notes: GTEx bone marrow and TCGA AML RNA-Seq data were retrieved from recount2 and RUVg normalized in R studio and $\log_2$ transformed in Microsoft excel prior to statistical analysis. The $\log_2$ fold change was calculated and compared to bone marrow control for all AML cohorts (n=126) and molecular subtypes including M0 (n=12), M1 (n=36), M2 (n=29), M3 (n=12), M4 (n=22), and M5 (n=14). Statistical significance was determined using the nonparametric Kruskal-Wallis test followed by Dunn's multiple comparisons. *$*p \leq 0.05$, $**p \leq 0.01$, $***p \leq 0.001$, $****p \leq 0.0001$.*

cohorts. Additionally, *LGALS8 (*0.3-fold, *p<0.001)* and *LGALS9* (0.3-fold, *p<0.001)* both demonstrated a significant downregulation in the M3 subtype relative to bone marrow cohorts. *LGALS4* (2.1-fold, *p<0.05*) and *LGALS12* both demonstrated a significant upregulation in the M3 subtype relative to bone marrow cohorts. Furthermore, a *LGALS12/LGALS9* ratio was specifically upregulated in the M3 FAB subtype that was not seen in other FAB subtypes or in bone marrow cohorts (*p<0.0001*). However, when looking at *LGALS7* and *CLC* FAB subtype expression profiles, there were no significant changes in any of the FAB subtypes relative to bone marrow cohorts (**Table 1**) (**Figure 23**).

To further evaluate the expression patterns of galectins in AML, differential expression analysis of *O*-GlcNAc cycle enzymes, granulocyte differentiation markers and stemness markers expression profiles were analyzed for FAB subtypes M0-M5. There were significant changes observed with downregulation of *O*-GlcNAc cycle enzymes *OGA* (0.7-fold, *p<0.05*) and *OGT* (0.7-fold, *p<0.05*) in the M5 subtype, and a significant upregulation of *GFAT1* (1.2-fold, *p<0.05*) in the M3 subtype relative to bone marrow cohorts (**Table 1**) (**Figure S2**). Additionally, an *OGT/GFAT1* ratio was significantly downregulated in the M0 FAB subtype that was not observed in other FAB subtypes or bone marrow cohorts (*p<0.0001*) (**Figure S2**). Furthermore, there were significant upregulations in the gene expression of granulocyte differentiation markers *NCF1* in the M4 (4.0-fold, *p<0.001*) and M5 (5.2-fold, *p<0.01*) subtypes, and *NCF2* in the M4 (3.4-fold, *p<0.0001*) and M5 (3.9-fold, *p<0.001*) subtypes relative to bone marrow cells (**Table 1**) (**Figure 23**). Other granulocytic differentiation markers and stemness markers including *CYBB, CYBA, MPO, KLF4,* and *CD34* demonstrated significant changes in the M3-M5 FAB subtypes, while *NCF1, NCF2, MPO, NANOG* and *CD34* demonstrated significant changes in expression in the M0-M2 FAB subtypes (**Table 1**) (**Figure S3**).

The relationship between galectin genes and the other markers of interest in this study have yet to be investigated. Therefore, pairwise correlations were performed between the various genes of interest of both AML and bone marrow cohorts. Correlation strengths of genes in bone marrow and AML cohorts are represented as heatmaps (**Figure 24A**). There were significant changes in the pairwise correlations of many genes when comparing

Figure 23: Differential expression analysis of TCGA AML subtypes reveals changes in LGALS gene expression in M3-M5 subtypes.

GTEx bone marrow (BM) and TCGA AML RNA-Seq data were retrieved from recount2 and RUVg normalized in R studio and $\log_2$ transformed in Microsoft excel prior to statistical analysis. The subtypes investigated include M0 (n=12), M1 (n=36), M2 (n=29), M3 (n=12), M4 (n=22), and M5 (n=14) and compared to BM control (n=70). Various galectin genes including *LGALS1, LGALS3, LGALS4, LGALS7, LGALS8, LGALS9, CLC, LGALS12,* and a ratio of *LGALS12/LGALS9* were examined. Granulocyte differentiation markers *NCF1* and *NCF2* were also examined. Data is represented as violin plots. Statistical significance was determined using the nonparametric Kruskal-Wallis test followed by Dunn's multiple comparisons and are represented as different letters with a $p<0.05$.

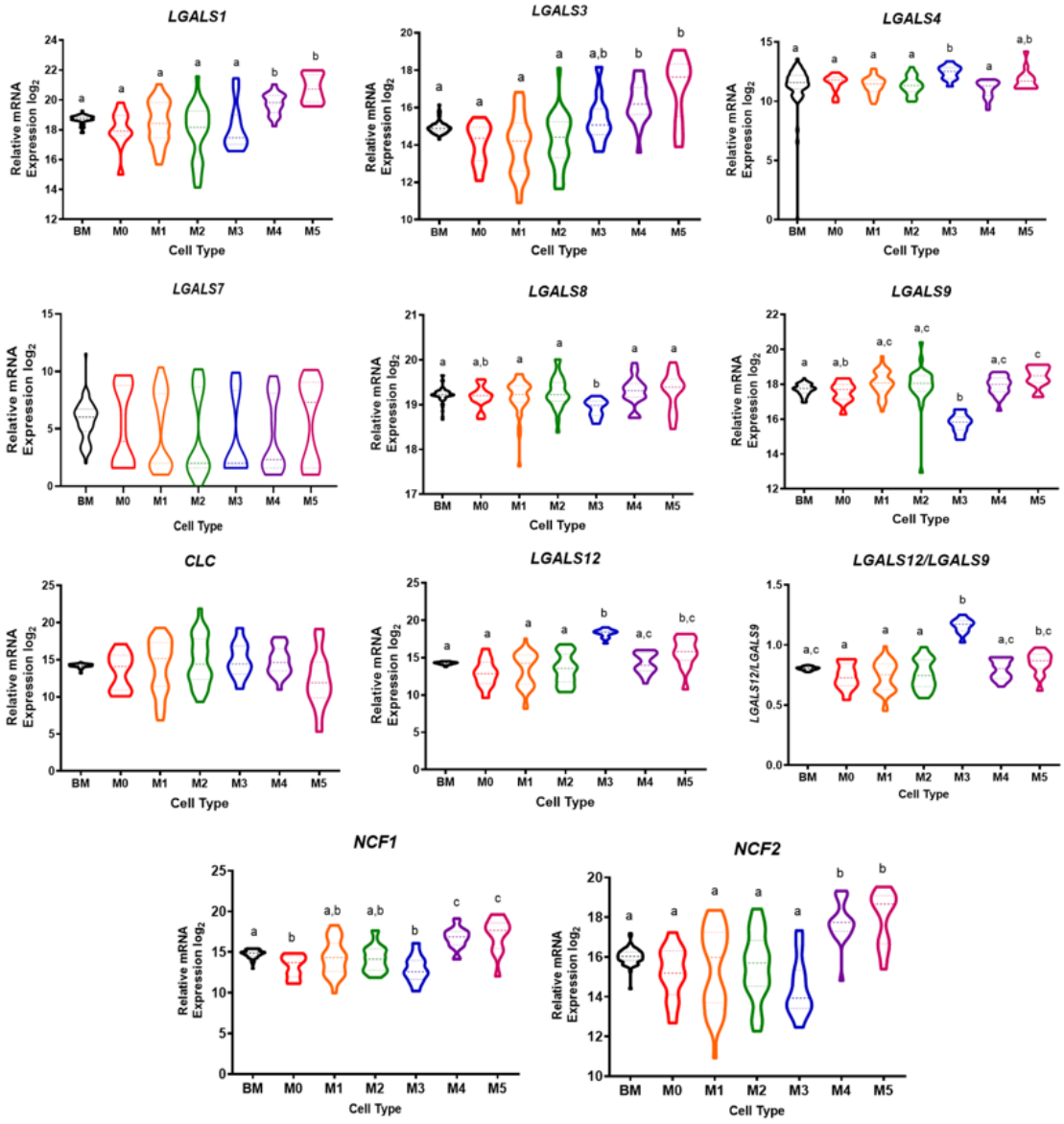
LGALS1
LGALS3
LGALS4
LGALS7
LGALS8
LGALS9
CLC
LGALS12
LGALS12/LGALS9
NCF1
NCF2
Relative mRNA Expression log2
LGALS12/LGALS9
Cell Type
BM M0 M1 M2 M3 M4 M5

Figure 24: Spearman's correlation of bone marrow and AML cohorts reveals global changes in glycobiological associations in AML patients.

GTEx bone marrow (BM) and TCGA AML RNA-Seq data were retrieved from recount2 and RUVg normalized in R studio and the data $\log_2$ transformed prior to statistical analysis. (A) Heatmaps for Spearman's correlation (ρ) of both BM (n=70) and AML (n=126) samples. (B) Changes in correlation between BM to AML were evaluated in R studios using the "cocor" package with blue indicating a change to positive correlation, red indicating a change to negative correlation, yellow indicating a change in correlation strength, and green indicating a loss in correlation in AML cohorts. *$*p \leq 0.05$, $**p \leq 0.01$, $***p \leq 0.001$, $****p \leq 0.0001$.*

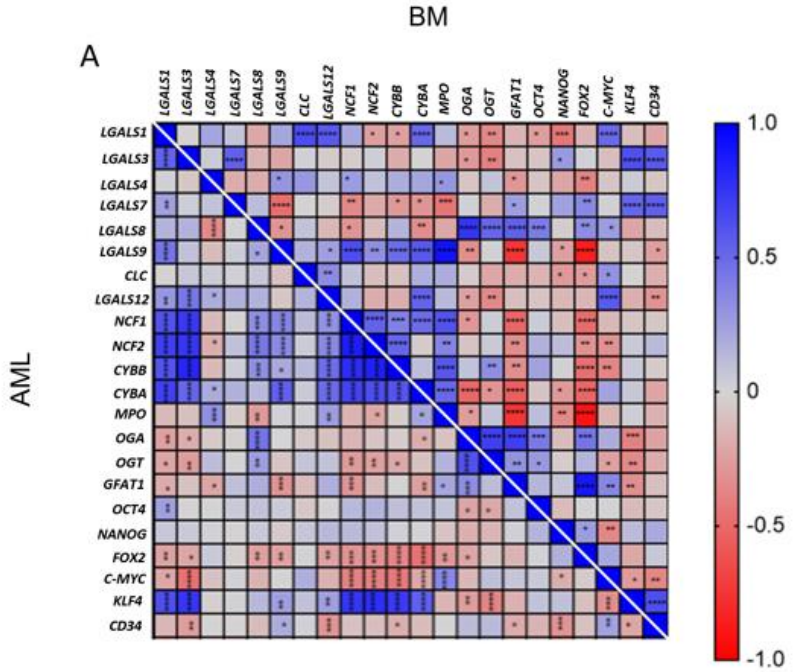
BM
A
AML
LGALS1
LGALS3
LGALS4
LGALS7
LGALS8
LGALS9
CLC
LGALS12
NCF1
NCF2
CYBB
CYBA
MPO
OGA
OGT
GFAT1
OCT4
NANOG
FOX2
C-MYC
KLF4
CD34
1.0
0.5
0
-0.5
-1.0

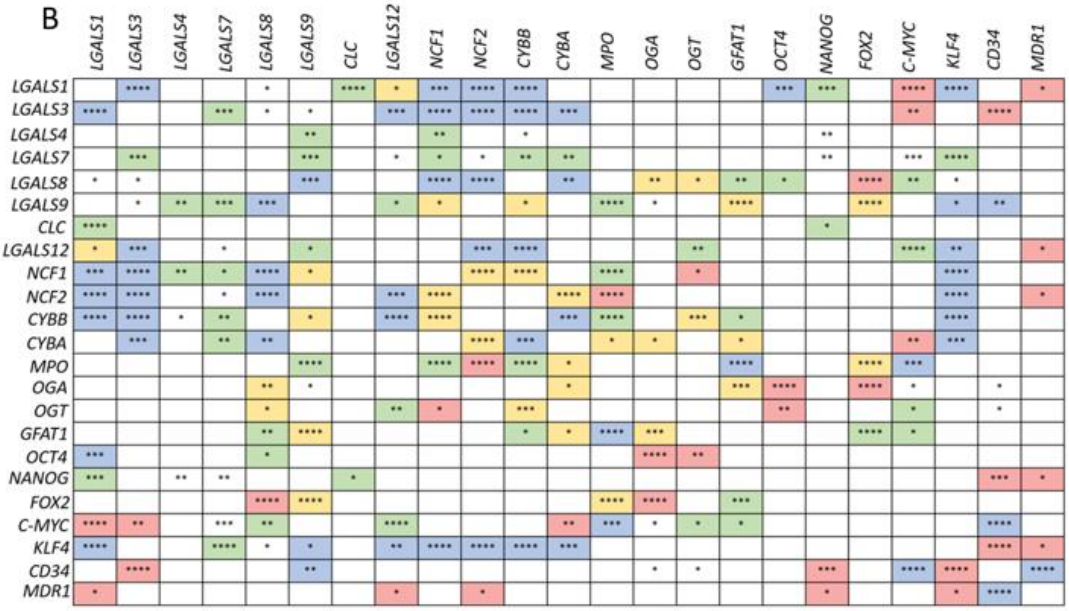
B
LGALS1
LGALS3
LGALS4
LGALS7
LGALS8
LGALS9
CLC
LGALS12
NCF1
NCF2
CYBB
CYBA
MPO
OGA
OGT
GFAT1
OCT4
NANOG
FOX2
C-MYC
KLF4
CD34
MDR1

between bone marrow and AML cohorts (**Figure 24B**). When looking particularly at the correlations between galectin genes, there were significant changes observed with a gain of positive association with *LGALS1* and *LGALS3* (*p<0.0001*), with *LGALS3* and *LGALS12* (*p<0.001*), with *LGALS8* and *LGALS9* (*p<0.001*), and a loss of association with *LGALS1* and *CLC* relative to bone marrow cohorts (**Figures 24, 25**). Additionally, there were significant changes in the correlation of galectin genes to granulocyte differentiation markers. More specifically, there was a significant correlation switch observed of a gain of positive association of *LGALS1* with *NCF1* (*p<0.001*) and *NCF2* (*p<0.0001*), *LGALS3* with *NCF1* (*p<0.0001*) and *NCF2* (*p<0.0001*), and *LGALS8* with *NCF1* (*p<0.0001)* and *NCF2* (*p<0.0001*) with reference to bone marrow cohort (**Figures 24, 26**).

To conclude the analysis of galectin gene expression in AML, patient survival was examined relative to galectin median gene expression of all AML cohorts and the M0-M5 FAB subtypes. Examining all AML cohorts revealed that an above median expression of *LGALS1* was significantly indicated of poor prognosis (*p<0.0001*) (**Figure 27A**). However, there were no other significant indications of prognosis observed for the expression of other galectin genes (**Figure S5**). When examining the M1-M5 FAB subtypes, there were no significant indications of prognosis observed for all galectin genes (Figure S10-15). However, when looking at the M0 FAB subtype, above median expression of *LGALS1* (*p<0.01*), *LGALS4* (*p<0.05*), and *CLC* (*p<0.05*) were significantly indicative of poor prognosis (**Figure 27B-D**).

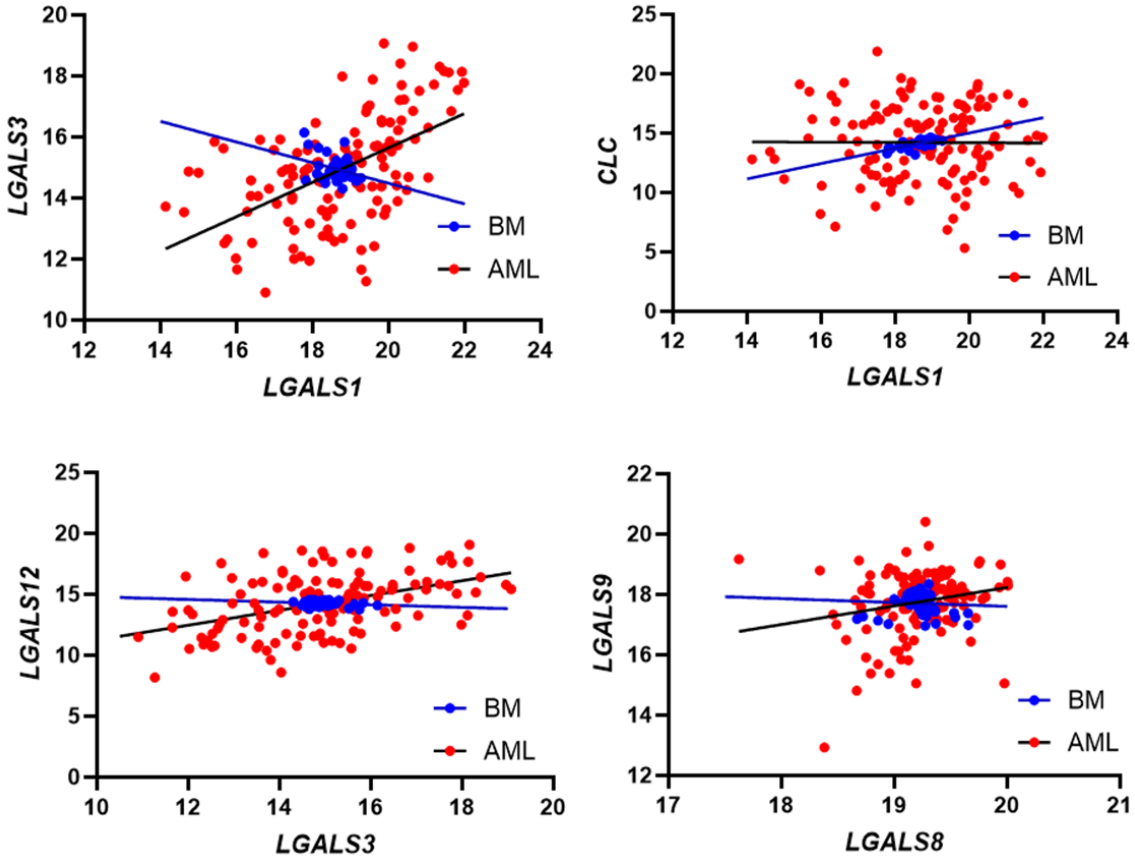

Figure 25: Pairwise scatter plots of Spearman's correlation indicates a change in LGALS gene expression regulation in AML patients.

GTEx bone marrow (BM) and TCGA AML RNA-Seq data were retrieved from recount2 and RUVg normalized in R studio and the data $\log_2$ transformed prior to statistical analysis. Correlations and regression line analysis between *LGALS1* and *LGALS3*, *LGALS1* and *CLC*, *LGALS3* and *LGALS12*, and *LGALS8* and *LGALS9* were evaluated for both BM (blue, n=70) and AML (red/black, n=126) galectin gene expression.

Figure 26: Pairwise scatter plots of Spearman's correlation indicates a change in LGALS and NCF1/2 gene expression regulation in AML patients.

GTEx bone marrow (BM) and TCGA AML RNA-Seq data were retrieved from recount2 and RUVg normalized in R studio and the data $\log_2$ transformed prior to statistical analysis. Correlations and regression line analysis between *LGALS1* and *NCF1/2*, *LGALS3* and *NCF1/2*, and *LGALS8* and *NCF1/2* were evaluated for both BM (blue, n=70) and AML (red/black, n=126) gene expressions.

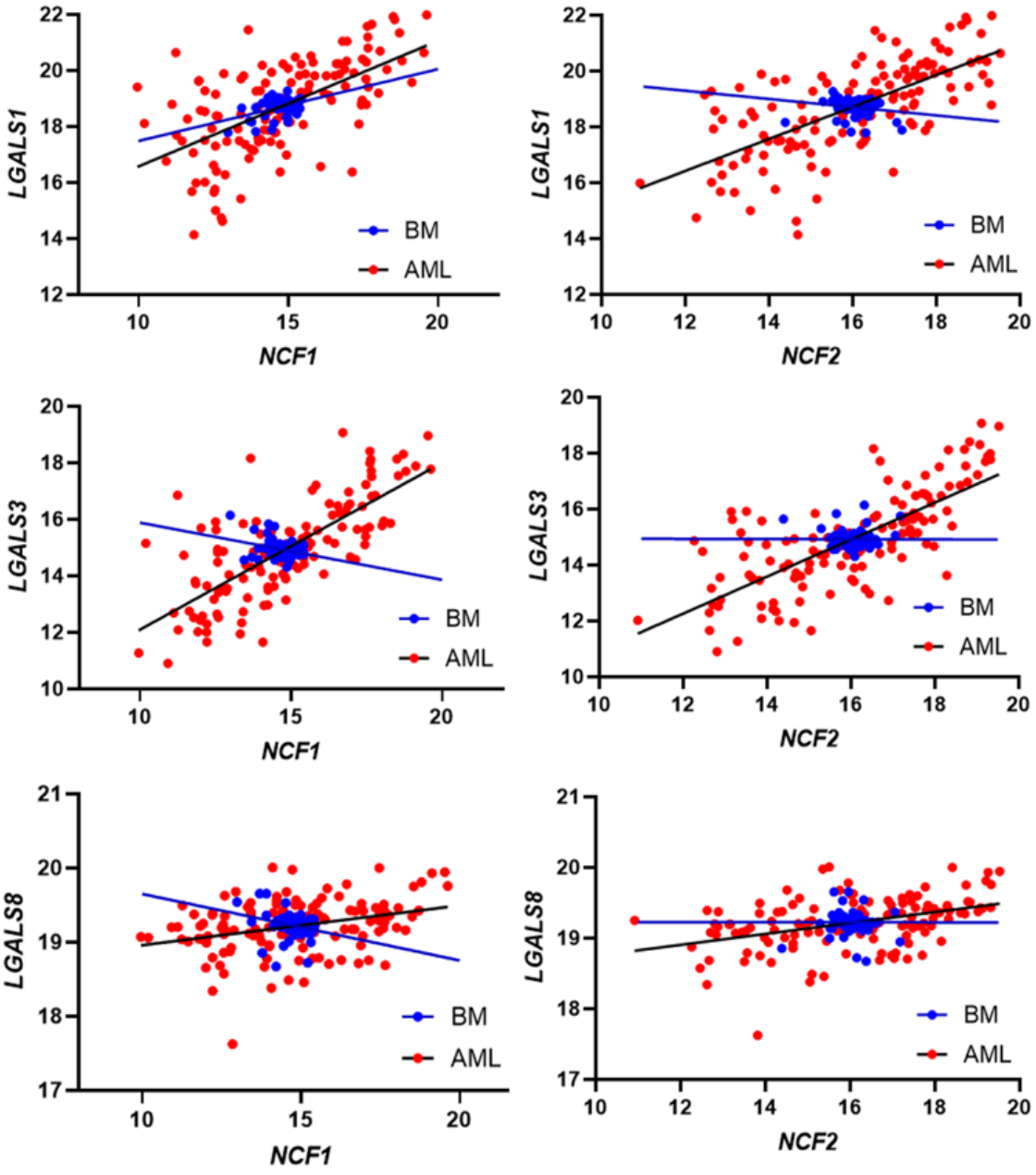
LGALS1
NCF1
BM
AML
LGALS1
NCF2
BM
AML
LGALS3
NCF1
BM
AML
LGALS3
NCF2
BM
AML
LGALS8
NCF1
BM
AML
LGALS8
NCF2
BM
AML

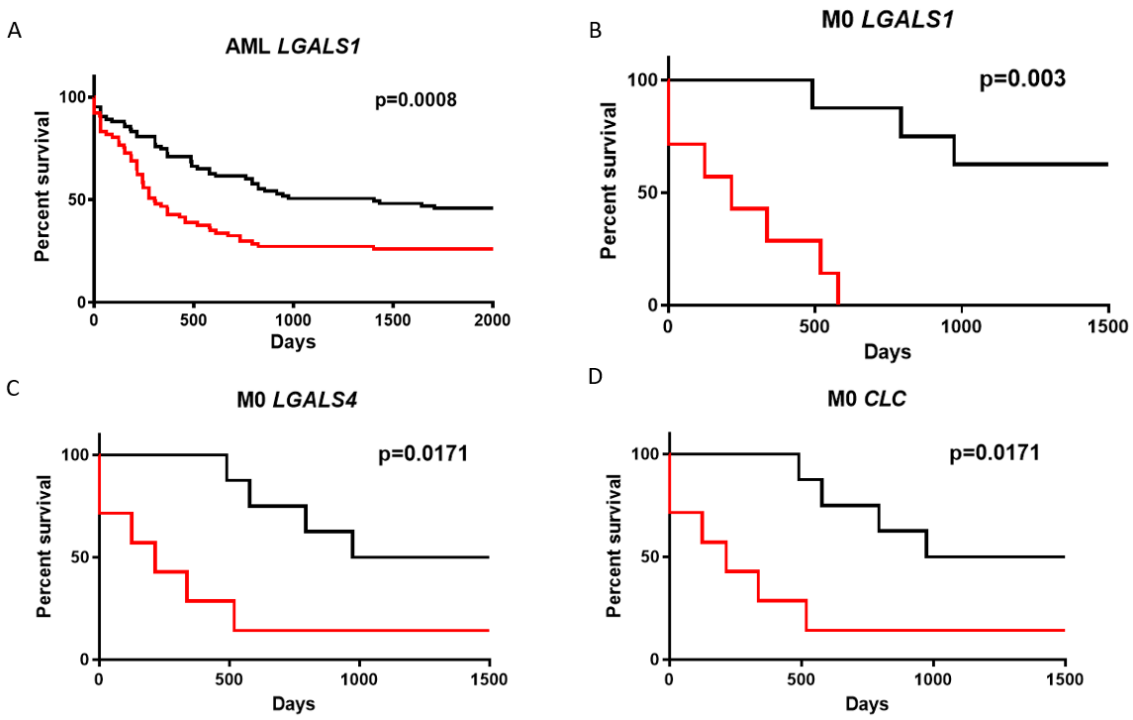

Figure 27: Survival curve analysis of TCGA AML patient data showed that LGALS gene expression is related to patient outlook.

RSEM AML patient data was retrieved from cBioPortal and $\log_2$ transformed. R Studio was used to access patient survival data from cBioPortal. Median gene expression was used to determine patients with above/equal (red) or below (black) expression when comparing patient prognosis for all AML cohorts (n=160) for *LGALS1* (A) and *LGALS1* (B), *LGALS4* (C), *CLC* (D) in all M0 subtype cohorts (n=15). Statistical significance was determined using the log-rank (Mantel-Cox) test.

Chapter 4

4 Discussion

The results obtained in this study indicate galectin specific effects on neutrophilic differentiation of HL-60 promyeloid leukemia cells. Additionally, HL-60 cells demonstrated resistance to galectin-induced apoptosis. Furthermore, I showed that specific galectin gene expression profiles can serve as new diagnostic and prognostic markers for AML and specific FAB subtypes. Lastly, correlation analysis revealed changes in galectin relationships between gene pairs.

I first showed that recombinant galectin-1 or -3 had no effect on neutrophilic differentiation of HL-60 cells based on dose-dependent and daily supplementation treatments. However, galectin-8 at 1000 ng/mL induced moderate levels of neutrophilic differentiation relative to ATRA treated cells, with no effect observed with daily supplementation. Galectin-9 induced a similar response to galectin-8 with increased *NCF1* expression, that was not observed with daily supplementation. Next, I demonstrated that permeable allosteric inhibitors specific to galectin-1 or -3 induced moderate levels of neutrophilic differentiation of HL-60 cells relative to ATRA-induced differentiation. These findings were confirmed by examining the segmentation of cell nuclei, genetically by expression of associated biomarkers, and through global changes in *O*-GlcNAcylation, with ATRA serving as a hallmark for these differentiation changes. Lastly, experiments related to the third objective of this study revealed that galectin gene expression does not change in leukemic cells relative to healthy cells, with more specific changes observed when investigating different AML FAB subtypes. The M0-M2 FAB subtypes revealed no changes in galectin gene expression, while the M4 and M5 subtypes demonstrated changes in *LGALS1* and *LGALS3* expression, and the M3 subtype demonstrated significant changes in galectin gene expression. Furthermore, correlation analysis revealed changes in the relationship of galectin gene pairs between AML and bone marrow cohorts. Finally, survival analysis revealed that above median expression of *LGALS1* in AML cohorts can serve as a marker for poor patient outlook, while above median expression of *LGALS1*, *LGALS4*, and *CLC* can serve as markers for poor patient outlook in the M0 subtype.

4.1 Interpretation

4.1.1 ATRA-induced differentiation provided insight into understanding potential mechanisms behind neutrophilic differentiation of HL-60 cells

ATRA has been used as a differentiation agent in research as well as a clinical treatment of APL (Lohse et al., 2018). There has also been increased interest in terminal differentiation treatments for leukemias to decrease leukemic burden. Signal transduction pathways related to terminal differentiation cause changes in gene expression that halt cell mitosis and drive cells to become mature leukocytes, losing their proliferative ability (Chaplinski et al., 1986; Mollinedo et al., 1998). ATRA-induced differentiation of HL-60 cells affects many signal transduction pathways and transcription factors including ERK1/2, p38/MAPK, STAT3 and many others (Hickestein et al., 1989; Song et al., 2013).

In this study, I showed that ATRA-induced differentiation of HL-60 cells resulted in increased segmentation of nuclei, upregulated *NCF1* expression and decreased global *O*-GlcNAcylation over 3 days. Olins et al. (2000) reported that ATRA-induced differentiation caused increased expression of lamin, cytoskeletal reorganization and related nuclear lobulation related to neutrophilic differentiation over 4 days. Additionally, Niggili et al. (2004) reported that the MAPK pathway is related in chemotactic peptide induced actin reorganization and polarity development in HL-60 cells. Previous research with ATRA revealed that RARα activation results in the formation of the RARα-RXR complex. This complex activates and upregulates transcription factors PU.1 and C/EPBα/β (Tasseff et al., 2017). Tasseff et al. (2017) also reported that ATRA activation results in the activation of ERK1/2 and MAPK pathway, causing binding of CEBPα/β, and PU.1 to promoter regions. This resulted in upregulation of neutrophil differentiation specific markers including CD11b (integrin αM) and *NCF1* in HL-60 cells. Furthermore, Hickstein et al. (1989) reported that undifferentiated HL-60 cells express integrin αM, with retinoic acid differentiated HL-60 cells expressing higher levels of integrin αM. ATRA-induced differentiation of HL-60 cells also downregulates signal transducers and activator of transcription 3 (SATA3) expression, a known signal transduction protein associated with

the continuous proliferation of undifferentiated cells, and CD44, a surface glycoprotein involved with cellular adhesion and migration (Liu et al., 2007; Song et al., 2013).

Prior research with HL-60 cells have shown that undifferentiated cells contain higher levels of global *O*-GlcNAcylation (Sherazi et al., 2018). Cancerous cells have been reported to have increased glycolysis for energy production, which allows for continuous proliferation and increased *O*-GlcNAcylation through the hexosamine biosynthetic pathway (Asthana et al., 2018). *O*-GlcNAcylation status in cancer cells is related to a variety of metabolism-sensing signaling pathways including MAPK, mTOR, and AMPK due to the protein being *O*-GlcNAcylated (Sanches-Garrido J & Shenoy AR, 2020). In mouse melanoma, increased levels of *O*-GlcNAcylation promoted cancer progression, while a downregulation of p38/MAPK and upregulation of ERK1/2 were observed (Moriwaki & Asahi, 2017). Additionally, Wu et al. (2020) reported that *O*-GlcNAcylation of phosphorylated STAT3 altered downstream gene activation of genes associated with proliferation.

While ATRA- and DMSO-induced differentiation revealed changes in nuclear morphology, *NCF1* regulation, and global *O*-GlcNAcylation, they also revealed changes in galectin gene expression. More specifically, *LGALS3* and *CLC* were upregulated in differentiated cells, *LGALS1* and *LGALS12* were downregulated in differentiated cells, and *LGALS8* and *LGALS9* were constantly expressed (Abedin et al., 2003; Timoshenko et al., 2016; Vinnai et al., 2017; Vakhrusnev et al., 2018). In this study, I demonstrated that galectins have no significant effect on ATRA-induced differentiation of HL-60 cells. HL-60 cells treated with 1 µM ATRA revealed strong stimulatory effects relative to galectin-induced differentiation. Therefore, an experiment was performed with 500 ng/mL recombinant galectin 1, 3, or 8 to investigate whether galectins influenced the differentiation of HL-60 cells with 5 nM ATRA. However, no significant changes were observed in nuclear morphology, *NCF1* expression or global *O*-GlcNAc. While 5 nM ATRA induced half the response of 1 µM ATRA, galectins exhibited no effects due to ATRA-induced strong stimulatory effects (**Figure S1**).

4.1.2 Proto-type galectins -1, -7 and -10

4.1.2.1 Galectin-1 allosteric inhibition induces moderate levels of cellular differentiation and demonstrates changes in gene expression related to AML FAB subtype and prognosis

To date, galectin-1 has been investigated in the differentiation of many cell models including eosinophil, macrophage, monocyte, trophoblast, keratinocyte, and hematopoietic stem cells (Abedin et al., 2003; Vas et al., 2004; Sarafian et al., 2006; Novak et al., 2012, Tang et al., 2018). Additionally, there are many instances where inhibition, knockdown, or use of recombinant galectin-1 has been investigated with respect to its role in differentiation and cancer progression. However, an understanding of the effects of galectin-1 in AML and granulocytic differentiation is lacking.

More specifically, Vas et al. (2004) reported that recombinant galectin-1 can induce differentiation of early hematopoietic stem cells. Furthermore, galectin-1 induced neutrophil migration during anti-inflammatory responses through the p38/MAPK pathway (Auvynet et al., 2013). To date, there are multiple galectin-1 inhibitors available including TDG, a broad functioning sugar inhibitor, and OTX008, a specific, permeable allosteric inhibitor. OTX008 is also under investigation in clinical trials with respect to its potential for cancer therapeutics through galectin-1 inhibition (Michael et al.,2016). In this study, I observed that HL-60 cells treated with TDG or recombinant galectin-1 did not demonstrate changes in neutrophilic differentiation, while OTX008 inhibition induced differentiation. This may indicate that the non-CRD region of galectin-1 plays a role in the regulation of promyeloid cells during neutrophilic differentiation of HL-60 cells. Previous investigations with OTX008 reported inhibition of the proliferation of HL-60 cells and the downregulation of ERK1/2 (Astorgues-Xerri et al., 2014). Additionally, treatment of HRAS-mutant cancers demonstrated that OTX008 inhibition blocked ERK1/2 MAPK signaling through prevention of galectin-1 and HRAS intracellular binding (Michael et al., 2016). In AML, galectin-1 is considered a pro-survival molecule through the assembly of RAS complex intracellularly, which causes activation of the ERK1/2 MAPK pathway (Ruvolo, 2019). Additionally, Paz et al. (2018) reported that OTX008 inhibition of galectin-1 in acute lymphocytic leukemia (ALL) inhibited integrin-mediated adhesion and

migration of ALL cells. Paz et al. (2018) also observed increased levels of galectin-1 surface expression. In addition, research using recombinant galectin-1 on stimulated neutrophils demonstrated inhibited expression of integrin αM, a known receptor associated with neutrophil function through ERK/p38/MAPK activation. siRNA mediated knockdown of galectin-1 resulted in enhanced neutrophil recruitment and emigration often associated with integrin binding, suggesting that galectin-1 may inhibit integrin αM responses (Cooper et al., 2008). Furthermore, Luo et al. (2016) demonstrated that galectin-1 in chronic myeloid leukemia (CML) K562 cells served as a mediator for drug resistance signaling through the MAPK pathway. Therefore, more investigation is needed to better understand the signal transduction mechanisms behind the role of galectin-1 in regulating neutrophil differentiation and function, with modulation of ERK1/2 MAPK signaling as a potential mechanism behind maintaining an undifferentiated and cancerous status.

Galectin-1 in blood cancers has been viewed as a pro-survival molecule and poor prognosis. Juszczynski et al. (2011) determined that galectin-1 gene expression was upregulated in 100% of MLL-related ALL, while Paz et al. (2018) indicated an upregulation in *LGALS1* in non-MLL related ALL. In this study, I found that *LGALS1* expression was constant when looking at all AML cohorts. However, *LGALS1* expression was elevated in the M4 and M5 FAB subtypes as was observed with neutrophil differentiation markers (*NCF1/2, CYBA/B*) and *LGALS3* (**Figure S3**). Ruvolo et al. (2020) reported that shRNA mediated knockdown of *LGALS1* in the M4 cell line OCI-AML3, demonstrated prolonged survival and a decreased the rate of leukemic burden in xenografted mice. This was also confirmed in this study where above median expression of *LGALS1* in all AML cohorts and the M0 subtype was indicative of poor prognosis. Above median expression of *LGALS1* also demonstrated a non-significant trend for poor prognosis in all AML FAB subtypes investigated in this study, except for the M5 subtype (**Figures S6-S10**). Knockdown of galectin-1 in multiple myeloma cells also results in decreased tumor size, indicating that in blood related cancers that galectin-1 serves as a poor prognostic marker (Storti et al., 2016). Finally, correlation analysis showed multiple changes in the relationships between *LGALS1* gene pairs including *LGALS3, CLC,* and *NCF1/2*. Almkvist et al. (2002) indicated that galectin-1 is involved with the activation of the NADPH-oxidase complex. However, the relationship between *LGALS1* and *NCF1/2*

in leukemia has yet to be investigated. Additionally, there has been no investigations into the relationship between *LGALS1* and *LGALS3* or *CLC*. This indicates that *LGALS1* has an important role in the progression of AML, with further investigations needed to understand the underlying mechanisms.

4.1.2.2 Galectin-10 gene expression indicated patient prognosis, while galectin-7 and galectin-10 gene expression remained constant in AML FAB subtypes

Previous research into galectin-7 expression has reported upregulation in keratinocyte differentiation and constant gene expression during enterocytic differentiation (Sarafian et al., 2006; Sherazi et al., 2018) Additionally, the gene expression of galectin-10 has only been examined during neutrophilic differentiation of HL-60 cells (Abedin et al., 2003; Vinnai et al., 2017). Galectin-7 and -10 are not as well-studied as the other galectins for their involvement in AML. Currently, galectin-7 and galectin-10 have been identified in AML (De Kouchkiveky & Abdul-Hay, 2016l Su, 2018). In this study, I showed that *LGALS7* and *CLC* exhibit constant expression. I also observed that above median expression of *CLC* was indicative of poor prognosis in the M0 subtype. To date, there are limited single studies of galectin-7 in cancer that are related to its gene expression changes. Galectin-7 has been reported to be upregulated in esophagus, breast, thyroid, pharynx and larynx cancers. Furthermore, galectin-7 has been reported to be downregulated in skin, cervix, and stomach cancers (Thijssen et al., 2015). In contrast, the expression patterns of galectin-10 are unreported in other cancers. Galectin-10 has been investigated for its involvement with eosinophils and its suppression function of Treg cells. However, galectin-10 suppression of T cells has yet to be investigated in leukemias. Therefore, more investigations are needed to fully understand the roles of galectin-7 and -10 in AML.

4.1.3 Chimeric type galectin-3 allosteric inhibition induces moderate levels of HL-60 cell differentiation

Galectin-3 is the sole chimeric-type galectin that is as well-studied as galectin-1. Galectin-3 exhibits increased expression in DMSO treated HL-60 cells and elicits responses through its CRD and N-terminal domains (Abedin et al.,2003; Vinnai et al., 2017; Sundqvist et al., 2018). Galectin-3 has been investigated in the differentiation of many cell models

including adipocyte, CD34+ mononuclear cells, enterocyte, eosinophil, keratinocyte M1 macrophages, monocyte, oligodendritic cell, osteoblast, B cells, and trophoblast cells (Tazhitdinova & Timoshenko, 2020). There have also been investigations into galectin-3 activities with mature neutrophils, expression patterns during neutrophilic differentiation, and AML cancer progression. Currently, there is little understanding of the involvement of galectin-3 in the differentiation of neutrophils.

In this study, I observed that recombinant galectin-3 or TDG demonstrated no effect on neutrophilic differentiation of HL-60 cells, whereas induction was observed with the permeable, specific allosteric inhibitor GB1107. This may indicate that galectin-3 regulated promyeloid cell neutrophilic differentiation through the N-terminal domain, rather than through CRD binding. Galectin-3 has been reported to be involved with primed neutrophil responses rather than naïve and unprimed neutrophils. Nieminen et al. (2005) reported that galectin-3 increased integrin expression in primed neutrophils, and elicited no effect on naïve, unprimed neutrophils. Additionally, Sundqvist et al. (2018) demonstrated that galectin-3 elicited ROS production in primed neutrophils that was unseen in unprimed neutrophils. Sundqvist et al. (2018) also demonstrated that the cleaved CRD portion of galectin-3 inhibited this response in primed neutrophils and that the N-terminal domain of the protein was required ROS production.

Furthermore, galectin-3 demonstrated properties that would enhance cellular proliferation and survival rather than differentiation. Galectin-3 is known to be involved with cellular division through interaction with NuMA (Magescas er al., 2017). Prior reports of galectin-3 indicated that it is involved with the activation of the Wnt/β-catenin pathway. The activation of the Wnt/β-catenin pathway is associated with poor prognosis and increased proliferation in AML and other cell types (Hu et al., 2015; Ruvolo et al, 2018). In human thyroid and orthotopic gastric cancer, galectin-3 inhibition by GB1107 resulted in increased levels of phosphorylated p38 and AKT, decreased phosphorylation of ERK, and decreased activation and expression of STAT3 and β-catenin (Kim et al., 2021; Lee et al., 2021). Previous research with gastric cancer also revealed that activation of STAT3 by Wnt required endogenous galectin-3 (Kim et al., 2021). Additionally, Kim et al. (2021) also demonstrated that overexpression of galectin-3 activated STAT3 through direct

binding by co-immunoprecipitation and regulated the DNA binding and transcriptional activation of STAT3. GB1107 inhibition also exhibited inhibited activation of both Wnt and STAT3 signaling pathways. Jeon et al. (2010) reported that galectin-3 demonstrated cytokine-like regulatory actions through the JAK-STAT pathway in brain immune cells. Bhattacharyya et al. (2014) also reported activity in Sp1 binding to Wnt promoter regions that was prevented by galectin-3 inhibition. Furthermore, in MSCs, elevated levels of galectin-3 were positively correlated with β-catenin, indicating a functional association (Ruvolo et al., 2018). Therefore, the N-terminal domain of galectin-3 potentially regulates promyeloid cell differentiation through Wnt/β-catenin and STAT3 pathways.

Currently, galectin-3 has been investigated for its relation to age, therapeutic enhanced resistance, and involvement in the cancer microenvironment of leukemias. Ruvolo et al. (2018) reported that galectin-3 protein expression was higher in AML MSC, Gao et al. (2016) demonstrated elevated gene expression in non-APL AML, and El Leithy et al. (2015) demonstrated no change in *LGASL3* expression. However, in this study, I found that *LGASL3* expression was unchanged in all AML cohorts. This difference could be due to the different sample subtype composition and leukemia burden. El Leithy et al. (2015) reported 53 patients (15 M0/M1, 17 M2, 5 M3, and 16 M4), while Ruvolo et al. (2018) reporting 106 MSC AML patients, and Gao et al. (2016) reported 298 non-APL AML patients. Furthermore, Cheng et al. (2013) reported a downregulation in *LGALS3* expression in the M1 subtype, and upregulation in the M4 and M5 FAB subtypes that was also observed in this study. Cheng et al. (2013) also indicated that older patients demonstrated increased *LGALS3* expression in bone marrow samples and were often associated with M4 and M5 subtypes, with no other variables influencing galectin-3 expression. Cheng et al (2013) also demonstrated that patients with lower *LGALS3* expression survived an additional 23.5 months. In this study, we observed that *LGALS3* expression demonstrated no diagnostic or prognostic potential. However, patient age was undetermined in this study and contained altered FAB subtype patient composition. Additionally, in this study, *LGALS3* gene pairs showed changes from negative to positive correlations with granulocyte differentiation markers *NCF1/2* and *CYBA/B*. While Sundqvist et al. (2018) showed that galectin-3 induces ROS production in neutrophils, this relationship has yet to be investigated in AML.

4.1.4 Tandem-repeat type galectins -4, -8, -9, and -12

4.1.4.1 Recombinant galectin-8 induces moderate levels of cellular differentiation, while galectin-4 gene expression indicates patient prognosis with constant gene expression in AML FAB subtypes

During HL-60 cell differentiation, galectin-8 demonstrates constant expression patterns (Abedin et al., 2003; Timoshenko et al., 2016; Vinnai et al., 2017). Galectin-8 gene expression has been reported to be downregulated in plasma cell differentiation and enterocyte differentiation, with constant gene expression observed in eosinophilic, monocytic, and trophoblastic differentiation (Abedin et al., 2003; Arikawa et al., 2012; Ikegame et al., 2016; Sherazi et al., 2018). In this study, I observed that recombinant galectin-8 induced neutrophilic differentiation of HL-60 cells. To date, little is known with respect to the regulatory functions of galectin-8 in neutrophils and their differentiation. However, in Jurkat T cells, the binding of galectin-8 to extracellular integrins results in strong stimulation of ERK1/2 (Cárcamo et al., 2006). Integrins are important for neutrophil function through ERK and p38/MPAK activation, which is involved in cellular adhesion and spreading, chemotaxis, and production of ROS. Nishi et al. (2003) reported that bound galectin-8 to integrin αM required the C-terminal CRD region for activation. Reports have also indicated that integrin αM expression is upregulated in differentiated cells, with a basal level observed in undifferentiated cells (Hickstein et al., 1989). However, galectin-8 induced differentiation was not observed with daily supplementation, indicating that activation through integrin αM is time sensitive. Therefore, galectin-8 induced differentiation through the proposed binding of the C-terminal CRD to integrin αM, activating p38/MAPK, with further investigations required.

However, recombinant galectin-8 demonstrated sustained *O*-GlcNAcylation status. To date, the involvement of the ERK or p38/MAPK pathways with *O*-GlcNAcylation in HL-60 cells is undetermined. In mouse melanoma, increased levels of *O*-GlcNAc promote cancer progression and downregulation in p38/MAPK, while also upregulating ERK1/2 (Moriwaki & Asahi, 2017). Additionally, Cárcamo et al. (2006) indicated that extracellular binding of galectin-8 to integrins results in the activation of ERK1/2. Therefore, this

suggests that galectin-8 binding to integrin αM not only activates p38/MPAK but also activates ERK1/2, maintaining *O*-GlcNAcylation status in HL-60 cells.

Galectin-8 is poorly studied with respect to its functions associated with leukemia. Investigations into other cancers have demonstrated upregulation in *LGALS8* (Nagi et al., 2002; Genetilini et al., 2017; Trebo et al., 2020). In this study, I found that *LGALS8* expression was unchanged in AML cohorts; and downregulated in the M3 subtype. El Leithy et al. (2015) reported that *LGALS8* expression was constant. El Leithy et al. (2015) also indicated that galectin-8 was not a marker for prognosis. I also observed that *LGALS8* expression was not indicative of prognosis in all AML cohort and FAB subtypes (**Figures S4-S10**). Additionally, *LGALS8* gene pair showed changes in relationships from negative to positive with *NCF1/2*. Nishi et al. (2003) indicated that galectin-8 induced ROS production in neutrophils. However, the relationship between *LGALS8* and *NCF1/2* in AML has yet to be investigated. Additionally, *LGALS8* also demonstrated a positive correlation with *LGALS9* expression in cancerous cells. To date, little is known with respect to how *LGALS8* expression is associated with other galectin gene expression in AML, indicating that further investigations are needed.

Studies of galectin-4 have reported downregulation in colon, prostate, and skin cancer, and an upregulation in pancreas, liver, ovary, and bladder cancer (Thijssen et al., 2015). El Leithy et al. (2015) reported that *LGALS4* exhibited constant gene expression. El Leithy et al. (2015) also indicated that *LGALS4* is upregulated in younger patients and is indicative of a better patient outlook. In this study, we found that *LGALS4* expression was constant in all AML cohorts, with upregulation observed in the M3 subtype. I also observed that above median expression of *LGALS4* was indicative of poor prognosis. There is little understanding on how galectin-4 is involved with AML, indicating additional investigations are needed.

4.1.4.2 Recombinant galectin-9 induces *NCF1* expression in relation to cellular differentiation, while galectin-9 and galectin-12 gene expression in the AML M3 subtype serves as a diagnostic marker

Galectin-9 is another galectin expressed in HL-60 cells that demonstrates constant expression during differentiation (Abedin et al., 2003; Timoshenko et al., 2016; Vinnai et al., 2017). To date, the interaction of galectin-9 and Tim-3 has been of primary focus in neutrophil activation and recruitment (Vega-Carrascal et al., 2011; Hirao et al., 2015; Robinson et al., 2019). Prior research into galectin-9 reported expression changes during eosinophil, macrophage, monocyte, osteoblast, trophoblast, and CD4+ T cell differentiation (Tazhitdinova & Timoshenko, 2020). However, overexpression of galectin-9 in macrophages increased activity and expression levels of STAT3. In healthy individuals, STAT3 has been reported to be involved in the upregulation of NADPH oxidase components, including *NCF1,* and binding of *C/EBPβ* during myelopoiesis (Lu et al., 2017). However, in HL-60 cells, STAT3 expression is associated with an undifferentiated state, allowing for continuous proliferation (Song et al., 2013). Tanikawa et al. (2010) indicated that galectin-9 induced osteoblast differentiation through binding of CD44. Liu et al. (2007) determined that ATRA-induced differentiation of HL-60 cells downregulated CD44. Additionally, Liu et al. (2007) indicated that CD44 activation in polymorphonuclear neutrophils activated ERK1/2 and p38/MAPK affecting actin polymerization and enhanced neutrophil function. In this study, I found that recombinant galectin-9 increased *NCF1* expression, exhibited a non-significant increasing trend in the percentage of segmented nuclei and elicited no change in *O*-GlcNAcylation. Furthermore, daily supplemented galectin-9 had no effect. Downregulation of CD44 could be a possible explanation for why galectin-9 was unable to induce differentiation. However, more investigations are required. Therefore, galectin-9 elicited a similar response to galectin-8 through CD44 activation, activating both p38/MAPK to induce nuclear reorganization and upregulation of *NCF1* and activating ERK1/2 to maintain *O*-GlcNAcylation levels.

Current investigations of galectin-9 in AML revolve around immune surveillance escape due to Tim-3 regulation of T cells and promoted myeloid-derived suppressor cells.

Gonçalves Silva et al. (2016) reported that Tim-3 is highly expressed in AML and is required for the secretion of galectin-9. Furthermore, Wdowiak et al. (2018) showed that galectin-9 levels were increased in the serum of chronic lymphocytic leukemia (CLL) patients that might have a role in the cancer progression. Taghiloo et al. (2017) also reported that galectin-9 expression is upregulated in CLL relative to peripheral blood mononuclear cells. El Leithy et al. (2015) investigated the expression of *LGALS9* in AML with constant gene expression being observe. El Leithy et al. (2015) also demonstrated that *LGALS9* expression was not indicative of patient prognosis. In this study, I found that *LGALS9* expression demonstrated upregulation in all AML cohorts and downregulation in the M3 subtype. Additionally, *LGALS9* in this study demonstrated no indications towards patient prognosis. However, the role galectin-9 has in leukemias is not fully understood. Kuroda et al. (2010) reported that galectin-9 induced apoptosis of chronic myeloid leukemia (CML) cells, while also re-sensitizing various treatments in resistant CML.

In this study, I found that *LGALS12/LGALS9* expression is a diagnostic marker for the M3 subtype. Currently, little is known with respect to the involvement of galectin-12 in AML. El Leithy et al. (2015) reported a downregulation in *LGALS12*, which served as an indicator of poor prognosis. Additionally, Zheng et al. (2019) stated *LGALS12* expression is upregulated in the M3 subtype. However, in this study, *LGALS12* expression in all AML cohorts remained constant, with an upregulation observed in the M3 subtype. El Leithy et al. (2015) demonstrated a different AML patient subtype composition relative to this study, indicating that a larger sample size or investigation into individualize subtypes is required. Furthermore, Helbawi et al. (2021) reported that methylation plays a role in the survival of patients when looking at *LGALS12* expression, with methylated *LGALS12* gene being indicative of poorer prognosis. However, in this study, *LGALS12* was not an indicator of patient outlook, with methylation status being uninvestigated.

4.1.5 HL-60 cells exhibit resistance to galectin-induced apoptosis

In this study, I also examined the degree of apoptosis of HL-60 cells. HL-60 cells were treated with various concentrations of brefeldin-A (BFA), a known inducer of apoptosis. Previous research with BFA has reported that BFA induces endoplasmic reticulum (ER) stress through inhibition of protein transport between ER and Golgi apparatus (Shao et al.,

1996). Additionally, Choi et al. (2010) and Namba et al. (2013) report that ER induced stress from BFA caused induction and activation of both CHOP and BAX, resulting in apoptotic cell death. Additionally, Wei et al. (2008) revealed that 24 hours treatments of BFA caused nuclear condensation and annexin V binding to phosphatidylserine of cell membranes. In this study, I demonstrated that BFA exhibited nuclear condensation, and upregulation of both *CHOP* and *BAX* in the HL-60 cell model.

In this study, I also examined the effect of ATRA on apoptosis of HL-60 cells. I revealed that 1 µM ATRA did not induce apoptosis of HL-60 cells over 3 days. Veselská et al. (2003) conducted a study with 1 µM ATRA and revealed that apoptotic cell death was achieved over 6 days. Furthermore, Ozeki et al. (2008) reported that 2 µM ATRA resulted in differentiation and apoptosis of HL-60 cells after 4 days. Based on the previous studies, HL-60 cells exhibited resistance to apoptosis from 1 µM ATRA treatments over 3 days.

Galectins -1, -3, -4, -7, -8, -9, -10, and -12 have all been reported to induce apoptosis in either immune or cancer cells (Timoshenko, 2015). However, the effects of galectins on HL-60 cell apoptosis have yet to be examined. In this study, I showed that recombinant galectins -1, -3, and -9 did not cause apoptosis of HL-60 cells. However, HL-60 cell treatments with recombinant galectin-8 revealed increased DNA condensation, with unchanged gene expression of *CHOP* and *BAX*. To date, treatments with only recombinant galectin-1 have been performed to investigate the effects of galectins on apoptosis. Vas et al. (2005) performed a study with 10 µg/mL recombinant galectin-1 on the differentiation and apoptosis of early hematopoietic stem cells and demonstrated apoptosis after 60 min and complete cell death after 14 days. Additionally, Rabinovich et al. (1999) revealed that 4 µg/mL of recombinant galectin-1 induced high levels of apoptosis over 18 hours. This indicates HL-60 cells are resistant to recombinant galectin-induced apoptosis under the parameters set in this study.

4.2 Conclusions and applications

In conclusion, galectins have a role in the regulation of neutrophilic differentiation of HL-60 cells and in AML. Galectins have similar structures and function, indicating evolutionary redundancies. In this study, I observed that galectins have their own

expression profiles in AML and had different effects on neutrophilic differentiation through different proposed signaling pathways. Furthermore, ATRA-induced differentiation of HL-60 cells demonstrated a strong stimulated response, which masked the effects of galectins and galectin inhibitors on neutrophilic differentiation. Finally, HL-60 cells exhibited resistance to galectins and ATRA induced apoptosis.

Galectin-1 exhibited increased gene expression in the M4 and M5 subtypes of AML. While *LGALS1* expression has yet to be investigated by others among AML FAB subtypes, *LGALS1* expression was reported to increase in ALL (Juszczynski et al., 2011; Paz et al., 2018). Additionally, above median gene expression of *LGALS1* was indicative of poor prognosis in all AML cohorts and the M0 subtype. Upregulation of *LGALS1* was also indicative of increased leukemia burden and poor prognosis in the M4 subtype as reported by Ruvolo et al. (2020). Furthermore, OTX008 inhibition of galectin-1 resulted in neutrophilic differentiation of HL-60 cells. Therefore, it is suggested that intracellular binding of non-CRD regions of galectin-1 to HRAS allows for p38/MAPK pathway activation, potentially maintaining the undifferentiated state of HL-60 cells (**Figure 28**). Inhibitory therapeutics, specifically OTX008, should be further investigated for AML.

Galectin-3 demonstrated similar trends as to galectin-1, except for upregulation being reported in differentiated HL-60 cells (Abedin et al., 2003; Vinnai et al., 2017). Various reports on *LGALS3* expression in AML indicated upregulation (Ruvolo et al., 2018; Gao et al., 2016), with upregulation of *LGALS3* expression also reported in more mature subtypes (Cheng et al., 2013). Cheng et al. (2013) also indicated that *LGALS3* expression increased with age, with older patients with AML being diagnosed with the M4 and M5 subtypes. Cheng et al. (2013) demonstrated that upregulation of *LGALS3* was indicative of poor prognosis, indicating that *LGALS3* does play a role in the M4 and M5 subtypes of AML. In undifferentiated HL-60 cells, the N-terminal domain of intracellular galectin-3 plays a potential role in the maintenance of an undifferentiated status by Wnt/β-catenin and STAT3 pathways (**Figure 28**). Furthermore, several reports have indicated that galectin-3 does not elicit any responses in unprimed neutrophils, indicating a complex system (Nieminen et al., 2005). Therefore, inhibitory therapeutics of galectin-3 should be further investigated for AML and proper immune cell function.

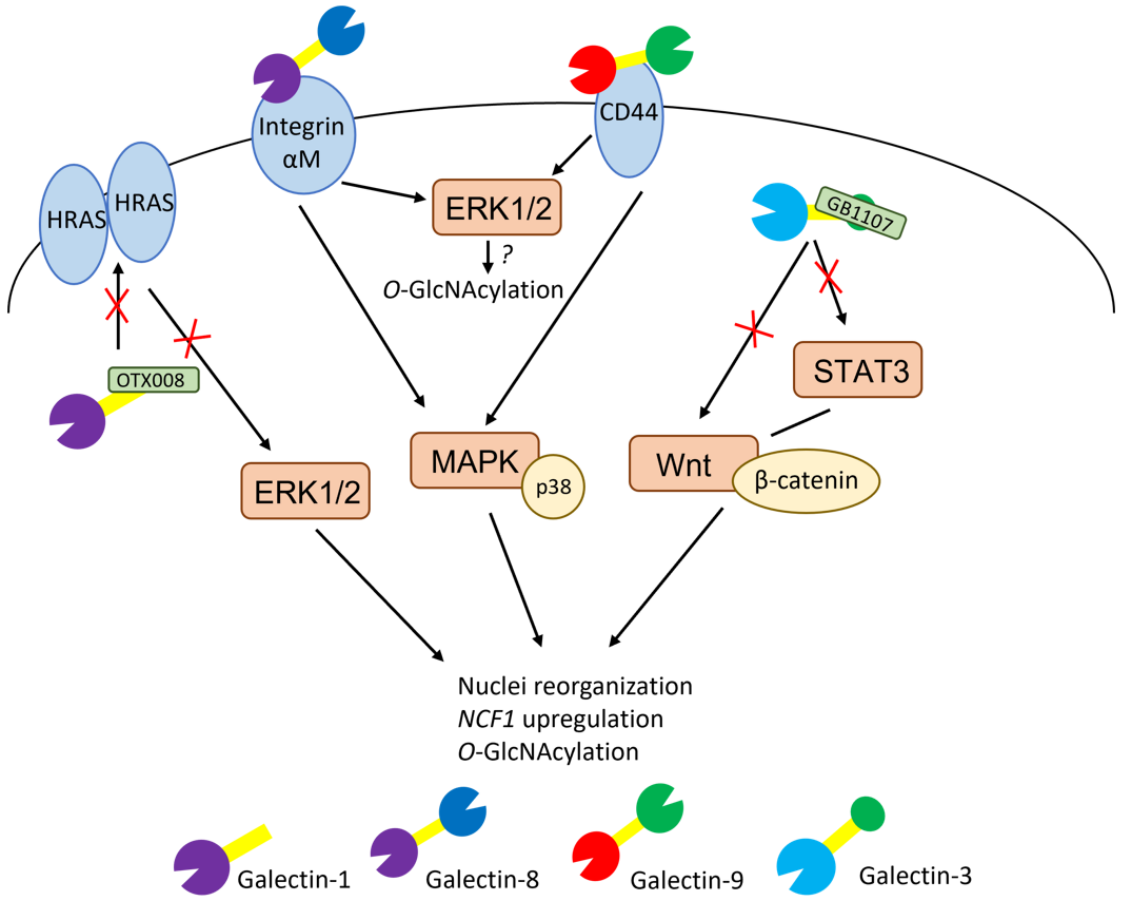

Figure 28: Hypothetical galectin mediated regulation of granulocytic differentiation of HL-60 cells.

OTX008 allosteric inhibition of galectin-1 intracellularly inhibits binding to HRAS, preventing complex formation and no activation of ERK1/2 MAPK, resulting in induced neutrophilic differentiation. Galectin-8 C-terminal CRD binding of integrin αM activates signal transduction for activation of both ERK1/2 and p38/MAPK. ERK1/2 activation maintains *O*-GlcNAcylation status while p38/MAPK activates the expression of genes associated with nuclear reorganization and NCF1 expression. Galectin-9 binding to CD44 induces mechanisms similarly to galectin-8. GB1107 allosteric inhibition of galectin-3 intracellularly inhibits activation of both STAT3 and Wnt/β-catenin, allowing for differentiation to occur.

Galectin-8 is one of the galectins in HL-60 cells and AML that demonstrated consistent expression patterns during neutrophilic differentiation and AML (Abedin et al., 2003; El Leithy et al., 2015; Vinnai et al., 2017). Little is known with respect to the role of galectin-8 in AML. However, recombinant galectin-8 demonstrated potential for a new differential therapeutic for AML. In the HL-60 cell model, galectin-8 induced moderate levels of differentiation. Several other reports indicated that the C-terminal CRD of galectin-8 binds to integrin αM in neutrophils, activating both ERK1/2 and p38/MAPK pathways that is time-dependent (**Figure 28**). This signal transduction pathway suggests a potential mechanism in which galetin-8 regulates neutrophilic differentiation of HL-60 cells.

Galectin-9 has been widely investigated for its interaction with Tim-3 in cancer progression through evasion of T cell surveillance. In leukemias, Tim-3 has increased expression that allows for increased secretion of galectin-9, detectable in patient serum (Wdowiak et al., 2018). However, due to the interaction of galectin-9 with Tim-3, it has gained more interest in lymphocytic leukemias. To date, there is one other study looking at *LGALS9* expression in AML that reported constant gene expression and no prognostic potential (El Leithy et al., 2015). However, in this study we found downregulation of *LGALS9* in the M3 subtype. *LGALS9* expression has also been reported to be constant during induced differentiation of HL-60 cells (Vinnai et al., 2017). I also found that recombinant galectin-9 demonstrated increased *NCF1* expression and potential increase in segmented nuclei that could be due to CD44 binding, activating both ERK1/2 and p38/MAPK similarly to galectin-8 (**Figure 28**).

Galectins 4, 7, 10, and 12 are poorly studied with respect to their expression patterns and roles in AML cancer progression and blood cell maturation. Galectin 4 and 7 have been demonstrated to exhibit changes in expression in other cancer models, with single reports only being investigated and no reports of galectin-10 (Thijssen et al., 2015). However, *LGALS4* and *LGALS10* served as poor prognostic indicators in the M0 subtype that require further investigations. Additionally, *LGALS12* is upregulated in the M3 subtype (Zheng et al., 2019). A specific ratio of *LGALS12/LGALS9* served as a new diagnostic marker of M3 subtype identified in this study. Additionally, the methylation status of the *LGALS12* gene demonstrated potential as a prognostic marker (Helbawi et al., 2021).

4.3 Study limitations and future directions

The results of this study showed that galectins do have a role in the neutrophilic differentiation of HL-60 cells. Additionally, galectins serve as new diagnostic and prognostic markers in AML. However, there are a few limitations with this study.

In the HL-60 cell model, a larger sample size is required for some treatments. When examining the effects of galectins on various aspects of neutrophilic differentiation, some variations were observed within treatments. A way to overcome these variations would be to increase sample size in order to get a more representative picture. Additionally, it is common practice in medicine to have independent experts to examine fluorescent images to eliminate bias. In this study, only one individual examined the percentage of segmented nuclei. Furthermore, neutrophil functions were not examined in this study. As such, increased *NCF1* expression indirectly indicate NADPH oxidase activity. Additional tests to assess neutrophilic function would help strengthen the results found this study.

HL-60 cells have been shown to produce ROS when differentiated into neutrophils (Vinnai et al., 2017). However, to produce ROS, activation and phosphorylation by protein kinase C is required to assemble the NADPH oxidase complex. In the HL-60 cell model, ROS can be activated using chemical stimulation, including phorbol 12-myristate 13-acetate, or bacterial cell wall components including formyl-methionyl-leucyl-phenylalanine (Dakik et al., 2021). Once activated, the NADPH oxidase complex will create superoxide ions, the precursor required for hydrogen peroxide production. Hydrogen peroxide production can then be measured by scopoletin/peroxidase fluorescence assay (Bedard & Krause 2007; Belambri et al., 2018). Additionally, flow cytometry of surface markers including an upregulation in CD11b and downregulation in CD44 and CD15 would be another method to assess neutrophilic differentiation. RT-qPCR of other genetic markers including downregulation in C-MYC and upregulation of lamin are other indicators to assess neutrophilic differentiation.

To date, there are no known specific inhibitors of galectin 8, 9, 10, or 12. Additionally, OTX008 and GB1107 may also have off targeting effects. Therefore, shRNA mediated silencing would be another method to determine the direct effects of inhibition of galectins

on HL-60 cell differentiation. shRNA mediated silencing allows for the effects of transfection to resolve before assessing neutrophilic differentiation by being a more stable and less transient method. Additionally, recombinant galectins 10 and 12 were not available for purchase and were not investigated in this study. Therefore, transfection of *E. coli* cells with a plasmid expressing human recombinant galectn-10 and -12 can be performed to obtain and test these recombinant galectins on differentiation of HL-60 cells.

In the HL-60 cell model, the mechanisms driving galectin regulated differentiation remains unknown. There are several signal transduction pathways and transcription factors that galectins interact with during various cellular processes. A method to assess these changes in the expression of various transcription factors would be to perform the RT^2 Profiler PCR Array (Garcia-Peterson et al., 2020). Additionally, investigations into the expression of ERK1/2, p38, MAPK, STAT3, HRAS, Wnt, β-catenin, and CD44 at a genetic and protein level, and inhibition of these proteins, would also be beneficial to determine if these are a part of the underlying mechanisms. Additionally, co-immunoprecipitation or fluorescent co-localization imaging are two methods with which to assess the interaction of galectins with the various proteins exogenously or endogenously.

To further assess the resistance of HL-60 cells to galectin-induced apoptosis, concentrations above 1 μg/mL should be tested. Additional tests are also required and can include annexin V staining and flow cytometry. Additionally, RT-qPCR and western blot analysis for other markers including BCL2 and caspases should be performed.

When examining the AML TCGA data used in this study, there are some differences in the results observed when compared to the literature. This could be due to several factors including patient subtype sample composition, leukemic burden, age, various genetic abnormalities, and sample size. Therefore, the same analysis performed in this study should be conducted on a different set of AML samples. Furthermore, investigations at the genetic level are half the picture. Assessment of galectins at the protein level, and their methylation status, would further enhance our understanding of their involvement in AML.

References

Abedin, M. J., Kashio, Y., Seki, M., Nakamura, K., & Hirashima, M. (2003). Potential roles of galectins in myeloid differentiation into three different lineages. *Journal of leukocyte biology*, *73*(5), 650–656.

Ackerman, S. J., Corrette, S. E., Rosenberg, H. F., Bennett, J. C., Mastrianni, D. M., Nicholson-Weller, A., Weller, P. F., Chin, D. T., & Tenen, D. G. (1993). Molecular cloning and characterization of human eosinophil Charcot-Leyden crystal protein (lysophospholipase). Similarities to IgE binding proteins and the S-type animal lectin superfamily. *Journal of immunology*, *150*(2), 456–468.

Acosta-Rodríguez, E. V., Montes, C. L., Motrán, C. C., Zuniga, E. I., Liu, F. T., Rabinovich, G. A., & Gruppi, A. (2004). Galectin-3 mediates IL-4-induced survival and differentiation of B cells: functional cross-talk and implications during *Trypanosoma cruzi* infection. *Journal of immunology*, *172*(1), 493–502.

Agarwal, A., Bolosky, W. J., Wilson, D. B., Eide, C. A., Olson, S. B., Fan, G., & Druker, B. J. (2019). Differentiation of leukemic blasts is not completely blocked in acute myeloid leukemia. *Proceedings of the National Academy of Sciences of the United States of America*, *116*(49), 24593–24599.

Ai, Z., & Udalova, I. A. (2020). Transcriptional regulation of neutrophil differentiation and function during inflammation. *Journal of leukocyte biology*, *107*(3), 419–430.

Akagi, T., Thoennissen, N. H., George, A., Crooks, G., Song, J. H., Okamoto, R., Nowak, D., Gombart, A. F., & Koeffler, H. P. (2010). *In vivo* deficiency of both C/EBPβ and C/EBPε results in highly defective myeloid differentiation and lack of cytokine response. *PloS one*, *5*(11), e15419.

Akella, N. M., Le Minh, G., Ciraku, L., Mukherjee, A., Bacigalupa, Z. A., Mukhopadhyay, D., Sodi, V. L., & Reginato, M. J. (2020). O-GlcNAc Transferase regulates cancer stem-like potential of breast cancer cells. *Molecular cancer research*, *18*(4), 585–598.

Almkvist, J., Dahlgren, C., Leffler, H., & Karlsson, A. (2002). Activation of the neutrophil nicotinamide adenine dinucleotide phosphate oxidase by galectin-1. *Journal of immunology*, *168*(8), 4034–4041.

Andresen, V., Erikstein, B. S., Mukherjee, H., Sulen, A., Popa, M., Sørnes, S., Reikvam, H., Chan, K. P., Hovland, R., McCormack, E., Bruserud, Ø., Myers, A. G., & Gjertsen, B. T. (2016). Anti-proliferative activity of the NPM1 interacting natural product avrainvillamide in acute myeloid leukemia. *Cell death & disease*, *7*(12), e2497.

Anginot, A., Espeli, M., Chasson, L., Mancini, S. J., & Schiff, C. (2013). Galectin 1 modulates plasma cell homeostasis and regulates the humoral immune response. *Journal of immunology*, *190*(11), 5526–5533.

Arthur, C. M., Baruffi, M. D., Cummings, R. D., & Stowell, S. R. (2015). Evolving mechanistic insights into galectin functions. *Methods in molecular biology*, *1207*, 1–35.

Arikawa, T., Simamura, E., Shimada, H., Nishi, N., Tatsuno, T., Ishigaki, Y., Tomosugi, N., Yamashiro, C., Hata, T., Takegami, T., Mogami, H., Yamaguchi, K., Nakamura, T., Otani, H., Hatta, T., & Shoji, H. (2012). Expression pattern of Galectin 4 in rat placentation. *Placenta*, *33*(10), 885–887.

Ashraf, G. M., Mahmoud, M. M., & Tabrez, S. (2018). Studies on immunological and degranulation properties of a galectin-1 purified from goat (*Capra hircus*) heart. *International journal of biological macromolecules*, *115*, 1183–1188.

Asthana, A., Ramakrishnan, P., Vicioso, Y., Zhang, K., & Parameswaran, R. (2018). Hexosamine biosynthetic pathway inhibition leads to AML cell differentiation and cell death. *Molecular cancer therapeutics*, *17*(10), 2226–2237.

Astorgues-Xerri, L., Riveiro, M. E., Tijeras-Raballand, A., Serova, M., Rabinovich, G. A., Bieche, I., Vidaud, M., de Gramont, A., Martinet, M., Cvitkovic, E., Faivre, S., & Raymond, E. (2014). OTX008, a selective small-molecule inhibitor of galectin-1,

downregulates cancer cell proliferation, invasion and tumour angiogenesis. *European journal of cancer*, *50*(14), 2463–2477.

Auvynet, C., Moreno, S., Melchy, E., Coronado-Martínez, I., Montiel, J. L., Aguilar-Delfin, I., & Rosenstein, Y. (2013). Galectin-1 promotes human neutrophil migration. *Glycobiology*, *23*(1), 32–42.

Bedard, K., & Krause, K. H. (2007). The NOX family of ROS-generating NADPH oxidases: physiology and pathophysiology. *Physiological reviews*, *87*(1), 245–313.

Belambri, S. A., Rolas, L., Raad, H., Hurtado-Nedelec, M., Dang, P. M., & El-Benna, J. (2018). NADPH oxidase activation in neutrophils: role of the phosphorylation of its subunits. *European journal of clinical investigation*, *48 Suppl 2*, e12951.

Bernerd, F., Sarasin, A., & Magnaldo, T. (1999). Galectin-7 overexpression is associated with the apoptotic process in UVB-induced sunburn keratinocytes. *Proceedings of the National Academy of Sciences of the United States of America*, *96*(20), 11329–11334.

Bhattacharyya, S., Feferman, L., & Tobacman, J. K. (2014). Increased expression of colonic Wnt9A through Sp1-mediated transcriptional effects involving arylsulfatase B, chondroitin 4-sulfate, and galectin-3. *The Journal of biological chemistry*, *289*(25), 17564–17575.

Bjerregaard, M. D., Jurlander, J., Klausen, P., Borregaard, N., & Cowland, J. B. (2003). The *in vivo* profile of transcription factors during neutrophil differentiation in human bone marrow. *Blood*, *101*(11), 4322–4332.

Breitman, T. R., Collins, S. J., & Keene, B. R. (1980). Replacement of serum by insulin and transferrin supports growth and differentiation of the human promyelocytic cell line, HL-60. *Experimental cell research*, *126*(2), 494–498.

Breitman, T. R., Selonick, S. E., & Collins, S. J. (1980). Induction of differentiation of the human promyelocytic leukemia cell line (HL-60) by retinoic acid. *Proceedings of the National Academy of Sciences of the United States of America*, *77*(5), 2936–2940.

Cárcamo, C., Pardo, E., Oyanadel, C., Bravo-Zehnder, M., Bull, P., Cáceres, M., Martínez, J., Massardo, L., Jacobelli, S., González, A., & Soza, A. (2006). Galectin-8 binds specific beta1 integrins and induces polarized spreading highlighted by asymmetric lamellipodia in Jurkat T cells. *Experimental cell research*, *312*(4), 374–386.

Chan, J., O'Donoghue, K., Gavina, M., Torrente, Y., Kennea, N., Mehmet, H., Stewart, H., Watt, D. J., Morgan, J. E., & Fisk, N. M. (2006). Galectin-1 induces skeletal muscle differentiation in human fetal mesenchymal stem cells and increases muscle regeneration. *Stem cells*, *24*(8), 1879–1891.

Chang, Y. H., Weng, C. L., & Lin, K. I. (2020). O-GlcNAcylation and its role in the immune system. *Journal of biomedical science*, *27*(1), 57.

Chaplinski, T. J., Bennett, T. E., & Caro, J. F. (1986). Alteration in insulin receptor expression accompanying differentiation of HL-60 leukemia cells. *Cancer research*, *46*(3), 1203–1207.

Cheng, C. L., Hou, H. A., Lee, M. C., Liu, C. Y., Jhuang, J. Y., Lai, Y. J., Lin, C. W., Chen, H. Y., Liu, F. T., Chou, W. C., Chen, C. Y., Tang, J. L., Yao, M., Huang, S. Y., Ko, B. S., Wu, S. J., Tsay, W., & Tien, H. F. (2013). Higher bone marrow *LGALS3* expression is an independent unfavorable prognostic factor for overall survival in patients with acute myeloid leukemia. *Blood*, *121*(16), 3172–3180.

Choi, J. H., Choi, A. Y., Yoon, H., Choe, W., Yoon, K. S., Ha, J., Yeo, E. J., & Kang, I. (2010). Baicalein protects HT22 murine hippocampal neuronal cells against endoplasmic reticulum stress-induced apoptosis through inhibition of reactive oxygen species production and CHOP induction. *Experimental & molecular medicine*, *42*(12), 811–822.

Collado-Torres, L., Nellore, A., Kammers, K., Ellis, S. E., Taub, M. A., Hansen, K. D., Jaffe, A. E., Langmead, B., & Leek, J. T. (2017). Reproducible RNA-seq analysis using recount2. *Nature biotechnology*, *35*(4), 319–321.

Collins, S. J., Gallo, R. C., & Gallagher, R. E. (1977). Continuous growth and differentiation of human myeloid leukaemic cells in suspension culture. *Nature*, *270*(5635), 347–349.

Cooper, D., Norling, L. V., & Perretti, M. (2008). Novel insights into the inhibitory effects of Galectin-1 on neutrophil recruitment under flow. *Journal of leukocyte biology*, *83*(6), 1459–1466.

Cortegano, I., del Pozo, V., Cárdaba, B., de Andrés, B., Gallardo, S., del Amo, A., Arrieta, I., Jurado, A., Palomino, P., Liu, F. T., & Lahoz, C. (1998). Galectin-3 down-regulates IL-5 gene expression on different cell types. *Journal of immunology*, *161*(1), 385–389.

Dakik, H., El Dor, M., Leclerc, J., Kouzi, F., Nehme, A., Deynoux, M., Debeissat, C., Khamis, G., Ducrocq, E., Ibrik, A., Stasia, M. J., Raad, H., Rezvani, H. R., Gouilleux, F., Zibara, K., Herault, O., & Mazurier, F. (2021). Characterization of NADPH oxidase expression and activity in acute myeloid leukemia cell lines: a correlation with the differentiation status. *Antioxidants*, *10*(3), 498.

Dalton, W. T., Jr, Ahearn, M. J., McCredie, K. B., Freireich, E. J., Stass, S. A., & Trujillo, J. M. (1988). HL-60 cell line was derived from a patient with FAB-M2 and not FAB-M3. *Blood*, *71*(1), 242–247.

De Kouchkovsky, I., & Abdul-Hay, M. (2016). Acute myeloid leukemia: a comprehensive review and 2016 update. *Blood cancer journal*, *6*(7), e441.

Diedenhofen, B., & Musch, J. (2015). cocor: a comprehensive solution for the statistical comparison of correlations. *PloS one*, *10*(3), e0121945.

Dunsmore, G., Rosero, E. P., Shahbaz, S., Santer, D. M., Jovel, J., Lacy, P., Houston, S., & Elahi, S. (2021). Neutrophils promote T-cell activation through the regulated release of CD44-bound Galectin-9 from the cell surface during HIV infection. *PLoS biology*, *19*(8), e3001387.

El Leithy, A. A., Helwa, R., Assem, M. M., & Hassan, N. H. (2015). Expression profiling of cancer-related galectins in acute myeloid leukemia. *Tumour biology*, *36*(10), 7929–7939.

Eliaz I. (2013). The role of Galectin-3 as a marker of cancer and inflammation in a stage IV ovarian cancer patient with underlying pro-inflammatory comorbidities. *Case reports in oncology*, *6*(2), 343–349.

Elola, M. T., Chiesa, M. E., & Fink, N. E. (2005). Activation of oxidative burst and degranulation of porcine neutrophils by a homologous spleen galectin-1 compared to N-formyl-L-methionyl-L-leucyl-L-phenylalanine and phorbol 12-myristate 13-acetate. *Comparative biochemistry and physiology*, *141*(1), 23–31.

Esmon C. T. (2005). The interactions between inflammation and coagulation. *British journal of haematology*, *131*(4), 417–430.

Espeli, M., Mancini, S. J., Breton, C., Poirier, F., & Schiff, C. (2009). Impaired B-cell development at the pre-BII-cell stage in galectin-1-deficient mice due to inefficient pre-BII/stromal cell interactions. *Blood*, *113*(23), 5878–5886.

Fardini, Y., Dehennaut, V., Lefebvre, T., & Issad, T. (2013). O-GlcNAcylation: a new cancer hallmark?. *Frontiers in endocrinology*, *4*, 99.

Ferrer, C. M., Lynch, T. P., Sodi, V. L., Falcone, J. N., Schwab, L. P., Peacock, D. L., Vocadlo, D. J., Seagroves, T. N., & Reginato, M. J. (2014). O-GlcNAcylation regulates cancer metabolism and survival stress signaling via regulation of the HIF-1 pathway. *Molecular cell*, *54*(5), 820–831.

Gao, N., Yu, W. Z., Guo, N. J., Wang, X. X., & Sun, J. R. (2017). Clinical significance of galectin-3 in patients with adult acute myeloid leukemia: a retrospective cohort study with long-term follow-up and formulation of risk scoring system. *Leukemia & lymphoma*, *58*(6), 1394–1402.

Garcia-Peterson, L. M., Ndiaye, M. A., Chhabra, G., Singh, C. K., Guzmán-Pérez, G., Iczkowski, K. A., & Ahmad, N. (2020). CRISPR/Cas9-mediated knockout of SIRT6 imparts remarkable antiproliferative response in human melanoma cells *in vitro* and *in vivo*. *Photochemistry and photobiology*, *96*(6), 1314–1320.

Gentilini, L. D., Jaworski, F. M., Tiraboschi, C., Pérez, I. G., Kotler, M. L., Chauchereau, A., Laderach, D. J., & Compagno, D. (2017). Stable and high expression of Galectin-8 tightly controls metastatic progression of prostate cancer. *Oncotarget*, *8*(27), 44654–44668.

Gonçalves Silva, I., Rüegg, L., Gibbs, B. F., Bardelli, M., Fruehwirth, A., Varani, L., Berger, S. M., Fasler-Kan, E., & Sumbayev, V. V. (2016). The immune receptor Tim-3 acts as a trafficker in a Tim-3/galectin-9 autocrine loop in human myeloid leukemia cells. *Oncoimmunology*, *5*(7), e1195535.

Guilbert, L. J., & Iscove, N. N. (1976). Partial replacement of serum by selenite, transferrin, albumin and lecithin in haemopoietic cell cultures. *Nature*, *263*(5578), 594–595.

Gupta, D., Shah, H. P., Malu, K., Berliner, N., & Gaines, P. (2014). Differentiation and characterization of myeloid cells. *Current protocols in immunology*, *104*, 22F.5.1–22F.5.28.

Hassan, K., Qureshi, M., Shafi, S., Ikram, N., & Akhtar, M. J. (1993). Acute myeloid leukemia-FAB classification and its correlation with clinico-haematological features. *The Journal of the Pakistan Medical Association*, *43*(10), 200–203.

Helbawi, F.M., Ahmed, S.M., Mahmoud, M.S., Assem, M.M., Kamal, T.M., Abdou, M.A.A. (2021). Methylation status of galectin-12 gene promoter in acute myeloid leukemia. *Egyptian journal of haematology, 46(1):*1-6.

Hickstein, D. D., Back, A. L., & Collins, S. J. (1989). Regulation of expression of the CD11b and CD18 subunits of the neutrophil adherence receptor during human myeloid differentiation. *The Journal of biological chemistry*, *264*(36), 21812–21817.

Hirao, H., Uchida, Y., Kadono, K., Tanaka, H., Niki, T., Yamauchi, A., Hata, K., Watanabe, T., Terajima, H., & Uemoto, S. (2015). The protective function of galectin-9 in liver ischemia and reperfusion injury in mice. *Liver transplantation*, *21*(7), 969–981.

Hokama, A., Mizoguchi, E., Sugimoto, K., Shimomura, Y., Tanaka, Y., Yoshida, M., Rietdijk, S. T., de Jong, Y. P., Snapper, S. B., Terhorst, C., Blumberg, R. S., & Mizoguchi, A. (2004). Induced reactivity of intestinal CD4(+) T cells with an epithelial cell lectin, galectin-4, contributes to exacerbation of intestinal inflammation. *Immunity*, *20*(6), 681–693.

Hu, K., Gu, Y., Lou, L., Liu, L., Hu, Y., Wang, B., Luo, Y., Shi, J., Yu, X., & Huang, H. (2015). Galectin-3 mediates bone marrow microenvironment-induced drug resistance in acute leukemia cells via Wnt/β-catenin signaling pathway. *Journal of hematology & oncology*, *8*, 1.

Huflejt, M. E., & Leffler, H. (2004). Galectin-4 in normal tissues and cancer. *Glycoconjugate journal*, *20*(4), 247–255.

Ikegame, M., Tabuchi, Y., Furusawa, Y., Kawai, M., Hattori, A., Kondo, T., & Yamamoto, T. (2016). Tensile stress stimulates the expression of osteogenic cytokines/growth factors and matricellular proteins in the mouse cranial suture at the site of osteoblast differentiation. *Biomedical research*, *37*(2), 117–126.

Iurisci, I., Tinari, N., Natoli, C., Angelucci, D., Cianchetti, E., & Iacobelli, S. (2000). Concentrations of galectin-3 in the sera of normal controls and cancer patients. *Clinical cancer research*, *6*(4), 1389–1393.

Jeon, S. B., Yoon, H. J., Chang, C. Y., Koh, H. S., Jeon, S. H., & Park, E. J. (2010). Galectin-3 exerts cytokine-like regulatory actions through the JAK-STAT pathway. *Journal of immunology*, *185*(11), 7037–7046.

Johannes, L., Jacob, R., & Leffler, H. (2018). Galectins at a glance. *Journal of cell science*, *131*(9), jcs208884.

Johnson, D. E., & Redner, R. L. (2015). An ATRActive future for differentiation therapy in AML. *Blood reviews*, *29*(4), 263–268.

Juszczynski, P., Rodig, S. J., Ouyang, J., O'Donnell, E., Takeyama, K., Mlynarski, W., Mycko, K., Szczepanski, T., Gaworczyk, A., Krivtsov, A., Faber, J., Sinha, A. U., Rabinovich, G. A., Armstrong, S. A., Kutok, J. L., & Shipp, M. A. (2010). MLL-rearranged B lymphoblastic leukemias selectively express the immunoregulatory carbohydrate-binding protein galectin-1. *Clinical cancer research*, *16*(7), 2122–2130.

Kashio, Y., Nakamura, K., Abedin, M. J., Seki, M., Nishi, N., Yoshida, N., Nakamura, T., & Hirashima, M. (2003). Galectin-9 induces apoptosis through the calcium-calpain-caspase-1 pathway. *Journal of immunology*, *170*(7), 3631–3636.

Kikushige, Y., Miyamoto, T., Yuda, J., Jabbarzadeh-Tabrizi, S., Shima, T., Takayanagi, S., Niiro, H., Yurino, A., Miyawaki, K., Takenaka, K., Iwasaki, H., & Akashi, K. (2015). A TIM-3/Gal-9 autocrine stimulatory loop drives self-renewal of human myeloid leukemia stem cells and leukemic progression. *Cell stem cell*, *17*(3), 341–352.

Kim, S. J., Kang, H. G., Kim, K., Kim, H., Zetterberg, F., Park, Y. S., Cho, H. S., Hewitt, S. M., Chung, J. Y., Nilsson, U. J., Leffler, H., & Chun, K. H. (2021). Crosstalk between WNT and STAT3 is mediated by galectin-3 in tumor progression. *Gastric cancer*, *24*(5), 1050–1062.

Kobayashi, S. D., Voyich, J. M., Burlak, C., & DeLeo, F. R. (2005). Neutrophils in the innate immune response. *Archivum immunologiae et therapiae experimentalis*, *53*(6), 505–517.

Kolaczkowska, E., & Kubes, P. (2013). Neutrophil recruitment and function in health and inflammation. *Nature reviews. Immunology*, *13*(3), 159–175.

Kubach, J., Lutter, P., Bopp, T., Stoll, S., Becker, C., Huter, E., Richter, C., Weingarten, P., Warger, T., Knop, J., Müllner, S., Wijdenes, J., Schild, H., Schmitt, E., & Jonuleit, H. (2007). Human CD4+CD25+ regulatory T cells: proteome analysis identifies galectin-10 as a novel marker essential for their anergy and suppressive function. *Blood*, *110*(5), 1550–1558.

Kuroda, J., Yamamoto, M., Nagoshi, H., Kobayashi, T., Sasaki, N., Shimura, Y., Horiike, S., Kimura, S., Yamauchi, A., Hirashima, M., & Taniwaki, M. (2010). Targeting activating transcription factor 3 by Galectin-9 induces apoptosis and overcomes various types of treatment resistance in chronic myelogenous leukemia. *Molecular cancer research*, *8*(7), 994–1001.

Lee, J. J., Hsu, Y. C., Li, Y. S., & Cheng, S. P. (2021). Galectin-3 inhibitors suppress anoikis resistance and invasive capacity in thyroid cancer cells. *International journal of endocrinology*, *2021*, 5583491.

Leffler, H., Carlsson, S., Hedlund, M., Qian, Y., & Poirier, F. (2002). Introduction to galectins. *Glycoconjugate journal*, *19*(7-9), 433–440.

Levi, G., Tarrab-Hazdai, R., & Teichberg, V. I. (1983). Prevention and therapy with electrolectin of experimental autoimmune myasthenia gravis in rabbits. *European journal of immunology*, *13*(6), 500–507.

Liu, F. T., & Rabinovich, G. A. (2010). Galectins: regulators of acute and chronic inflammation. *Annals of the New York Academy of Sciences*, *1183*, 158–182.

Liu, J., Bi, G., Wen, P., Yang, W., Ren, X., Tang, T., Xie, C., Dong, W., & Jiang, G. (2007). Down-regulation of CD44 contributes to the differentiation of HL-60 cells induced by ATRA or HMBA. *Cellular & molecular immunology*, *4*(1), 59–63.

Lohse, I., Statz-Geary, K., Brothers, S. P., & Wahlestedt, C. (2018). Precision medicine in the treatment stratification of AML patients: challenges and progress. *Oncotarget*, *9*(102), 37790–37797.

Lu, Y., Lotan, D., & Lotan, R. (2000). Differential regulation of constitutive and retinoic acid-induced galectin-1 gene transcription in murine embryonal carcinoma and myoblastic cells. *Biochimica et biophysica acta*, *1491*(1-3), 13–19.

Lu, Y., & Lotan, R. (1999). Transcriptional regulation by butyrate of mouse galectin-1 gene in embryonal carcinoma cells. *Biochimica et biophysica acta*, *1444*(1), 85–91.

Luczak, M., Kaźmierczak, M., Handschuh, L., Lewandowski, K., Komarnicki, M., & Figlerowicz, M. (2012). Comparative proteome analysis of acute myeloid leukemia with and without maturation. *Journal of proteomics*, *75*(18), 5734–5748.

Luo, W., Song, L., Chen, X. L., Zeng, X. F., Wu, J. Z., Zhu, C. R., Huang, T., Tan, X. P., Lin, X. M., Yang, Q., Wang, J. Z., Li, X. K., & Wu, X. P. (2016). Identification of galectin-1 as a novel mediator for chemoresistance in chronic myeloid leukemia cells. *Oncotarget*, *7*(18), 26709–26723.

Lv, R., Bao, Q., & Li, Y. (2017). Regulation of M1-type and M2-type macrophage polarization in RAW264.7 cells by Galectin-9. *Molecular medicine reports*, *16*(6), 9111–9119.

Magescas, J., Sengmanivong, L., Viau, A., Mayeux, A., Dang, T., Burtin, M., Nilsson, U. J., Leffler, H., Poirier, F., Terzi, F., & Delacour, D. (2017). Spindle pole cohesion requires glycosylation-mediated localization of NuMA. *Scientific reports*, *7*(1), 1474.

Mastrianni, D. M., Eddy, R. L., Rosenberg, H. F., Corrette, S. E., Shows, T. B., Tenen, D. G., & Ackerman, S. J. (1992). Localization of the human eosinophil Charcot-Leyden crystal protein (lysophospholipase) gene (CLC) to chromosome 19 and the human ribonuclease 2 (eosinophil-derived neurotoxin) and ribonuclease 3 (eosinophil cationic protein) genes (RNS2 and RNS3) to chromosome 14. *Genomics*, *13*(1), 240–242.

McKeehan, W. L., Hamilton, W. G., & Ham, R. G. (1976). Selenium is an essential trace nutrient for growth of WI-38 diploid human fibroblasts. *Proceedings of the National Academy of Sciences of the United States of America*, *73*(6), 2023–2027.

Michael, J. V., Wurtzel, J. G., & Goldfinger, L. E. (2016). Inhibition of galectin-1 sensitizes HRAS-driven tumor growth to rapamycin Treatment. *Anticancer research*, *36*(10), 5053–5061.

Mollinedo, F., Santos-Beneit, A.M., Gajate, C. (1998). The human leukemia cell line HL-60 as a cell culture model 465 to study neutrophil functions and inflammatory cell responses. *Animal cell culture techniques*, 264–97.

Moriwaki, K., & Asahi, M. (2017). Augmented TME *O*-GlcNAcylation promotes tumor proliferation through the inhibition of p38 MAPK. *Molecular cancer research*, *15*(9), 1287–1298.

Nagy, N., Bronckart, Y., Camby, I., Legendre, H., Lahm, H., Kaltner, H., Hadari, Y., Van Ham, P., Yeaton, P., Pector, J. C., Zick, Y., Salmon, I., Danguy, A., Kiss, R., & Gabius, H. J. (2002). Galectin-8 expression decreases in cancer compared with normal and dysplastic human colon tissue and acts significantly on human colon cancer cell migration as a suppressor. *Gut*, *50*(3), 392–401.

Namba, T., Tian, F., Chu, K., Hwang, S. Y., Yoon, K. W., Byun, S., Hiraki, M., Mandinova, A., & Lee, S. W. (2013). CDIP1-BAP31 complex transduces apoptotic signals from endoplasmic reticulum to mitochondria under endoplasmic reticulum stress. *Cell reports*, *5*(2), 331–339.

Nellore, A., Jaffe, A. E., Fortin, J. P., Alquicira-Hernández, J., Collado-Torres, L., Wang, S., Phillips, R. A., III, Karbhari, N., Hansen, K. D., Langmead, B., & Leek, J. T. (2016). Human splicing diversity and the extent of unannotated splice junctions across human RNA-seq samples on the Sequence Read Archive. *Genome biology*, *17*(1), 266.

Nieminen, J., St-Pierre, C., & Sato, S. (2005). Galectin-3 interacts with naive and primed neutrophils, inducing innate immune responses. *Journal of leukocyte biology*, *78*(5), 1127–1135.

Niggli, V., Meszaros, A. V., Oppliger, C., & Tornay, S. (2004). Impact of cholesterol depletion on shape changes, actin reorganization, and signal transduction in neutrophil-like HL-60 cells. *Experimental cell research*, *296*(2), 358–368.

Nishi, N., Shoji, H., Seki, M., Itoh, A., Miyanaka, H., Yuube, K., Hirashima, M., & Nakamura, T. (2003). Galectin-8 modulates neutrophil function via interaction with integrin alphaM. *Glycobiology*, *13*(11), 755–763.

Nishikawa, H., & Suzuki, H. (2018). Possible role of inflammation and galectin-3 in brain injury after subarachnoid hemorrhage. *Brain sciences*, *8*(2), 30.

Norambuena, A., Metz, C., Vicuña, L., Silva, A., Pardo, E., Oyanadel, C., Massardo, L., González, A., & Soza, A. (2009). Galectin-8 induces apoptosis in Jurkat T cells by phosphatidic acid-mediated ERK1/2 activation supported by protein kinase A down-regulation. *The Journal of biological chemistry*, *284*(19), 12670–12679.

Novak, R., Dabelic, S., & Dumic, J. (2012). Galectin-1 and galectin-3 expression profiles in classically and alternatively activated human macrophages. *Biochimica et biophysica acta*, *1820*(9), 1383–1390.

Olins, A. L., Herrmann, H., Lichter, P., & Olins, D. E. (2000). Retinoic acid differentiation of HL-60 cells promotes cytoskeletal polarization. *Experimental cell research*, *254*(1), 130–142.

Olins, A. L., & Olins, D. E. (2004). Cytoskeletal influences on nuclear shape in granulocytic HL-60 cells. *BMC cell biology*, *5*, 30.

Ozeki, M., & Shively, J. E. (2008). Differential cell fates induced by all-*trans* retinoic acid-treated HL-60 human leukemia cells. *Journal of leukocyte biology*, *84*(3), 769–779.

Pan, L. L., Deng, Y. Y., Wang, R., Wu, C., Li, J., Niu, W., Yang, Q., Bhatia, M., Gudmundsson, G. H., Agerberth, B., Diana, J., & Sun, J. (2018). Lactose induces phenotypic and functional changes of neutrophils and macrophages to alleviate acute pancreatitis in mice. *Frontiers in immunology*, *9*, 751.

Paz, H., Joo, E. J., Chou, C. H., Fei, F., Mayo, K. H., Abdel-Azim, H., Ghazarian, H., Groffen, J., & Heisterkamp, N. (2018). Treatment of B-cell precursor acute lymphoblastic leukemia with the Galectin-1 inhibitor PTX008. *Journal of experimental & clinical cancer research*, *37*(1), 67.

Perillo, N. L., Pace, K. E., Seilhamer, J. J., & Baum, L. G. (1995). Apoptosis of T cells mediated by galectin-1. *Nature*, *378*(6558), 736–739.

Polyak, K., Xia, Y., Zweier, J. L., Kinzler, K. W., & Vogelstein, B. (1997). A model for p53-induced apoptosis. *Nature*, *389*(6648), 300–305.

Rabinovich, G. A., Daly, G., Dreja, H., Tailor, H., Riera, C. M., Hirabayashi, J., & Chernajovsky, Y. (1999). Recombinant galectin-1 and its genetic delivery suppress collagen-induced arthritis via T cell apoptosis. *The Journal of experimental medicine*, *190*(3), 385–398.

Risso, D., Ngai, J., Speed, T. P., & Dudoit, S. (2014). Normalization of RNA-seq data using factor analysis of control genes or samples. *Nature biotechnology*, *32*(9), 896–902.

Robinson, B. S., Arthur, C. M., Evavold, B., Roback, E., Kamili, N. A., Stowell, C. S., Vallecillo-Zúniga, M. L., Van Ry, P. M., Dias-Baruffi, M., Cummings, R. D., & Stowell, S. R. (2019). The sweet-side of leukocytes: galectins as master regulators of neutrophil function. *Frontiers in immunology*, *10*, 1762.

Rodríguez-Alcázar, J. F., Ataide, M. A., Engels, G., Schmitt-Mabmunyo, C., Garbi, N., Kastenmüller, W., Latz, E., & Franklin, B. S. (2019). Charcot-Leyden Crystals activate the NLRP3 inflammasome and cause IL-1β inflammation in H=human macrophages. *Journal of immunology*, *202*(2), 550–558.

Rossi, B., Espeli, M., Schiff, C., & Gauthier, L. (2006). Clustering of pre-B cell integrins induces galectin-1-dependent pre-B cell receptor relocalization and activation. *Journal of immunology*, *177*(2), 796–803.

Ruvolo, P. P., Ma, H., Ruvolo, V. R., Zhang, X., Post, S. M., & Andreeff, M. (2020). *LGALS1* acts as a pro-survival molecule in AML. *Biochimica et biophysica acta. Molecular cell research*, *1867*(10), 118785.

Ruvolo, P. P., Ruvolo, V. R., Burks, J. K., Qiu, Y., Wang, R. Y., Shpall, E. J., Mirandola, L., Hail, N., Jr, Zeng, Z., McQueen, T., Daver, N., Post, S. M., Chiriva-Internati, M., Kornblau, S. M., & Andreeff, M. (2018). Role of MSC-derived galectin 3 in the AML microenvironment. *Biochimica et biophysica acta. Molecular cell research*, *1865*(7), 959–969.

Ruvolo P. P. (2016). Galectin 3 as a guardian of the tumor microenvironment. *Biochimica et biophysica acta*, *1863*(3), 427–437.

Ruvolo P. P. (2019). Galectins as regulators of cell survival in the leukemia niche. *Advances in biological regulation*, *71*, 41–54.

Sarafian, V., Jans, R., & Poumay, Y. (2006). Expression of lysosome-associated membrane protein 1 (Lamp-1) and galectins in human keratinocytes is regulated by differentiation. *Archives of dermatological research*, *298*(2), 73–81.

Sanchez-Garrido, J., & Shenoy, A. R. (2021). Regulation and repurposing of nutrient sensing and autophagy in innate immunity. *Autophagy*, *17*(7), 1571–1591.

Sciacchitano, S., Lavra, L., Morgante, A., Ulivieri, A., Magi, F., De Francesco, G. P., Bellotti, C., Salehi, L. B., & Ricci, A. (2018). Galectin-3: one molecule for an alphabet of diseases, from A to Z. *International journal of molecular sciences*, *19*(2), 379.

Shao, R. G., Shimizu, T., & Pommier, Y. (1996). Brefeldin A is a potent inducer of apoptosis in human cancer cells independently of p53. *Experimental cell research*, *227*(2), 190–196.

Sherazi, A. A., Jariwala, K. A., Cybulski, A. N., Lewis, J. W., Karagiannis, J., Cumming, R. C., & Timoshenko, A. V. (2018). Effects of global O-GlcNAcylation on galectin gene-expression profiles in human cancer cell lines. *Anticancer research*, *38*(12), 6691–6697.

Short, N. J., Rytting, M. E., & Cortes, J. E. (2018). Acute myeloid leukaemia. *Lancet*, *392*(10147), 593–606.

Snarr, B. D., St-Pierre, G., Ralph, B., Lehoux, M., Sato, Y., Rancourt, A., Takazono, T., Baistrocchi, S. R., Corsini, R., Cheng, M. P., Sugrue, M., Baden, L. R., Izumikawa, K., Mukae, H., Wingard, J. R., King, I. L., Divangahi, M., Satoh, M. S., Yipp, B. G., Sato, S., Sheppard, D. C. (2020). Galectin-3 enhances neutrophil motility and extravasation into the airways during *Aspergillus fumigatus* infection. *PLoS pathogens*, *16*(8), e1008741.

Soddu, S., Blandino, G., Citro, G., Scardigli, R., Piaggio, G., Ferber, A., Calabretta, B., & Sacchi, A. (1994). Wild-type p53 gene expression induces granulocytic differentiation of HL-60 cells. *Blood*, *83*(8), 2230–2237.

Song, G., Li, Y., Zhang, Z., Ren, X., Li, H., Zhang, W., Wei, R., Pan, S., Shi, L., Bi, K., & Jiang, G. (2013). c-myc but not Hif-1α-dependent downregulation of VEGF influences the proliferation and differentiation of HL-60 cells induced by ATRA. *Oncology reports*, *29*(6), 2378–2384.

Steichen, A. L., Simonson, T. J., Salmon, S. L., Metzger, D. W., Mishra, B. B., & Sharma, J. (2015). Alarmin function of galectin-9 in murine respiratory tularemia. *PloS one*, *10*(4), e0123573.

Storti, P., Marchica, V., Airoldi, I., Donofrio, G., Fiorini, E., Ferri, V., Guasco, D., Todoerti, K., Silbermann, R., Anderson, J. L., Zhao, W., Agnelli, L., Bolzoni, M., Martella, E., Mancini, C., Campanini, N., Noonan, D. M., Petronini, P. G., Neri, A., Aversa, F., Roodman, G.D., Giuliani, N. (2016). Galectin-1 suppression delineates a new strategy to inhibit myeloma-induced angiogenesis and tumoral growth *in vivo*. *Leukemia*, *30*(12), 2351–2363.

Stowell, S. R., Qian, Y., Karmakar, S., Koyama, N. S., Dias-Baruffi, M., Leffler, H., McEver, R. P., & Cummings, R. D. (2008). Differential roles of galectin-1 and galectin-3 in regulating leukocyte viability and cytokine secretion. *Journal of immunology*, *180*(5), 3091–3102.

Su J. (2018). A brief history of Charcot-Leyden Crystal Protein/Galectin-10 research. *Molecules*, *23*(11), 2931.

Sumimoto H. (2008). Structure, regulation and evolution of Nox-family NADPH oxidases that produce reactive oxygen species. *The FEBS journal*, *275*(13), 3249–3277.

Sundqvist, M., Welin, A., Elmwall, J., Osla, V., Nilsson, U. J., Leffler, H., Bylund, J., & Karlsson, A. (2018). Galectin-3 type-C self-association on neutrophil surfaces; the carbohydrate recognition domain regulates cell function. *Journal of leukocyte biology*, *103*(2), 341–353.

Tang, M., You, J., Wang, W., Lu, Y., Hu, X., Wang, C., Liu, A., & Zhu, Y. (2018). Impact of galectin-1 on trophoblast stem cell differentiation and invasion in *in vitro* implantation model. *Reproductive sciences*, *25*(5), 700–711.

Tanikawa, R., Tanikawa, T., Hirashima, M., Yamauchi, A., & Tanaka, Y. (2010). Galectin-9 induces osteoblast differentiation through the CD44/Smad signaling pathway. *Biochemical and biophysical research communications*, *394*(2), 317–322.

Tasseff, R., Jensen, H. A., Congleton, J., Dai, D., Rogers, K. V., Sagar, A., Bunaciu, R. P., Yen, A., & Varner, J. D. (2017). An effective model of the retinoic acid induced HL-60 differentiation program. *Scientific reports*, *7*(1), 14327.

Tazhitdinova, R., & Timoshenko, A. V. (2020). The emerging role of galectins and *O*-GlcNAc homeostasis in processes of cellular differentiation. *Cells*, *9*(8), 1792.

Teichberg, V. I., Silman, I., Beitsch, D. D., & Resheff, G. (1975). A beta-D-galactoside binding protein from electric organ tissue of *Electrophorus electricus*. *Proceedings of the National Academy of Sciences of the United States of America*, *72*(4), 1383–1387.

Thijssen, V. L., Heusschen, R., Caers, J., & Griffioen, A. W. (2015). Galectin expression in cancer diagnosis and prognosis: A systematic review. *Biochimica et biophysica acta, 1855*(2), 235–247.

Timoshenko A. V. (2015). Towards molecular mechanisms regulating the expression of galectins in cancer cells under microenvironmental stress conditions. *Cellular and molecular life sciences, 72*(22), 4327–4340.

Timoshenko, A. V., Lanteigne, J., & Kozak, K. (2016). Extracellular stress stimuli alter galectin expression profiles and adhesion characteristics of HL-60 cells. *Molecular and cellular biochemistry, 413*(1-2), 137–143.

Trebo, A., Ditsch, N., Kuhn, C., Heidegger, H. H., Zeder-Goess, C., Kolben, T., Czogalla, B., Schmoeckel, E., Mahner, S., Jeschke, U., & Hester, A. (2020). High galectin-7 and low galectin-8 expression and the combination of both are negative prognosticators for breast cancer patients. *Cancers, 12*(4), 953.

Tribulatti, M. V., Figini, M. G., Carabelli, J., Cattaneo, V., & Campetella, O. (2012). Redundant and antagonistic functions of galectin-1, -3, and -8 in the elicitation of T cell responses. *Journal of immunology, 188*(7), 2991–2999.

Tsai, C. M., Chiu, Y. K., Hsu, T. L., Lin, I. Y., Hsieh, S. L., & Lin, K. I. (2008). Galectin-1 promotes immunoglobulin production during plasma cell differentiation. *Journal of immunology, 181*(7), 4570–4579.

Tsai, C. M., Guan, C. H., Hsieh, H. W., Hsu, T. L., Tu, Z., Wu, K. J., Lin, C. H., & Lin, K. I. (2011). Galectin-1 and galectin-8 have redundant roles in promoting plasma cell formation. *Journal of immunology, 187*(4), 1643–1652.

Vakhrushev, I. V., Novikova, S. E., Tsvetkova, A. V., Karalkin, P. A., Pyatnitskii, M. A., Zgoda, V. G., & Yarygin, K. N. (2018). Proteomic profiling of HL-60 cells during ATRA-induced differentiation. *Bulletin of experimental biology and medicine, 165*(4), 530–543.

van der Leij, J., van den Berg, A., Blokzijl, T., Harms, G., van Goor, H., Zwiers, P., van Weeghel, R., Poppema, S., & Visser, L. (2004). Dimeric galectin-1 induces IL-10 production in T-lymphocytes: an important tool in the regulation of the immune response. *The Journal of pathology*, *204*(5), 511–518.

van Hattum, H., Branderhorst, H. M., Moret, E. E., Nilsson, U. J., Leffler, H., & Pieters, R. J. (2013). Tuning the preference of thiodigalactoside- and lactosamine-based ligands to galectin-3 over galectin-1. *Journal of medicinal chemistry*, *56*(3), 1350–1354.

Vas, V., Fajka-Boja, R., Ion, G., Dudics, V., Monostori, E., & Uher, F. (2005). Biphasic effect of recombinant galectin-1 on the growth and death of early hematopoietic cells. *Stem cells*, *23*(2), 279–287.

Vega-Carrascal, I., Bergin, D. A., McElvaney, O. J., McCarthy, C., Banville, N., Pohl, K., Hirashima, M., Kuchroo, V. K., Reeves, E. P., & McElvaney, N. G. (2014). Galectin-9 signaling through TIM-3 is involved in neutrophil-mediated gram-negative bacterial killing: an effect abrogated within the cystic fibrosis lung. *Journal of immunology*, *192*(5), 2418–2431.

Veselská, R., Zitterbart, K., Jelínková, S., Neradil, J., & Svoboda, A. (2003). Specific cytoskeleton changes during apoptosis accompanying induced differentiation of HL-60 myeloid leukemia cells. *Oncology reports*, *10*(4), 1049–1058.

Vinnai, J. R., Cumming, R. C., Thompson, G. J., & Timoshenko, A. V. (2017). The association between oxidative stress-induced galectins and differentiation of human promyelocytic HL-60 cells. *Experimental cell research*, *355*(2), 113–123.

Vuong, L., Kouverianou, E., Rooney, C. M., McHugh, B. J., Howie, S., Gregory, C. D., Forbes, S. J., Henderson, N. C., Zetterberg, F. R., Nilsson, U. J., Leffler, H., Ford, P., Pedersen, A., Gravelle, L., Tantawi, S., Schambye, H., Sethi, T., & MacKinnon, A. C. (2019). An orally active galectin-3 antagonist inhibits lung adenocarcinoma growth and augments response to PD-L1 blockade. *Cancer research*, *79*(7), 1480–1492.

Walter, R. B., Othus, M., Burnett, A. K., Löwenberg, B., Kantarjian, H. M., Ossenkoppele, G. J., Hills, R. K., van Montfort, K. G., Ravandi, F., Evans, A., Pierce, S. R., Appelbaum, F. R., & Estey, E. H. (2013). Significance of FAB subclassification of "acute myeloid leukemia, NOS" in the 2008 WHO classification: analysis of 5848 newly diagnosed patients. *Blood*, *121*(13), 2424–2431.

Wang, L., Zhao, Y., Wang, Y., & Wu, X. (2018). The role of galectins in cervical cancer biology and progression. *BioMed research international*, *2018*, 2175927.

Wdowiak, K., Gallego-Colon, E., Francuz, T., Czajka-Francuz, P., Ruiz-Agamez, N., Kubeczko, M., Grochoła, I., Wybraniec, M. T., Chudek, J., & Wojnar, J. (2019). Increased serum levels of Galectin-9 in patients with chronic lymphocytic leukemia. *Oncology letters*, *17*(1), 1019–1029.

Wei, H., Kim, S. J., Zhang, Z., Tsai, P. C., Wisniewski, K. E., & Mukherjee, A. B. (2008). ER and oxidative stresses are common mediators of apoptosis in both neurodegenerative and non-neurodegenerative lysosomal storage disorders and are alleviated by chemical chaperones. *Human molecular genetics*, *17*(4), 469–477.

Wu, D., Jin, J., Qiu, Z., Liu, D., & Luo, H. (2020). Functional analysis of *O*-GlcNAcylation in cancer metastasis. *Frontiers in oncology*, *10*, 585288.

Wu, S. Y., Huang, J. H., Chen, W. Y., Chan, Y. C., Lin, C. H., Chen, Y. C., Liu, F. T., & Wu-Hsieh, B. A. (2017). Cell intrinsic galectin-3 attenuates neutrophil ROS-dependent killing of *Candida* by modulating CR3 downstream Syk activation. *Frontiers in immunology*, *8*, 48.

Xue, H., Yang, R. Y., Tai, G., & Liu, F. T. (2016). Galectin-12 inhibits granulocytic differentiation of human NB4 promyelocytic leukemia cells while promoting lipogenesis. *Journal of leukocyte biology*, *100*(4), 657–664.

Yamamoto, H., Nishi, N., Shoji, H., Itoh, A., Lu, L. H., Hirashima, M., & Nakamura, T. (2008). Induction of cell adhesion by galectin-8 and its target molecules in Jurkat T-cells. *Journal of biochemistry*, *143*(3), 311–324.

Yang, R. Y., Hsu, D. K., Yu, L., Chen, H. Y., & Liu, F. T. (2004). Galectin-12 is required for adipogenic signaling and adipocyte differentiation. *The Journal of biological chemistry*, *279*(28), 29761–29766.

Yang, R. Y., Rabinovich, G. A., & Liu, F. T. (2008). Galectins: structure, function and therapeutic potential. *Expert reviews in molecular medicine*, *10*, e17.

Yang, X., & Qian, K. (2017). Protein O-GlcNAcylation: emerging mechanisms and functions. *Nature reviews. Molecular cell biology*, *18*(7), 452–465.

Yang, X., Su, K., Roos, M. D., Chang, Q., Paterson, A. J., & Kudlow, J. E. (2001). O-linkage of N-acetylglucosamine to Sp1 activation domain inhibits its transcriptional capability. *Proceedings of the National Academy of Sciences of the United States of America*, *98*(12), 6611–6616.

Zheng, Y., Feng, W., Wang, Y. J., Sun, Y., Shi, G., & Yu, Q. (2019). Galectins as potential emerging key targets in different types of leukemia. *European journal of pharmacology*, *844*, 73–78.

Zhu, C., Anderson, A. C., Schubart, A., Xiong, H., Imitola, J., Khoury, S. J., Zheng, X. X., Strom, T. B., & Kuchroo, V. K. (2005). The Tim-3 ligand galectin-9 negatively regulates T helper type 1 immunity. *Nature immunology*, *6*(12), 1245–1252.

Appendix A: Supplementary Material

Table S1: Gene names, PCR primer sequences and amplicon sizes, cycling conditions, efficiencies, and references.

Gene name mRNA RefSeq	Sequence 5'-3'	Size (bp)	2 step cycling	PMID reference
NCF1	F GTCAGATGAAAGCAAAGCGA	93	95°C (5 s)	23147401
NM_000265.7	R CATAGTTGGGCTCAGGGTCT		62°C (25 s)	
ACTB	F TCAGCAAGCAGGAGTATGACGAG	265	95°C (5 s)	30504378
NM_001101.5	R ACATTGTGAACTTTGGGGGATG		60°C (25 s)	
*CHOP**	F CAGACTGATCCAACTGCAG	280	95°C (5 s)	Designed
NM_004083.6 *NM_001195057.1* *NM_001195056.1* *NM_001195055.1* *NM_001195054.1* *NM_001195053.1*	R GACTGGAATCTGGAGAGT		62°C (25 s)	
*BAX***	F TGGCAGCTGACATGTTTTCTGAC	195	95°C (5 s)	30069445
NM_001291429.2 *NM_004324.4*	R TCACCCAACCACCCTGGTCTT		62°C (25 s)	

Note: *CHOP transcript variant 1 (NM_001195053.1), transcript variant 2 (NM_001195054.1), transcript variant 3 (NM_001195055.1), transcript variant 4 (NM_001195056.1), transcript variant 5 (NM_004083.6), and transcript variant 6 (NM_001195057.1) are recognized by this primer pair. **_BAX_ transcript variant gamma (NM_001291429.2) and transcript variant beta (NM_004324.4) are recognized by this primer pair.

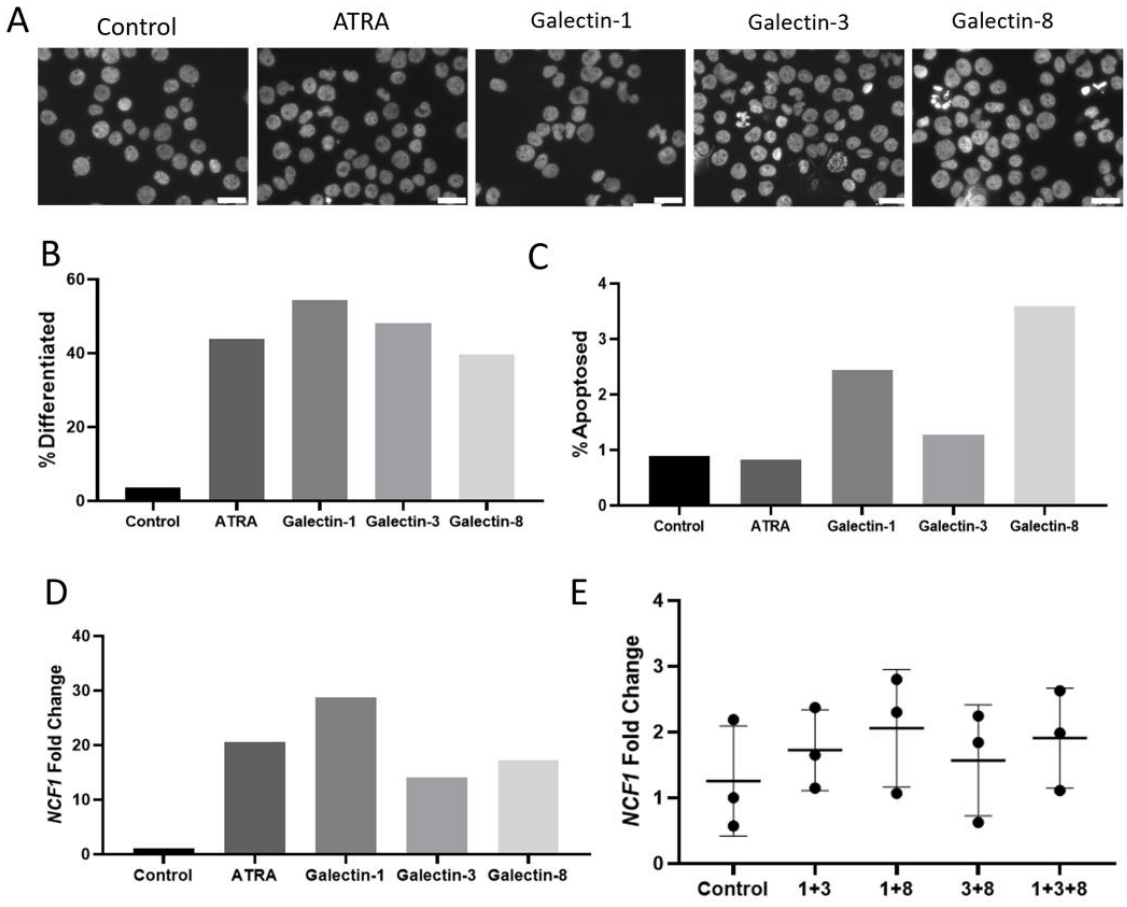

Figure S1: **Combination treatments with recombinant galectins and 50 nM ATRA had no effect on granulocytic differentiation of HL-60 cells.**

HL-60 cells were treated with combinations of 500 ng/mL of recombinant galectin-1, -3 or -8 or treatments with 500 ng/mL galectin-1, -3 or -8 and 50 nM ATRA were conducted over 72 hr. See Chapter 2 Materials and Methods for detailed explanation of techniques. (A) Nuclear morphology of cells; (B) cell differentiation index; (C) cell apoptotic index; *NCF1* gene expression of recombinant galectins + ATRA treated cells (D) and galectin combination treatments (E). Recombinant galectins + ATRA data represented as n=1. Galectin combination data are presented as means ± SD, n=3. Significant differences were determined using One-way ANOVA followed by Tukey's HSD test with a $p<0.05$.

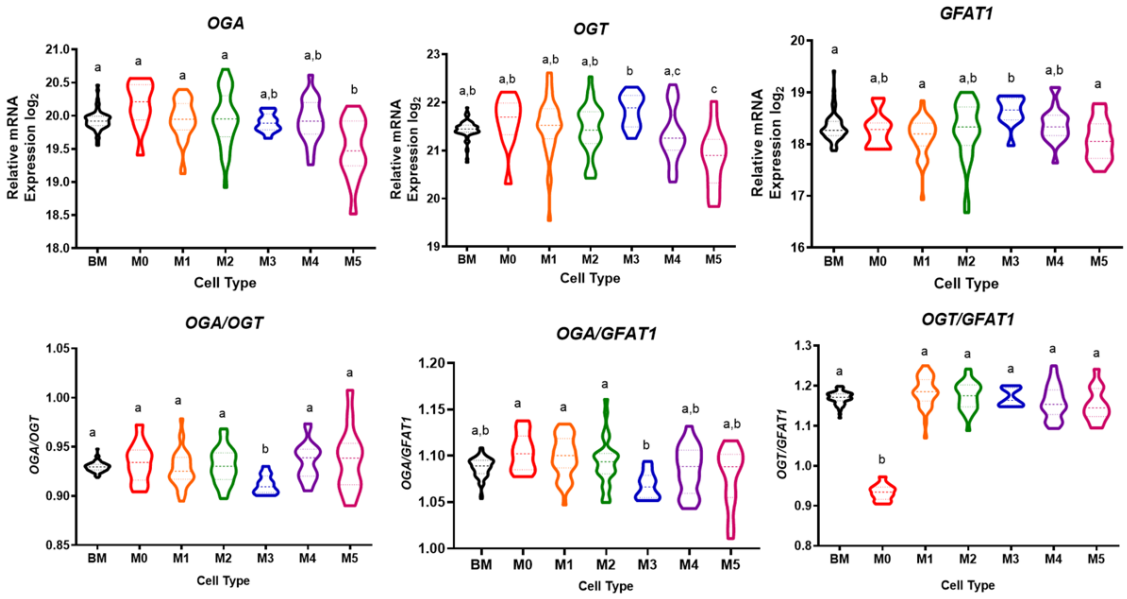

Figure S2: *O*-GlcNAc related enzymes *OGA, OGT,* and *GFAT1* exhibits constant gene expression patterns in TCGA AML subtypes M0-M5.

GTEx bone marrow (BM) and TCGA AML RNA-Seq data were retrieved from recount2 and RUVg normalized in R studio and $\log_2$ transformed in Microsoft excel prior to statistical analysis. The subtypes investigated include M0 (n=12), M1 (n=36), M2 (n=29), M3 (n=12), M4 (n=22), and M5 (n=14) and compared to BM control (n=70). *O*-GlcNAc related enzymes gene expression profiles of *OGA, OGT,* and *GFAT1* were examined as well as related ratios of *OGA/OGT, OGA/GFAT1*, and *OGT/GFAT1*. Data are represented as violin plots. Statistical significance was determined using the nonparametric Kruskal-Wallis test followed by Dunn's multiple comparisons and are represented as different letters with a $p<0.05$.

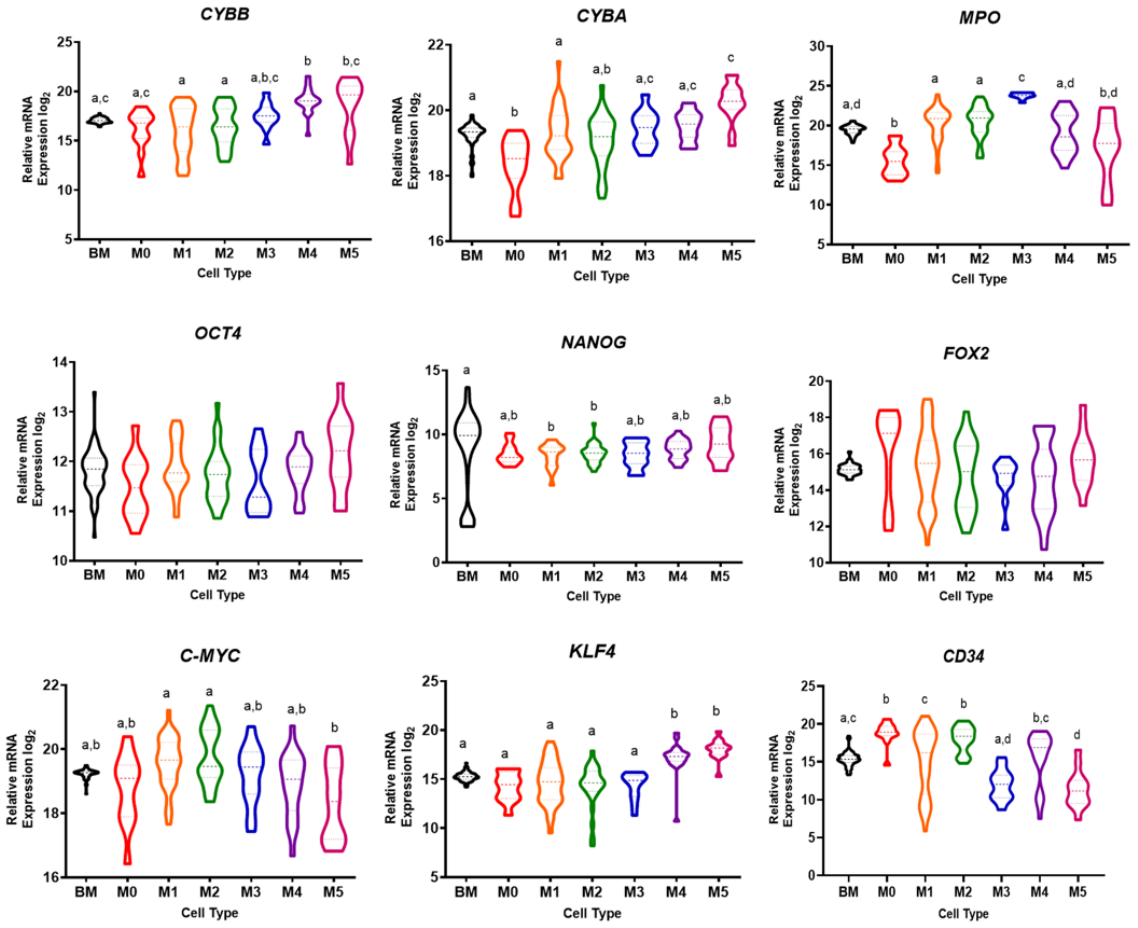

Figure S3: **Granulocyte differentiation markers and stemness markers demonstrates changes in expression profiles in TCGA AML subtypes M0-M5.**

GTEx bone marrow (BM) and TCGA AML RNA-Seq data were retrieved from recount2 and RUVg normalized in R studio and $\log_2$ transformed in Microsoft excel prior to statistical analysis. The subtypes investigated include M0 (n=12), M1 (n=36), M2 (n=29), M3 (n=12), M4 (n=22), and M5 (n=14) and compared to BM control (n=70). Granulocyte differentiation markers *NCF1*, *NCF2*, *CYBB*, *CYBA* and *MPO* were investigated as well as stemness markers *OCT4*, *NANOG*, *FOX2*, *C-MYC*, *KLF4*, and *CD34*. Data are represented as violin plots. Statistical significance was determined using the nonparametric Kruskal-Wallis test followed by Dunn's multiple comparisons and are represented as different letters with a $p<0.05$.

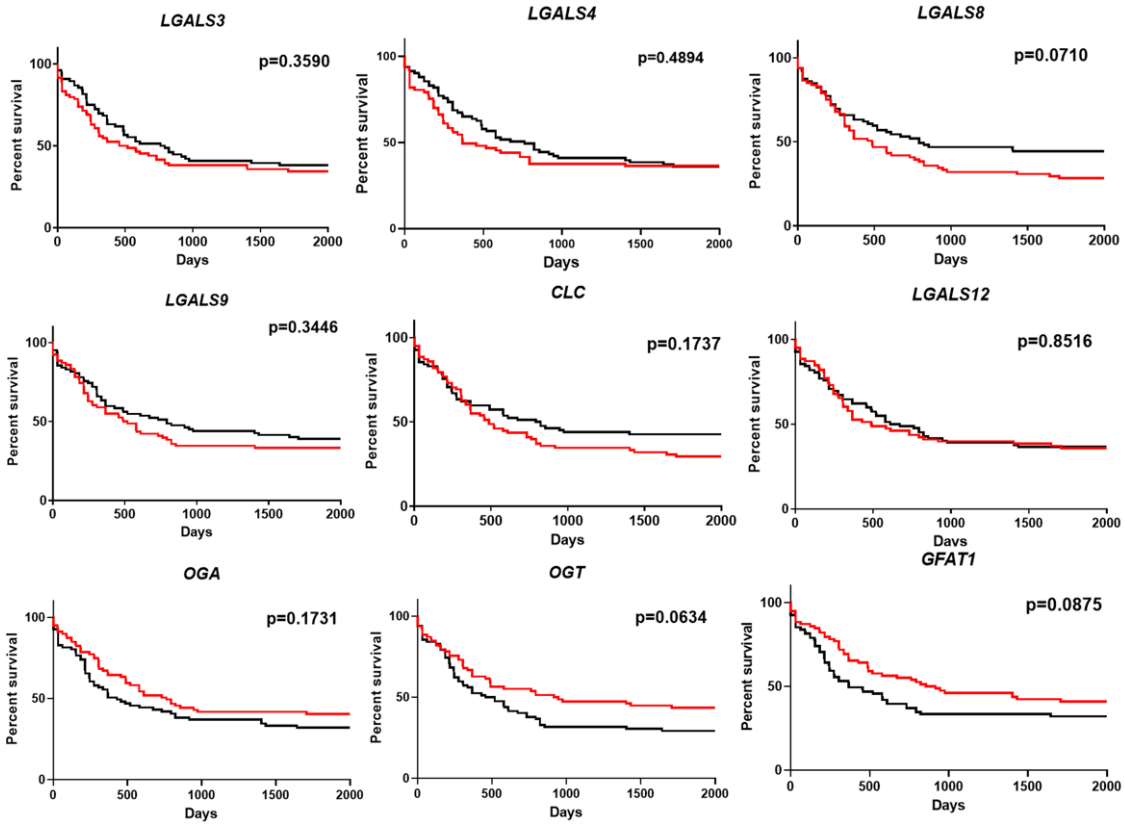

Figure S4: **Survival curve analysis of TCGA AML patient data of galectin and *O*-GlcNAc genes expression is not associated with patient prognosis.**

RSEM AML patient data was retrieved from cBioPortal and $\log_2$ transformed. R Studio was used to access patient survival data from cBioPortal. Median gene expression was used to determine patients with above/equal (red) or below (black) expression. Galectin genes including *LGASL3, LGALS4, LGALS8, LGALS9, CLC,* and *LGALS12* as well as *O*-GlcNAc related enzymes *OGA, OGT,* and *GFAT1* were investigated in all AML cohorts (n=160). Statistical significance was determined using the log-rank (Mantel-Cox) test.

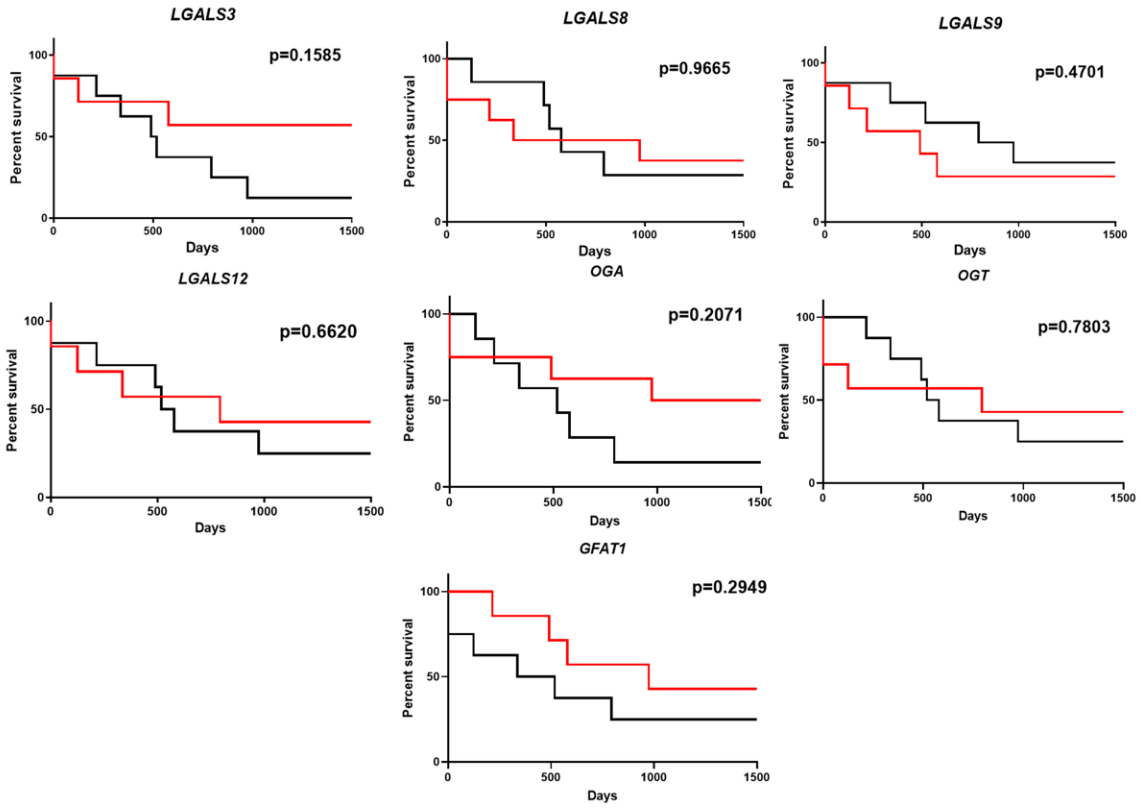

Figure S5: **Survival curve analysis of TCGA AML patient data of galectin and *O*-GlcNAc genes expression is not associated with patient prognosis in FAB subtype M0.**

RSEM AML patient data was retrieved from cBioPortal and put to the $\log_2$ transformed. R Studio was used to access patient survival data from cBioPortal. Median gene expression was used to determine patients with above/equal (red) or below (black) expression. Galectin genes including *LGASL3, LGALS8, LGALS9,* and *LGALS12* as well as *O*-GlcNAc related enzymes *OGA, OGT,* and *GFAT1* were investigated in all AML M0 FAB subtype (n=15). Statistical significance was determined using the log-rank (Mantel-Cox) test.

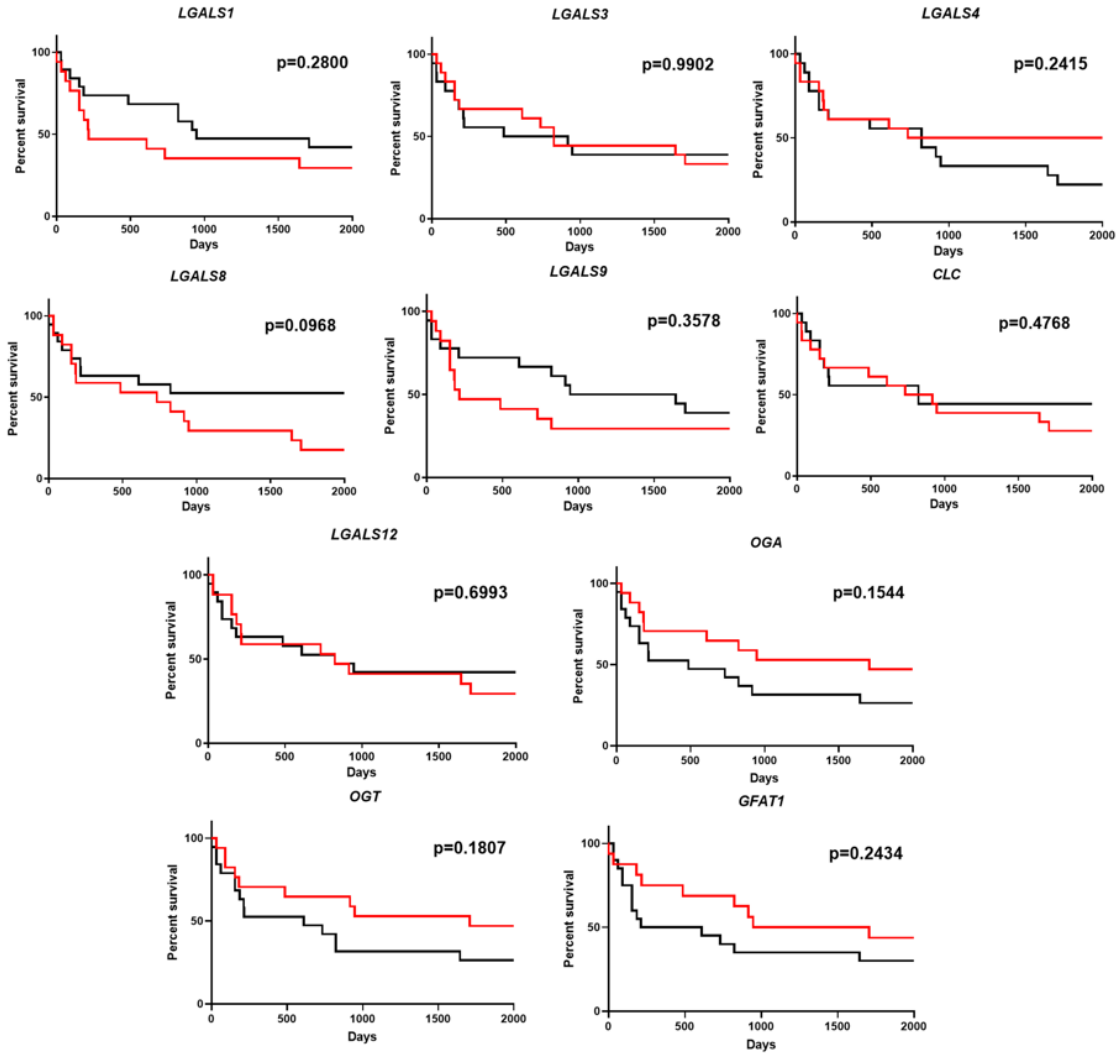

Figure S6: **Survival curve analysis of TCGA AML patient data of galectin and *O*-GlcNAc genes expression is not associated with patient prognosis in FAB subtype M1.**

RSEM AML patient data was retrieved from cBioPortal and $\log_2$ transformed. R Studio was used to access patient survival data from cBioPortal. Median gene expression was used to determine patients with above/equal (red) or below (black) expression. Galectin genes including *LGALS1*, *LGASL3*, *LGALS4*, *LGALS8*, *LGALS9*, *CLC*, and *LGALS12* as well as *O*-GlcNAc related enzymes *OGA*, *OGT*, and *GFAT1* were investigated in all AML M1 FAB subtype (n=36). Statistical significance was determined using the log-rank (Mantel-Cox) test.

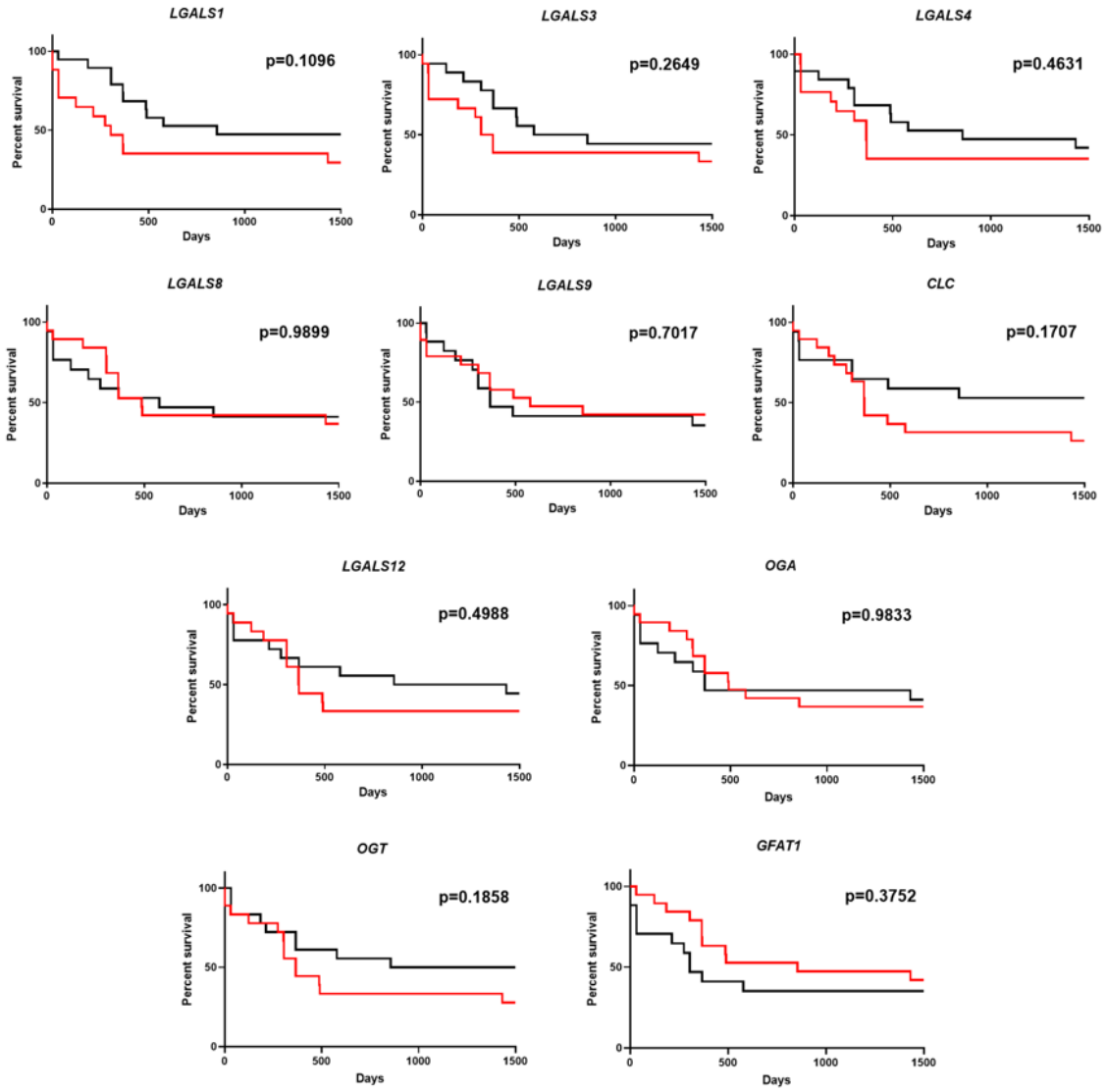

Figure S7: **Survival curve analysis of TCGA AML patient data of galectin and *O*-GlcNAc genes expression is not associated with patient prognosis in FAB subtype M2.**

RSEM AML patient data was retrieved from cBioPortal and $\log_2$ transformed. R Studio was used to access patient survival data from cBioPortal. Median gene expression was used to determine patients with above/equal (red) or below (black) expression. Galectin genes including *LGALS1*, *LGASL3*, *LGALS4*, *LGALS8*, *LGALS9*, *CLC*, and *LGALS12* as well as *O*-GlcNAc related enzymes *OGA*, *OGT*, and *GFAT1* were investigated in all AML M2 FAB subtype (n=36). Statistical significance was determined using the log-rank (Mantel-Cox) test.

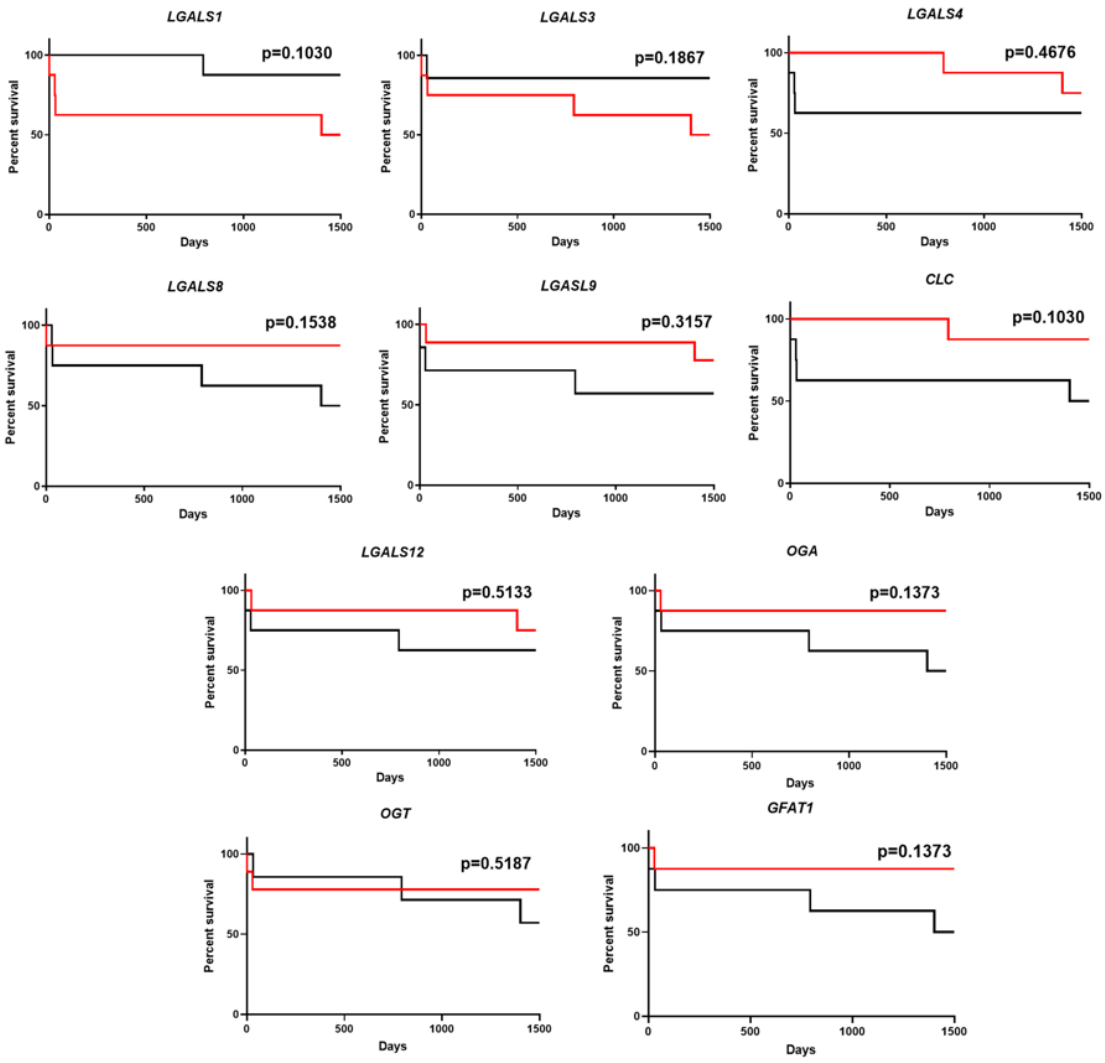

Figure S8: **Survival curve analysis of TCGA AML patient data of galectin and *O*-GlcNAc genes expression is not associated with patient prognosis in FAB subtype M3.**

RSEM AML patient data was retrieved from cBioPortal and $\log_2$ transformed. R Studio was used to access patient survival data from cBioPortal. Median gene expression was used to determine patients with above/equal (red) or below (black) expression. Galectin genes including *LGALS1*, *LGASL3*, *LGALS4*, *LGALS8*, *LGALS9*, *CLC*, and *LGALS12* as well as *O*-GlcNAc related enzymes *OGA*, *OGT*, and *GFAT1* were investigated in all AML M3 FAB subtype (n=16). Statistical significance was determined using the log-rank (Mantel-Cox) test.

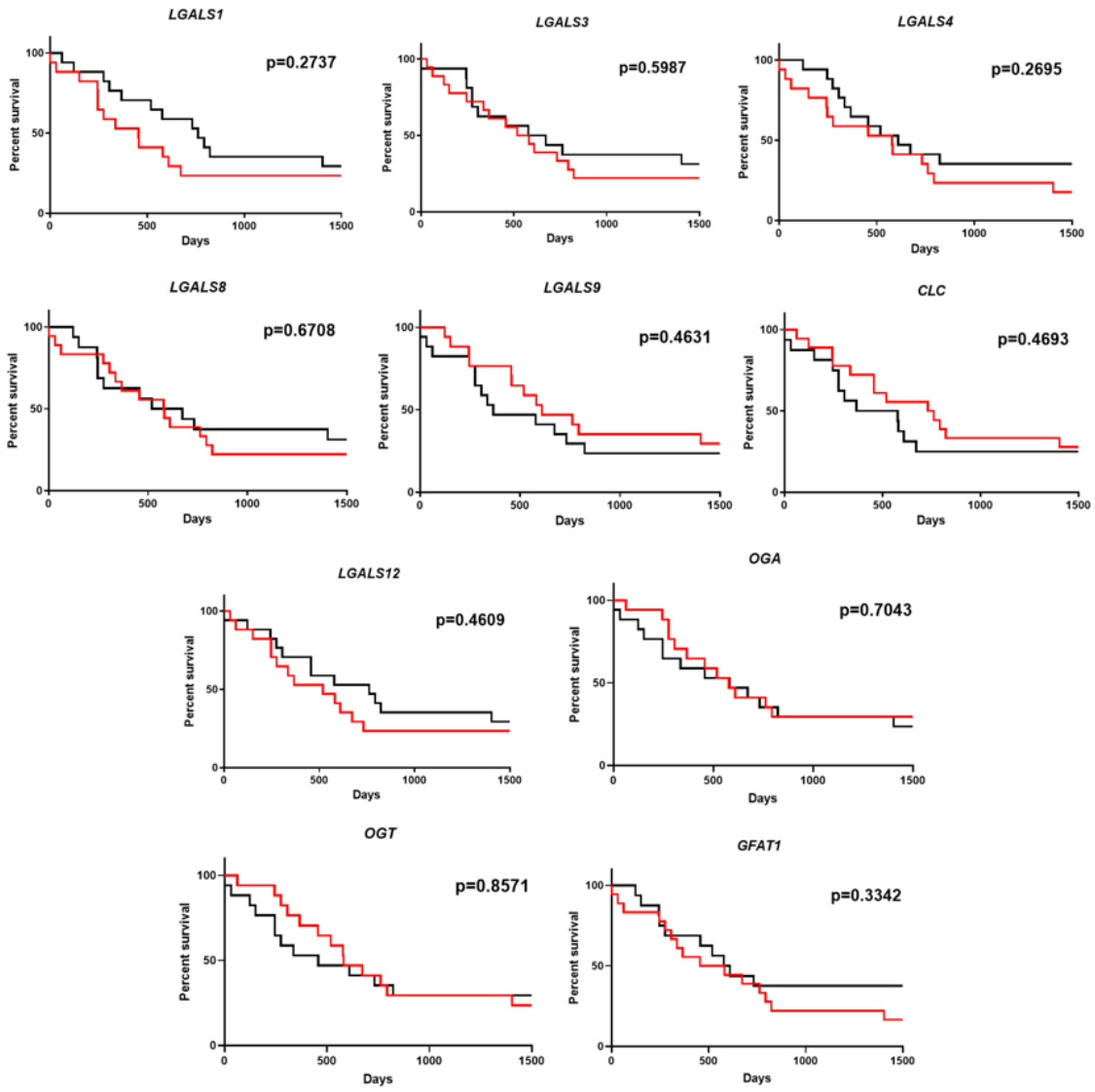

Figure S9: **Survival curve analysis of TCGA AML patient data of galectin and *O*-GlcNAc genes expression is not associated with patient prognosis in FAB subtype M4.**

RSEM AML patient data was retrieved from cBioPortal and $\log_2$ transformed. R Studio was used to access patient survival data from cBioPortal. Median gene expression was used to determine patients with above/equal (red) or below (black) expression. Galectin genes including *LGALS1*, *LGASL3*, *LGALS4*, *LGALS8*, *LGALS9*, *CLC*, and *LGALS12* as well as *O*-GlcNAc related enzymes *OGA*, *OGT*, and *GFAT1* were investigated in all AML M4 FAB subtype (n=34). Statistical significance was determined using the log-rank (Mantel-Cox) test.

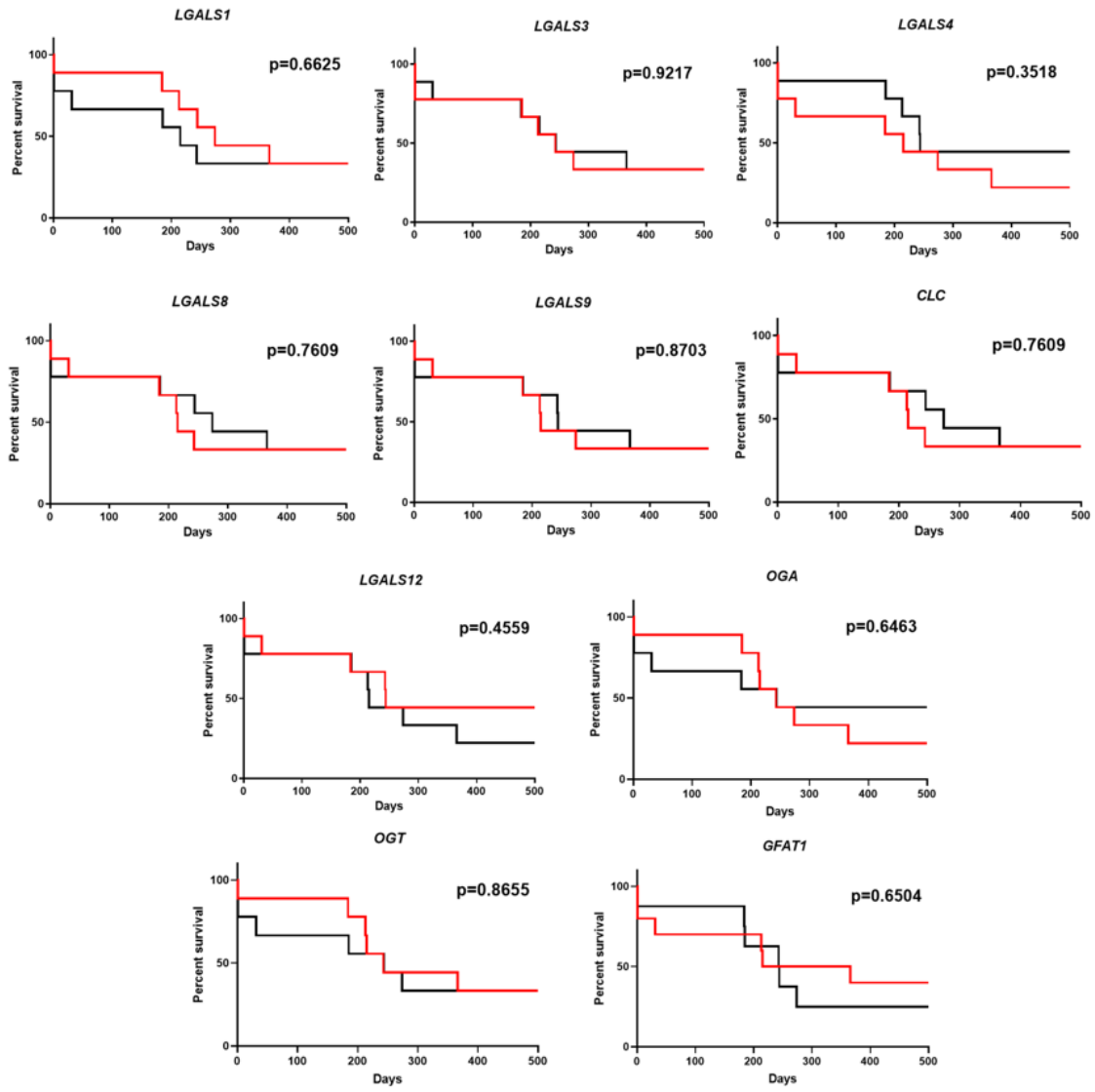

Figure S10: **Survival curve analysis of TCGA AML patient data of galectin and *O*-GlcNAc genes expression is not associated with patient prognosis in FAB subtype M5.**

RSEM AML patient data was retrieved from cBioPortal and $\log_2$ transformed. R Studio was used to access patient survival data from cBioPortal. Median gene expression was used to determine patients with above/equal (red) or below (black) expression. Galectin genes including *LGALS1*, *LGASL3*, *LGALS4*, *LGALS8*, *LGALS9*, *CLC*, and *LGALS12* as well as *O*-GlcNAc related enzymes *OGA*, *OGT*, and *GFAT1* were investigated in all AML M5 FAB subtype (n=18). Statistical significance was determined using the log-rank (Mantel-Cox) test

Curriculum Vitae

Name: Jolaine Smtih

Post-secondary Education and Degrees:

The University of Western Ontario
London, Ontario, Canada
2019-Present M.Sc. in Biology

University of Waterloo
Waterloo Ontario, Canada
2015-2019 B.Sc. in Honours Biology, Specialization in Microbiology

Honours and Awards:

Western Graduate Research Scholarship (WGRS)
The University of Western Ontario, London, Ontario
Sept 2019-Aug 2021

Dean's Honours List
University of Waterloo, Waterloo, Ontario
Sept 2016-April 2019

Related Work Experience:

Teaching Assistant
The University of Western Ontario
Sept 2019 – Dec 2021

Volunteer Experience:

Science Open House
University of Waterloo, Waterloo, Ontario
2018

Abstracts and Posters:

Smith J, Timoshenko AV (2021) The role of galectins in neutrophilic differentiation of HL-60 cells. Ontario Cell Biology Symposium (online), July 12-16, 2021.

Smith J, Guevorguian P, Timoshenko AV (2021) *In silico* analysis of galectin and *O*-GlcNAc cycle enzyme expression patterns in acute myeloid leukemia. 17th Annual Oncology Research & Education "Day" (online), June 14-18, 2021.

Smith J, Timoshenko AV (2021) The role of galectins and *O*-GlcNAcylation in acute myeloid leukemia. Virtual Canadian Cancer Research Conference, November 8-11, 2021.